DUDLEY KNOX LIBRARY
NAVAL POSTGRADUATE SCHOOL
MONTEREY, CALIFORNIA 93943-5002

NPS 68-87-002

NAVAL POSTGRADUATE SCHOOL
Monterey, California

THESIS

MESOSCALE VARIABILITY IN THE WEST
SPITSBERGEN CURRENT
AND ADJACENT WATERS IN FRAM STRAIT

by

Alan M. Weigel

March 1987

Thesis Advisor R.H. Bourke

Approved for public release; distribution is unlimited.

Prepared for:
Director, Arctic Submarine Laboratory,
Naval Ocean Systems Center,
San Diego, Ca., 92152

T233163

NAVAL POSTGRADUATE SCHOOL
Monterey, California

Rear Admiral R. C. Austin
Superintendent

David A. Schrady
Provost

This thesis prepared in conjunction with research sponsored by the Arctic Submarine Laboratory, Naval Ocean Systems Center, San Diego, CA under Work Order N66001-86-WR-00131.

Reproduction of all or part of this report is authorized

Released by:

NCLASSIFIED
URITY CLASSIFICATION OF THIS PAGE

REPORT DOCUMENTATION PAGE

REPORT SECURITY CLASSIFICATION UNCLASSIFIED	1b RESTRICTIVE MARKINGS
SECURITY CLASSIFICATION AUTHORITY	3 DISTRIBUTION/AVAILABILITY OF REPORT Approved for public release; distribution unlimited.
DECLASSIFICATION/DOWNGRADING SCHEDULE	
ERFORMING ORGANIZATION REPORT NUMBER(S) NPS 68-87-002	5 MONITORING ORGANIZATION REPORT NUMBER(S)
NAME OF PERFORMING ORGANIZATION val Postgraduate School 6b OFFICE SYMBOL (If applicable) Code 68	7a NAME OF MONITORING ORGANIZATION Arctic Submarine Laboratory
ADDRESS (City, State, and ZIP Code) nterey, CA 93943	7b ADDRESS (City, State, and ZIP Code) Code 19, Bldg. 271 Naval Ocean Systems Center San Diego, CA 92152
NAME OF FUNDING/SPONSORING ORGANIZATION rctic Submarine Lab. 8b OFFICE SYMBOL (If applicable) Code 19	9 PROCUREMENT INSTRUMENT IDENTIFICATION NUMBER N6600186WR00131
ADDRESS (City, State, and ZIP Code) ldg. 271 aval Ocean Systems Center an Diego, CA 92152	10 SOURCE OF FUNDING NUMBERS PROGRAM ELEMENT NO / PROJECT NO / TASK NO / WORK UNIT ACCESSION NO

TLE (Include Security Classification)
SOSCALE VARIABILITY IN THE WEST SPITSBERGEN CURRENT AND ADJACENT WATERS
FRAM STRAIT

ERSONAL AUTHOR(S)
igel, Alan M.

TYPE OF REPORT	13b TIME COVERED FROM ___ TO ___	14 DATE OF REPORT (Year Month Day)	15 PAGE COUNT
ster's Thesis		1987 March	100

SUPPLEMENTARY NOTATION
epared in conjunction with R.H. Bourke and R.G. Paquette.

COSATI CODES		
FIELD	GROUP	SUB-GROUP

18 SUBJECT TERMS (Continue on reverse if necessary and identify by block number)
West Spitsbergen Current
East Greenland Current
NORTHWIND
Fram Strait

ABSTRACT (Continue on reverse if necessary and identify by block number)

A dense network of conductivity-temperature-depth (CTD) measurements as carried out between 76°N and 81°N in order to define the distribution f temperature and salinity in Fram Strait. Although weakly baroclinic, he WSC flow was found to be strongly influenced by the 2000 m deep ipnovich Ridge which separated the flow into several streams. In ddition, filaments of warm Atlantic Water (AW) were found to spread out ver the top of the Greenland Gyre. The WSC branches near 80°N. pproximately 20% of the baroclinic transport enters the Arctic Ocean orth of Spitsbergen as the eastern branch. The other branch (80% of he baroclinic transport) turns westward, apparently under the influence f the Yermak Plateau, and joins with the southward flowing East reenland Current (EGC). The entire turning takes place south of 81°N ear the ice edge with baroclinic speeds of up to 0.03 m/s. The

STRIBUTION/AVAILABILITY OF ABSTRACT ☒ UNCLASSIFIED/UNLIMITED ☐ SAME AS RPT ☐ DTIC USERS	21 ABSTRACT SECURITY CLASSIFICATION UNCLASSIFIED
NAME OF RESPONSIBLE INDIVIDUAL R. H. Bourke	22b TELEPHONE (Include Area Code) 408-646-3270 22c OFFICE SYMBOL 68Bf

FORM 1473, 84 MAR 83 APR edition may be used until exhausted
All other editions are obsolete

SECURITY CLASSIFICATION OF THIS PAGE

Block 19 continued:

structure of the East Greenland Polar Front (EGPF) and associated mesoscale features were also examined. The EGPF was found to leave the Greenland continental slope north of 79°N and turn northeastward across the Yermak Plateau and into the Arctic basin. A cold core mesoscale eddy having a length scale of approximately 60 km and a closed baroclinic circulation up to 0.15 m/s was found associated with the front. Also associated with the front was extensive temperature and salinity finestructure which occurred near the maximum temperature in the water column. This finestructure was often associated with strong double diffusive activity.

Block 18 continued:

Marginal Ice Zone
Finestructure
East Greenland Polar Front
Yermak Plateau
Greenland Sea

Approved for public release; distribution is unlimited.

Mesoscale Variability in the West Spitsbergen Current and Adjacent Waters in Fram Strait

by

Alan M. Weigel
Lieutenant, United States Navy
B.S., United States Naval Academy, 1979

Submitted in partial fulfillment of the
requirements for the degree of

MASTER OF SCIENCE IN METEOROLOGY AND OCEANOGRAPHY

from the

NAVAL POSTGRADUATE SCHOOL
March 1987

ABSTRACT

A dense network of conductivity-temperature-depth (CTD) measurements was carried out between 76°N and 81°N in order to define the distribution of temperature and salinity in Fram Strait. Although weakly baroclinic, the WSC flow was found to be strongly influenced by the 2000 m deep Kipnovich Ridge which separated the flow into several streams. In addition, filaments of warm Atlantic Water (AW) were found to spread out over the top of the Greenland Gyre. The WSC branches near 80°N. Approximately 20% of the baroclinic transport enters the Arctic Ocean north of Spitsbergen as the eastern branch. The other branch (80% of the baroclinic transport) turns westward, apparently under the influence of the Yermak Plateau, and joins with the southward flowing East Greenland Current (EGC). The entire turning takes place south of 81°N near the ice edge with baroclinic speeds of up to 0.03 m/s. The structure of the East Greenland Polar Front (EGPF) and associated mesoscale features were also examined. The EGPF was found to leave the Greenland continental slope north of 79°N and turn northeastward across the Yermak Plateau and into the Arctic basin. A cold core mesoscale eddy having a length scale of approximately 60 km and a closed baroclinic circulation up to 0.15 m/s was found associated with the front. Also associated with the front was extensive temperature and salinity finestructure which occurred near the maximum temperature in the water column. This finestructure was often associated with strong double diffusive activity.

TABLE OF CONTENTS

I. INTRODUCTION 11
A. PURPOSE 11
B. BACKGROUND 12
C. BATHYMETRY 12
D. GENERAL CIRCULATION 15
E. WATER MASSES 20

II. METHODS AND MEASUREMENTS 25
A. CRUISE SUMMARY 25
B. DATA ACQUISTION 25
C. DATA REDUCTION AND ANALYSIS 27

III. TEMPERATURE-SALINITY DISTRIBUTION 29
A. INTRODUCTION 29
B. WEST SPITSBERGEN CURRENT 29
1. Water Mass Characteristics 29
2. East Branch 32
3. Westward Turning 34
C. HISTORICAL COMPARISONS 36
D. EAST GREENLAND CURRENT 42
1. Water Mass Characteristics 42
2. East Greenland Polar Front 44
3. Mesoscale Features 45
E. FINESTRUCTURE 46

IV. CIRCULATION AND TRANSPORT 63
A. INTRODUCTION 63
B. DYNAMIC HEIGHT 64
C. BAROCLINIC FLOW 68
D. CIRCULATION 70

V. CONCLUSIONS 83

LIST OF REFERENCES 85

INITIAL DISTRIBUTION LIST 90

LIST OF TABLES

1. A SUMMARY OF THE DEFINITIONS OF WATER MASSES FOUND IN FRAM STRAIT 22

LIST OF FIGURES

1.1 Bathymetric features of Fram Strait (from Hurdle, 1986, p. 699) 13

1.2 A chart showing the bathymetry of Fram Strait (from Bourke et al., 1986). Depths are in hundreds of meters 14

1.3 The general circulation and bathymetry of the Greenland Sea (from Paquette et al, 1985) 16

1.4 Temperature-salinity limits defining the basic water masses found in Fram Strait (from Greisman, 1976) 21

1.5 Temperature-salinity envelopes for the water mass regimes in Fram Strait (from Greisman, 1976) 23

2.1 NORTHWIND 1985 cruise track and location of CTD stations. The heavy dashed line shows the position of the ice edge 26

3.1 A chart showing the locations of transects made in Fram Strait. The dashed line is the location of the ice edge 30

3.2 A temperature/salinity plot for stations in the core of the WSC. Symbols are at 50 m intervals 32

3.3 Surface temperature (°C) distribution 37

3.4 Surface salinity distribution 38

3.5 The maximum temperature at each station 39

3.6 The temperature of the 28.0 sigma-t surface 40

3.7 The depth of the 28.0 sigma-t surface 41

3.8 A temperature-salinity plot of stations along 78°N in the vicinity of the EGPF 43

3.9 Stations exhibiting significant vertical structure. The solid line is the location of the EGPF and the dashed line is the ice edge. Other symbols are defined in the text 47

3.10 Temperature profiles for stations along 80°30′N 48

3.11 Salinity profiles for stations along 80°30′N 49

3.12 The Turner angle for Station 96 in the EGPF 52

3.13 Transect 1, along 78°N. The 2000 m feature between Stations 21 and 22 is the Kipnovich Ridge. The arrow at the top indicates the location of the ice edge 53

3.14 Transect 2 along 79°N. Note the effect of the Kipnovich Ridge between Stations 31 and 32 creating a wave-like structure in the isotherms and isohalines 54

3.15 Transect 3 along 79°30′N. The Kipnovich Ridge is very pronounced at this latitude. 55

3.16 Transect 5 along 80°N 56
3.17 Transect 4 along the top of the Yermak Plateau 57
3.18 Transect 6 north of Spitsbergen 58
3.19 Transect 7 along 81°N 59
3.20 Transect 8 along 80°30′N 60
3.21 Transect 9 along 2°E shows the core of westward turning as the 3° lens between Stations 36 and 99 61
3.22 Transect 10 along 2°W through the center of the eddy 62
4.1 Surface dynamic topography referenced to 150 decibars in dynamic centimeters 65
4.2 Surface dynamic topography referenced to 500 decibars in dynamic centimeters 66
4.3 150 decibar dynamic topography referenced to 500 decibars in dynamic centimeters 67
4.4 A plan view of Fram Strait summarizing the transport calculations. 71
4.5 A plot of the surface circulation suggested by the dynamic topography and geostrophic velocities 72
4.6 Section 1, along 78°N. Southward flow is indicated by postive isotachs spaced at 0.01 m/s intervals. 73
4.7 Section 2, along 79°N 74
4.8 Section 3, along 79°30′N 75
4.9 Section 4, along the top of the Yermak Plateau 76
4.10 Section 5, along 80°N 77
4.11 Section 6, extending northwestward from the Spitsbergen coast 78
4.12 Section 7, along 81°N 79
4.13 Section 8, along 80°30′N 80
4.14 Section 9, along 2°E, showing the core of the westward turning 81
4.15 Section 10 along 2°W, through the center of the eddy 82

ACKNOWLEDGEMENTS

Funding for the work described in this thesis was provided by the Arctic Submarine Laboratory, Naval Ocean Systems Center, San Diego, California under Work Order N-66001-86-WR00131.

I wish to thank Dr. R.G. Paquette for his careful reading of this thesis and for many of the computer programs which were used in it's preparation. M.D. Tunnicliffe also provided programs, programming assistance and helpful advice. The assistance of K.O. McCoy and Dr. J.L. Newton was instrumental in the data acquistion as was the assistance and enthusiasm of the crew of the USCGC NORTHWIND, especially the Marine Science Technicians and her Commanding Officer, Captain W. Caster.

The success of this thesis was due, in large measure, to the advice and guidance of Dr. R.H. Bourke. He continues to be a fine friend and shipmate and a source of inspiration to all who know him.

Finally, I wish to acknowledge the love and support of my wife, Diana. Without her numerous personal sacrifices and many hours of typing throughout the past year this thesis would never have been completed.

I. INTRODUCTION

A. PURPOSE

During September 1985 the USCGC NORTHWIND conducted an oceanographic measurement program, MIZLANT 85, in the northern Greenland Sea between Greenland and Spitsbergen. A relatively dense network of conductivity-temperature-depth profiler (CTD) stations provided extensive information on the circulation and water mass structure of the major oceanographic features in the region known as Fram Strait. MIZLANT 85 was the fourth in a series of hydrographic surveys under the sponsorship of the Arctic Submarine Laboratory designed to investigate the oceanographic characteristics of the Greenland Sea north of 75°N. This thesis is an analysis of the data set acquired during the 1985 cruise.

The overall objective of the cruise was to quantify the physical oceanographic properties of the northern Greenland Sea waters and to define the oceanographic processes responsible for property distributions and their variability. Specific objectives of the measurement program included: (1) study of the westward turning of the warm, saline West Spitsbergen Current (WSC) and its interaction with the cold, fresh southward flowing East Greenland Current (EGC); (2) measurement of the temperature and salinity distribution across Fram Strait in at least two locations to define the water mass characteristics and structure of water entering and exiting the Arctic Ocean; (3) assessment of the bathymetric effects of the shallow Yermak Plateau on the flow of warm Atlantic Water (AW) into Fram Strait and the Arctic Ocean; and (4) study of the dynamic characteristics of the East Greenland Polar Front (EGPF), a sharp boundary between the EGC and the warmer water of the Greenland Sea, north of 79°N. A secondary objective was the assessment of the circulation in the area of the Molloy Deep, a 5500 m depression located near 79° 10′ N, 003°E where a large cyclonic eddy has frequently been observed. To a large extent, all these objectives were met.

The objectives of the CTD data analysis presented in this thesis will be to: (1) infer the water masses of Fram Strait using temperature-salinity transects; (2) describe the baroclinic circulation and transport in Fram Strait using contours of the geostrophic current velocity field; (3) describe the role of bathymetric steering on the

baroclinic circulation in Fram Strait; and (4) assess the characteristics and formation processes of mesoscale eddies and temperature-salinity finestructure usually found in or near the EGPF.

B. BACKGROUND

Fram Strait is the major connection for the transfer of heat, mass, and momentum between the Arctic and Atlantic Oceans. Aagaard and Greisman (1975) have shown that the WSC provides the major inflow of mass, salt, and thermal energy into the Arctic Basin. Aagaard and Coachman (1968a) have shown that the EGC is the major outlet for Arctic Ocean surface water into the Atlantic Ocean.

Carmack (1972) cites the work of Zordrager, in 1723, as the earliest known description of the Greenland Sea. The first modern description of the physical oceanography of the region was done by Helland-Hansen and Nansen (1909) who described the Greenland and Norwegian Seas gyres. Killerich (1945) discussed the hydrography and circulation of the Greenland Sea based on data acquired from 1891 to 1933. Other reviews have been conducted by Lee (1963), Trangeled (1974), Carmack (1972) and Coachman and Aagaard (1974)

Aagaard and Coachman (1968a) provided a comprehensive review of the studies of the EGC and the waters of the Greenland Sea. More recently Paquette et al. (1985), Tunnicliffe (1985), and Bourke et al. (in press, a) have studied the characteristics of the EGC and the Polar Front, while Greisman (1976) and Hanzlick (1983) have done in-depth studies of the characteristics of the WSC.

C. BATHYMETRY

Fig. 1.1 shows the geographic setting and major bathymetric features of the northern Greenland Sea. The bathymetry of the region is characterized by deep basins separated by submarine ridges; glaciated continental shelves form the lateral boundaries. A detailed bathymetry of Fram Strait is shown in Fig. 1.2. Perry (1986) provides a comprehensive discussion of the bathymetry of the Greenland Sea; only the salient features will be summarized here.

The bathymetry of the continental shelf and slope in Fram Strait is based on limited soundings by ships with ice-strengthend hulls because the area is ice covered most of the year. The East Greenland continental shelf is a region of shallow banks and local depressions with large troughs extending seaward from the shore line. The continental slope has an average relief of approximately 1:10 and varies in depth from

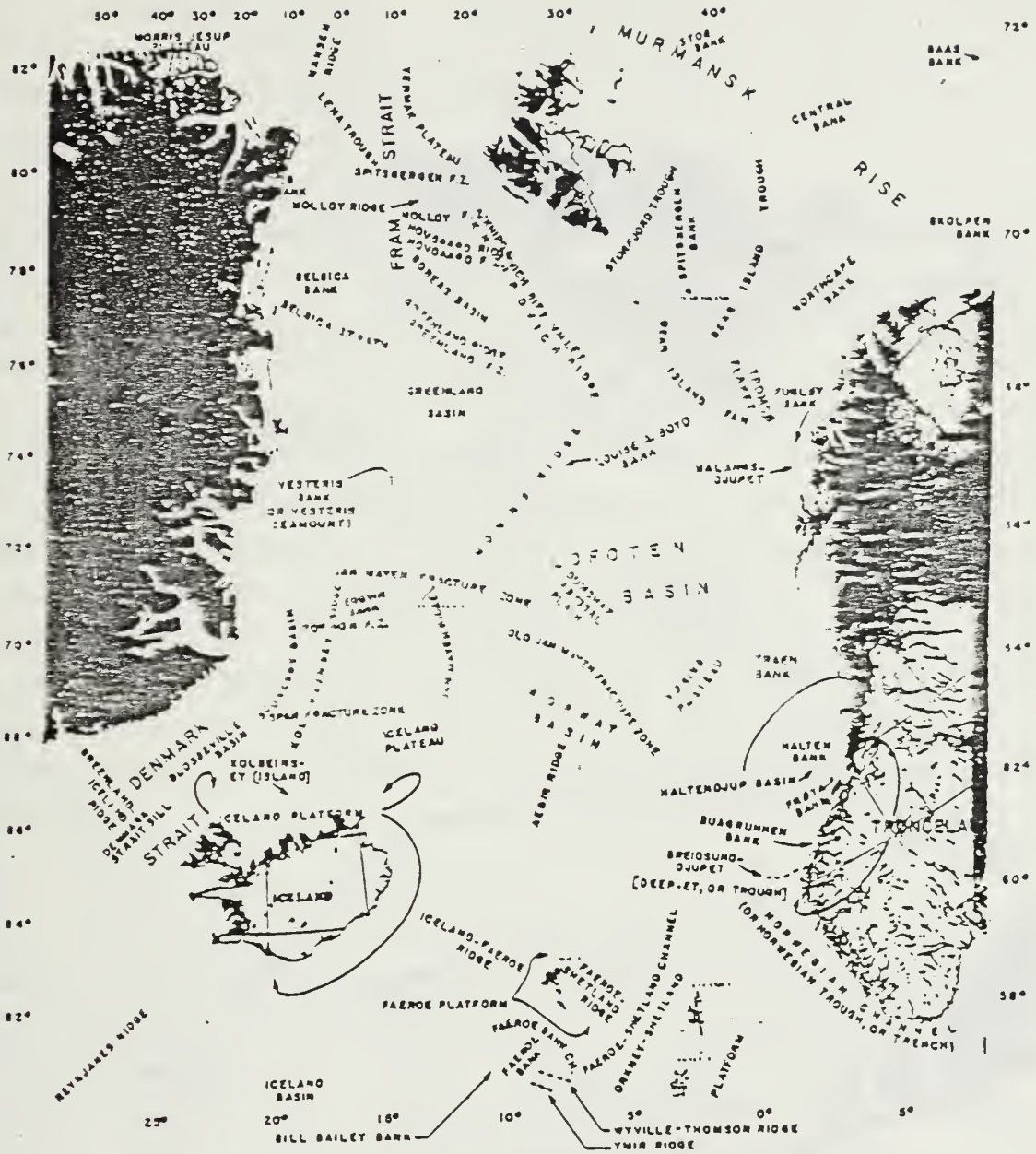

Figure 1.1 Bathymetric features of Fram Strait (from Hurdle, 1986, p. 699).

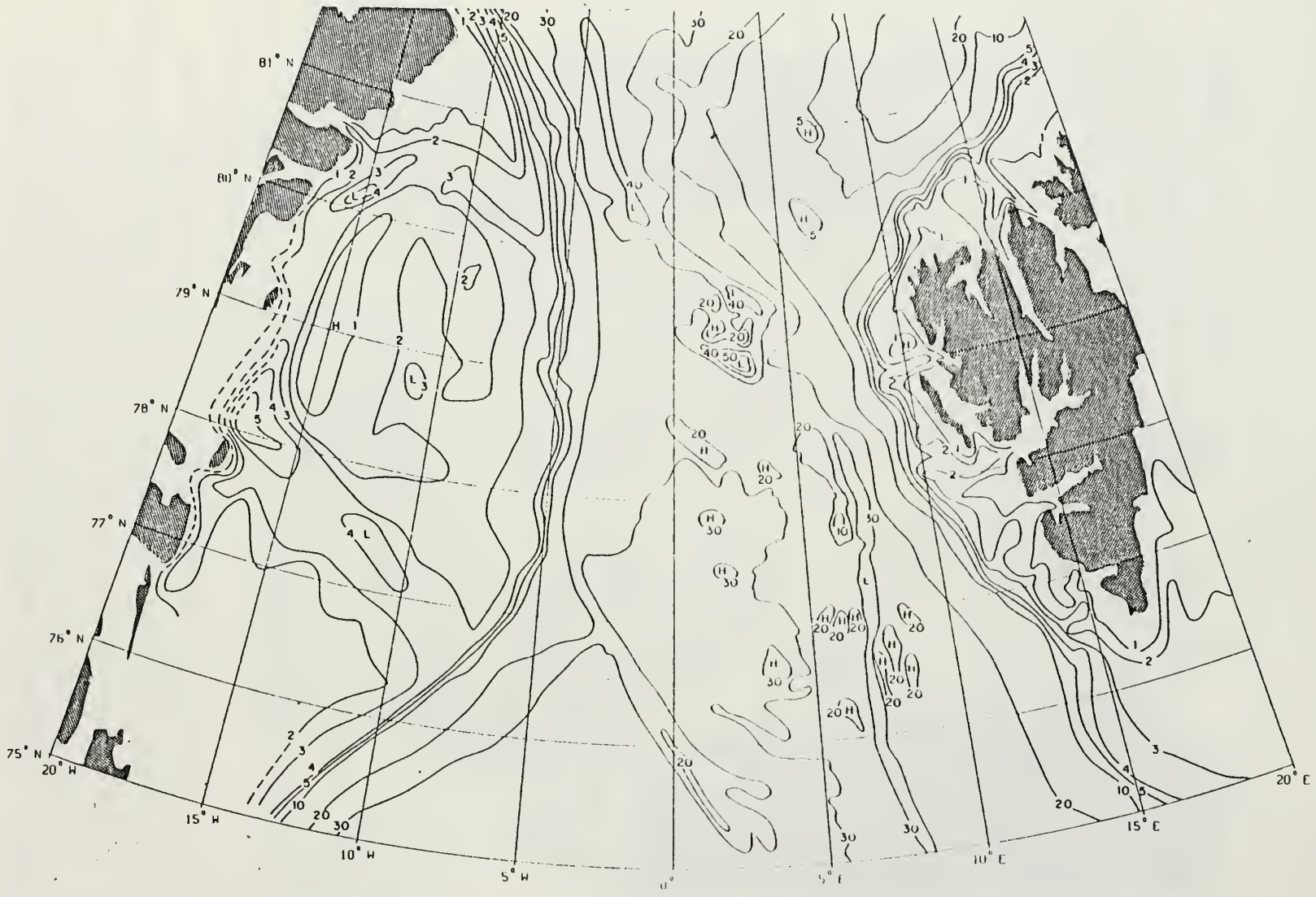

Figure 1.2 A chart showing the bathymetry of Fram Strait (from Bourke et al., 1986). Depths are in hundreds of meters.

400 to 3400 m (Perry, 1986, p.219). The Yermak Plateau, on the eastern side of Fram Strait, is an extension of the Barents Sea continental slope projecting into the Arctic Ocean (Perry, 1986, p. 219) The shallowest depth measured on a ridge topping the plateau is 425 m. The western slope of the plateau drops to the floor of the Lena Trough and the Spitsbergen Fracture Zone, a northwest-southeast tending trough with a maximum depth of 4532 m.

The Boreas Basin is a small abyssal plain lying in the southern end of Fram Strait. The basin is bordered on the east by the Knipovich Ridge, an extension of the Mid-Atlantic Ridge system. The ridge is characterized by widely spaced groups of seamounts, most of which are between 900 and 1600 m deep. A rift valley 3200 to 3400 m deep lies along the length of the ridge.

To the north of the Boreas Basin is the Greenland-Spitsbergen sill. Perry (1986, p. 232) describes this feature as a "damlike" structure with a maximum depth of 2650 m. The sill may limit the exchange of deep bottom water between the Greenland Sea and the Arctic Ocean although Aagaard et al. (1985) present evidence for exchange through Fram Strait of intermediate-depth waters above the sill. The southern part of the sill contains the Hovgaard and Molloy Fracture Zones. The Hovgaard Fracture zone consists of a 2600 m deep trough between two ridges which shoal to an average depth of 1250 m. The Molloy Fracture Zone contains an elliptical depression, the 5570 m Molloy Deep, and is ringed to the north by three 1500 m deep seamounts named the Molloy Ridge.

D. GENERAL CIRCULATION

Helland-Hansen and Nansen (1909) first defined the cyclonic surface circulation of the Greenland Sea. The Greenland Gyre is centered on the prime meridian between 74°-76°N (Fig. 1.3). The northward flowing WSC forms the eastern boundary of the gyre while the southward flowing EGC forms the western boundary. The eastward zonal flow known as the Jan Mayen Polar Current closes the circulation to the south and the westward turning of the WSC into the EGC closes the circulation to the north in a flow known as the Return Atlantic Current (RAC) (Paquette et al.,1985).

The WSC is formed when warm, saline water from the North Atlantic enters the Norwegian Sea and flows northward along the continental slope as the Norwegian Atlantic Current. Off the southern tip of Spitsbergen near 74°N it mixes with colder, fresher water from the Jan Mayen Polar Current and the East Spitsbergen Current and

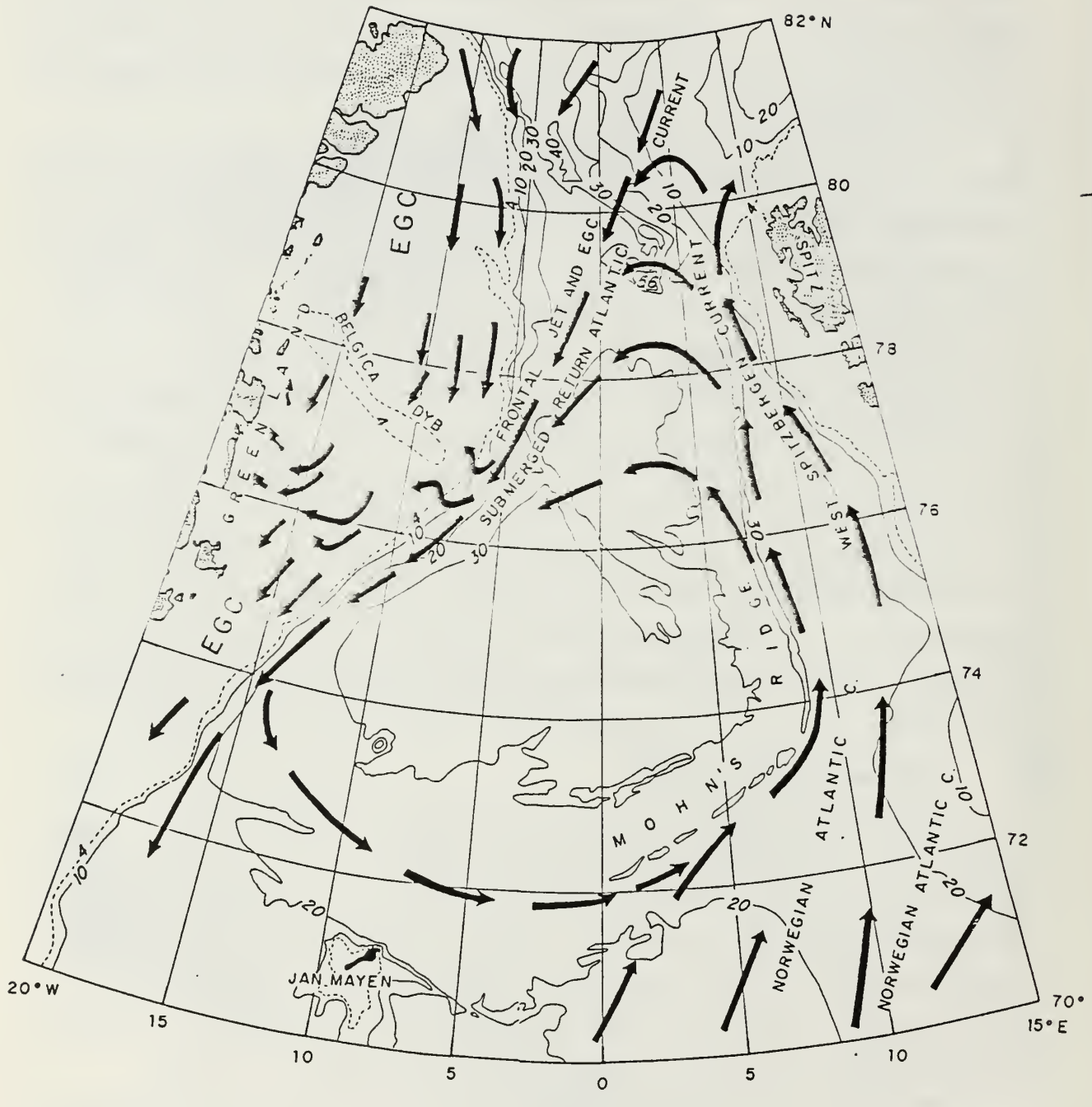

Figure 1.3 The general circulation and bathymetry of the Greenland Sea (from Paquette et al, 1985).

continues flowing north along the west coast of Spitsbergen. Along the continental slope the flow is deep, extending to about 800 m (Hanzlick, 1983, p. 7). North of about 75°N it loses heat and is diluted as it spreads out in a thin layer over the top of the Greenland Gyre. Near 80°N one branch of the current turns northeastward (Aagaard and Foldvik, 1985), sinking to about 200 m depth as it passes under the ice edge, and eventually enters the Arctic Basin (Johannessen et al., 1983) This branch of the current is the principal supply for the warm Atlantic layer observed throughout the Arctic Ocean (Aagaard et al., 1985b). The second branch of the current turns westward and mixes with the southward flowing EGC as the RAC. The RAC forms the eastern boundary of the EGPF.

Hanzlick (1983) summarized the transport calculations of earlier investigators. Based on hydrographic data from 1933 to 1960, as gleaned from various sources (Hill and Lee, 1957; Kislyakov, 1960; and Timofeyev, 1962), the mean baroclinic transport across the WSC was estimated to be 3 to 4 Sv[1] northward. Greisman (1976) estimated the mean total transport, using long-term direct current measurements, obtained during 1971-72, as about 7 Sv northward, with a 10.7 Sv maximum in September and a 3 Sv minimum in February. Using hydrographic data Greisman estimated the mean baroclinic transport to be 3.5 Sv, or about one-half of the total. During 1976-77 Hanzlick (1983) estimated a mean transport of 5.6 Sv from current meter data, with a maximum in the fall and a minimum in the spring. The mean baroclinic transport for the same period was only 1 Sv.

The WSC is rich in temporal and spatial variability. Greisman (1976) and Hanzlick (1983) have shown that both volume flow and core temperatures of the WSC are variable over time scales that range from days to years. For example, Hanzlick (1983) showed evidence, based largely on hydrographic data, that the interannual variability in the volume and heat transport was on the order of 50%. He also presented data showing that for 1976-77 the volume transport ranged from 1.4 Sv southward to 11.9 Sv northward, while the core temperature of the WSC ranged from a maximum of 6°C to a minimum of -1°C. There is also evidence to suggest that there is significant short term variability in the WSC flow. Hill and Lee (1957) reported baroclinic transports west of Bear Island which changed from 0.1 Sv southward to 1.0 northward within 48 hours. Direct current measurements made in Fram Strait during 1984-85 (Aagaard et al., 1985a) showed a northward flow in the core of the WSC in

[1] $10^6\ m^3 s^{-1}$

excess of 0.4 m/s in the latter half of August 1984. By the first week in September 1984 the flow had reversed, with southward speeds of approximately 0.05 m/s being observed. An important conclusion which arises from these various data sets is that the changes between successive yearly surveys may in fact be due to short term variability and are not true interannual changes.

Various investigators have also shown evidence of spatial variation in the WSC flow and temperature. Dickson (1972) discussed the spatial variability of the Norwegian Atlantic Current. This variation takes the form of banded structures or northward flowing filaments. The spatial variability of the WSC is probably an extension of this structure. Hanzlick (1985, p. 23) suggested that the scale of the lateral structures is about 15 km.

The mean wind stress over the Greenland-Norwegian sea region is apparently the major factor affecting the interannual and shorter time scale variability of the WSC (Greisman, 1976; Hanzlick, 1983). Aagaard (1970) computed the wind-driven transport in the Greenland Sea for 1965 and found a circulation which quantitatively resembled the known circulation. Greisman and Aagaard (1979) suggested that the WSC is driven by large scale variations in the atmospheric forcing over the Greenland and Norwegian Seas on time scales of less than one month and that there was considerable month to month variation in the forcing. Hanzlick (1983) suggested that baroclinic instability and coastally trapped waves were also possible contributors to shorter time scale variability. Greisman (1976) showed that the WSC also has a strong tidal component.

The cold, fresh EGC together with the warmer, saltier RAC form the western branch of the Greenland Gyre. The ECG originates in the Arctic Ocean and carries Arctic surface water and ice southward, through Fram Strait and over the East Greenland continental shelf. The eastern boundary of the EGC is tied to the shelf break south of 79°N and is separated from the RAC by the EGPF, a zone exhibiting sharp horizontal gradients of water properties. On the eastern side of the front the RAC has a width of approximately 100 km and is submerged under the EGPF to depths of 50-300 m (Paquette et al., 1985). Paquette et al. (1985) and Bourke et al. (in press, a) found a high speed jet associated with the EGPF, with baroclinic speeds as high as 0.96 m/s, but more typically 0.40 to 0.60 m/s.

Aagaard and Coachman (1968b) computed a volume transport of 35 Sv for the EGC based on current meter measurements made from the ice island ARLIS II and by

the EDISTO in 1965. More recent observations, however, do not support this estimate. Paquette et al. (1985) estimated the baroclinic transport in 1981 to be approximately 2 Sv. Bourke et al. (in press, a) found the baroclinic transport of the EGC in 1984 to be approximately 1 Sv. Current meter measurements taken by Muench et al. (1986) suggest that the total transport may be twice the baroclinic component, rather than the order of magnitude suggested by Aagaard and Coachman (1968b).

The EGC also shows considerable spatial and temporal variation. Aagaard and Coachman (1968a) have shown that the position of the EGPF, which they define by the location of the 0°C isotherm at 50 m, can vary up to 100 km in several days, most probably a result of wind forcing. As the surface manifestation of the front moves, the RAC may be overrun by the colder water of the EGC (Perdue, 1982). Associated with the front are mesoscale ice-ocean meanders and eddies. These eddies have been studied extensively by Wadhams and Squire (1983), Johannessen et al. (1983), Paquette et al. (1985), Bourke et al. (in press, b) and others. Of particular interest is a quasi-stationary cyclonic eddy occuring at about 79° 10'N, 001°E, which appears to be associated with the complex bathymetry near the Molloy Deep. Various theories have been suggested concerning the generation of these eddies including baroclinic instability (Griffiths and Linden, 1981), barotropic instability (Johannessen et al., 1983), topographic interaction (Smith et al., 1984), differential Ekman pumping along the ice edge (Hakkinen, 1986) and advection of open ocean eddies into the Greenland Sea (Davidson et al., 1986).

Another important mesoscale feature found along the EGPF is temperature and salinity finestructure. These features consist mainly of an interleaving of the warm water of the RAC with the colder water of the EGC. Paquette et al. (1985) found alternating lenses of warm and cool water with peak-to-peak temperature differences of 0.5°C to 1.0°C at depths between 75 and 300 m. They suggest that the average length of these lenses is 27 km. Tunnicliffe (1985) found similar structures in his data with peak-to-peak variations up to 3.5°C. Paquette et al. (1985) proposed that these structures form when warm water east of the EGPF descends along isopycnal surfaces from at or near the surface. They also proposed that these finestructure elements dissipate through double diffusive processes.

E. WATER MASSES

For an area so dynamically active and so well studied, it is not suprising that Swift and Aagaard report "the water mass terminology for the entire area is rich and often confusing." (1981, p. 1110) The basic water masses of the EGC and the WSC have been defined by Coachman and Aagaard (1974) and while their definitions have been accepted by much of the succeding literature, the definitions have also been successively modified. Fig. 1.4 shows the basic water masses, which will also be adopted for this thesis, as well as the modifications proposed by other authors. Table 1 summarizes the temperature and salinity limits for the various water masses.

The temperature-salinity envelopes for the water mass regimes found in Fram Strait are portrayed in Fig. 1.5. Two water masses are found in the WSC. Atlantic Water (AW) extends from the surface to about 800 m and is warmer than 0°C. Surface temperatures in summer may be higher than 6°C, while during the winter the surface temperatures are typically warmer than 2°C keeping the west coast of Spitsbergen ice free. The salinity of the AW increases in the upper 100 m so that at the core of the WSC the salinity may be greater than 35.2.[2] Below 100 m the salinity decreases to about 34.95. Warm water, properly called AW, can also be found with salinities as low as 34.7. This low salinity fraction of AW is primarily a surface phenomenon and is the result of dilution by ice melt. This area of low salinity is generally found near the ice edge or in more southerly areas where ice melt water has been advected. Beneath the AW is found Greenland Sea Deep Water (GSDW). This water mass forms a large dome at the center of the Greenland Gyre with temperatures colder than 0°C and salinity between 34.87 and 34.95. Carmack (1972) proposed that GSDW was formed by convective subsurface modification of AW. Carmack and Aagaard (1973) and Aagaard et al. (1985b) suggest that chimney formation and double-diffusive mixing between PW and AW may also be involved with the production of GSDW.

PW is generated in the Arctic Ocean, but over the Greenland shelf is modified by local processes such as ice melt and mixing (Bourke et al., in press, a). Thus, the water masses of the EGC are similar to those of the Arctic Ocean. Polar Water, colder than 0°C, extends from the surface to below 150 m. In summer the effects of insolation create a temperature minimum at a depth of about 50 m. The surface salinity may be

---

[2]Salinity will be reported in the practical salinity scale (gm/kg) as dimensionless quantities (UNESCO, 1981)

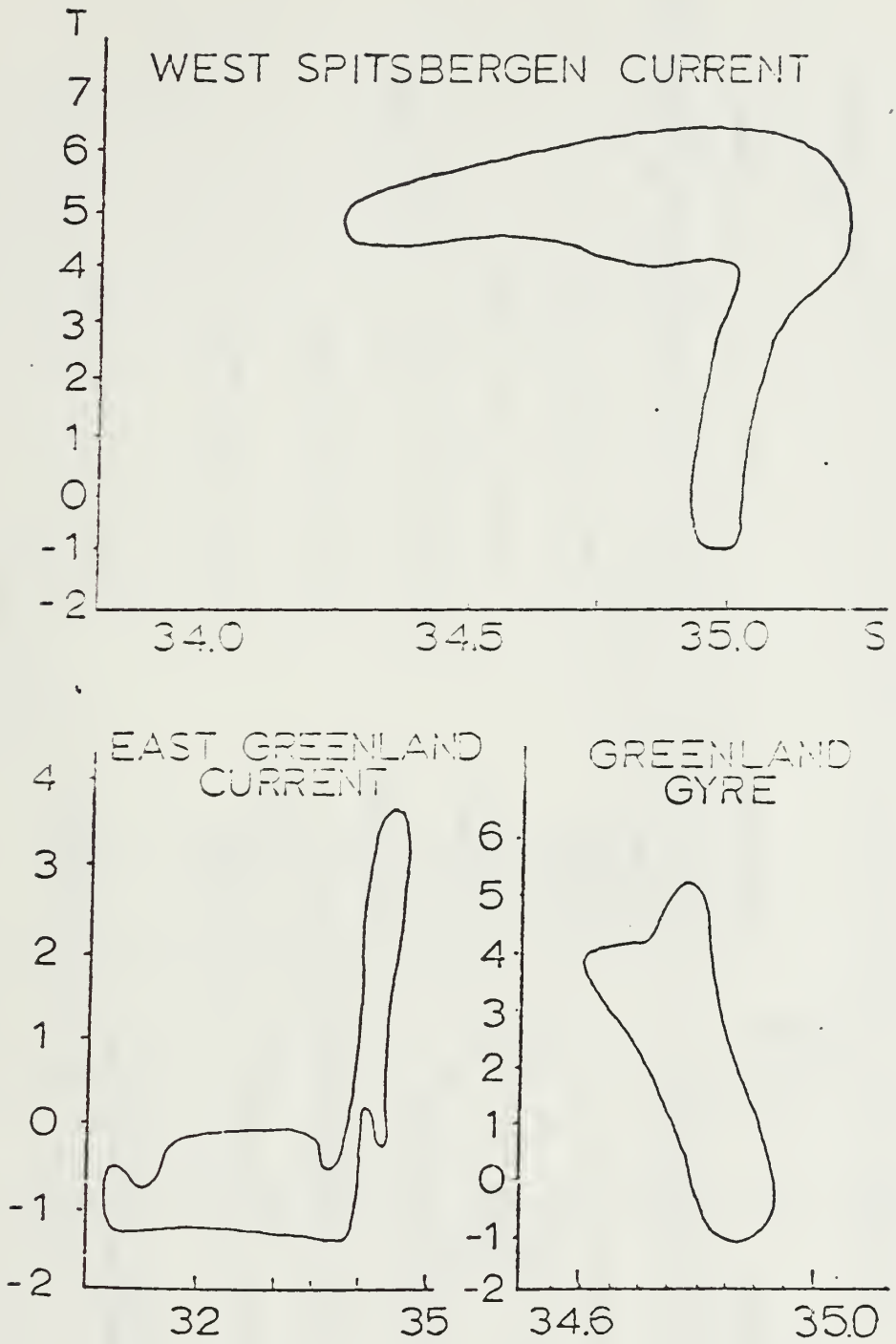

Figure 1.4 Temperature-salinity limits defining the basic water masses found in Fram Strait (from Greisman, 1976).

TABLE 1

A SUMMARY OF THE DEFINITIONS OF WATER MASSES FOUND IN FRAM STRAIT

WATER MASS	PROPERTY LIMITS	REFERENCE	REMARKS
Surface Waters			
Atlantic Water (AW)	T: >0°C S: 34.9-35.2 D: <800 m	Coachman and Aagaard (1974)	Swift and Aagard (1981) define AW as > 3°C
Polar Water (PW)	T: <0°C S: <34.4 D: <150 m	Aagaard and Coachman (1968a)	
Atlantic Intermediate Water (AIW)	T: >0°C S: 34.4-34.9 D: 150-800 m	Aagaard and Coachman (1968a)	
Arctic Surface Water (ASW)	T: >0°C S: 34.4-34.7 D: above UAIW	Swift and Aagaard (1981)	Alternate limits: T>2°C if S 34.7-34.9
Upper Arctic Intermediate Water (UAIW)	T: <2°C S: 34.7-34.9 D: above LAIW	Swift and Aagaard (1981)	
Lower Arctic Intermediate Water (LAIW)	T: 0-3°C S: >34.9 D: <800 m	Swift and Aagard (1981)	
Deep Waters			
Greenland Sea Deep Water (GSDW)	T: <0°C S: 34.87-34.95 D: >800 m	Aagaard and Coachman (1968a)	

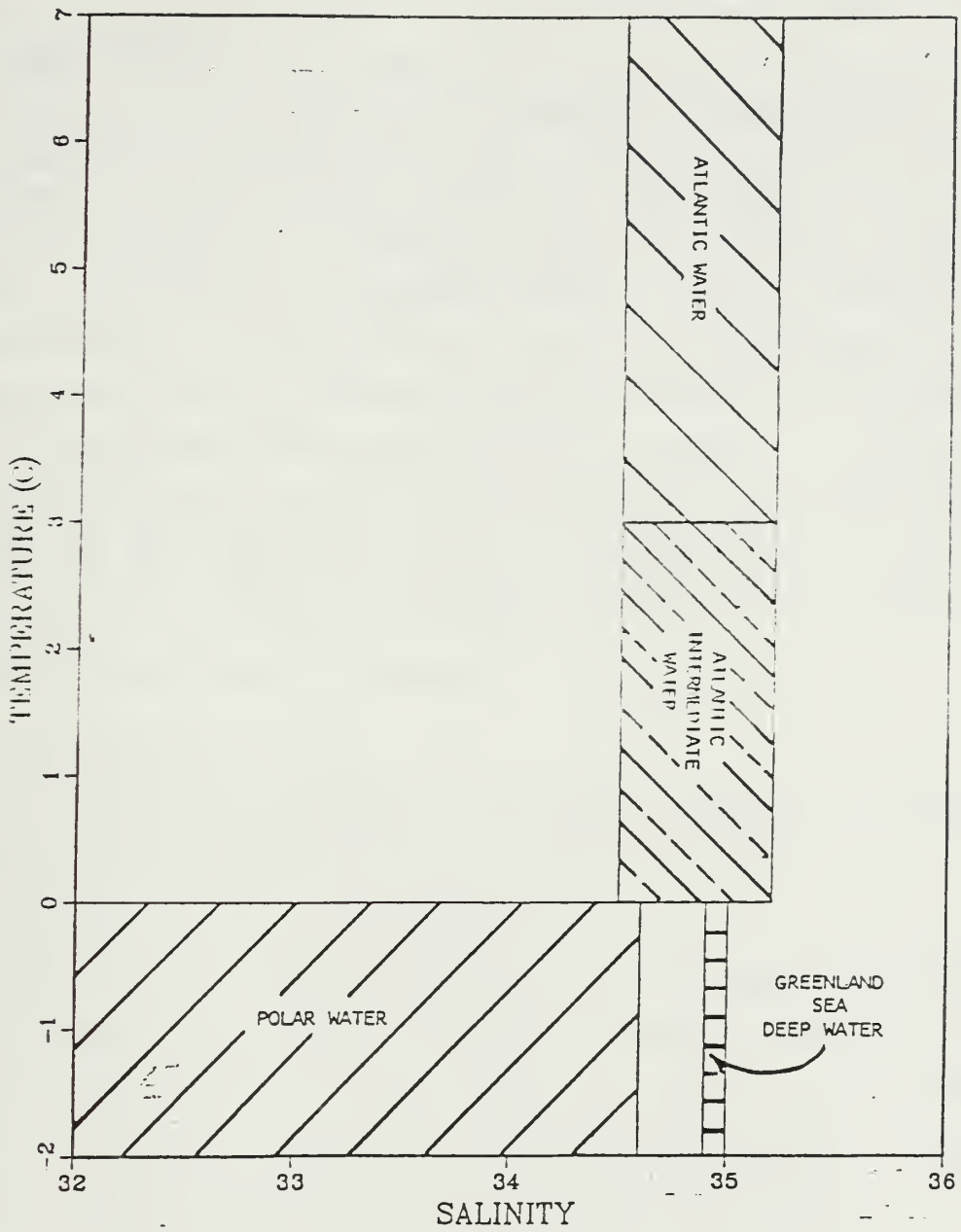

Figure 1.5 Temperature-salinity envelopes for the water mass regimes in Fram Strait (from Greisman, 1976).

less than 30 but increases rapidly to 34 at the bottom of the PW layer. In winter wind and convective mixing causes the temperature to be uniformly near freezing to about 75 m, often to depths exceeding 100 m.

Atlantic Intermediate Water (AIW) is found below the PW to approximately 800 m. The temperature of this water mass is greater than 0°C with a temperature maximum occuring between 200 and 400 m. Although the upper limit of temperature is set at 3°C, warmer water definable as AW may be found in the RAC in summer and may be seen to cool continuously with distance to below 3°C. Hence, so far as the mechanisms of the RAC are concerned, the 3°C limit is arbitrary. The salinity increases from 34 at the base of the PW to between 34.88 and 35.00 at about 400 m, remaining nearly constant below that depth. AIW has its origin in the warm WSC. In part, AIW may be advected from the Arctic Ocean into the RAC. It may also be formed from AW by processes of surficial cooling, limited mixing with PW and exchange of heat with PW by double diffusion (Paquette et al., 1985). Just as for the WSC, GSDW is found below the EGC at depths greater than 800 m, with temperatures below 0°C and salinities between 34.87 and 34.95.

II. METHODS AND MEASUREMENTS

A. CRUISE SUMMARY

Between 1 and 26 September 1985, the USCGC NORTHWIND conducted a series of closely spaced (approximately 10 km) CTD stations between Greenland and Spitsbergen in the region known as Fram Strait. NORTHWIND covered over 1270 km while conducting 156 CTD stations in Fram Strait and in the area north of Svalbard. NORTHWIND's two embarked helicopters were used extensivly in an ice reconnaissance role. Forty sorties were flown for a total of 80 flight hours. The cruise track and location of CTD stations are indicated in Figure 2.1. The limit of the ice edge, defined by ice concentration greater than 0.1, is shown in Fig. 2.1 as a heavy dashed line. The ice edge position was determined by observation from the ship and helicopter, therefore the line shown in Fig. 2.1 is a quasi-synoptic depiction of the ice edge for the 26 days of the cruise. The intent is to show the limit of the significant ice cover; there were areas encountered outside the depicted edge where ice had accumulated in narrow bands or where grease ice had formed.

B. DATA ACQUISTION

The instrumentation and methods used for data acquistion and reduction have been previously described in detail by Perdue (1982) and Tunnicliffe (1985). Thus, only a brief description of the procedures will be given here.

The primary oceanographic instrument was the Neil Brown Instrument Systems (NBIS) Mark III CTD. Data were acquired, stored, and displayed using a Hewlett-Packard 9835A computer and a 9872A flat-bed X-Y plotter. Additionally, the 10 kHz modulated signal from the CTD was recorded for back-up on a Sony audio tape recorder. As in the past, a wire cage was constructed around the base of the CTD to protect the sensors from damage by ice. As discussed by Paquette et al. (1985), no apparent deviation in sensor accuracy has been noted using this technique.

Prior to lowering the instrument for a cast, it was flushed by lowering and hoisting it over a depth range of at least 50 m to minimize temperature errors caused by stored heat in the body of the instrument. Perdue (1982) noted difficulties with water freezing in the sensors between casts when the air temperature dropped below -1.8°C. This was only a minor problem as the air temperature remained above freezing

Figure 2.1 NORTHWIND 1985 cruise track and location of CTD stations. The heavy dashed line shows the position of the ice edge.

during most of the cruise. When the problem did occur, the flush of the instrument to 50 m was sufficient to melt any ice crystals that may have formed.

Bourke et al. (1986) discuss the pre- and post-cruise calibration of the temperature and conductivity sensors. The calibrated 3200 dbar pressure sensor installed at NPS failed early in the cruise, at Station 18, and was replaced with the 1600 dbar sensor. This reduced-depth capability had no impact on the cruise as no casts were conducted below 1200 m.

Standardization of the instrument was by means of a reversing bottle clamped to the line approximately 1 m above the sensors. The resulting samples were analyzed with a portable induction salinometer referenced to standard water. The average differences between the instruments and the standards were approximately 0.01°C in temperature and 0.01 in salinity, not notably greater than the probable error in the reversing thermometer and the deck salinometer measurements.

The primary navigation aid was the ship's Magnavox MX 1107 Satellite Navigation System. The combination of high latitude and polar orbiting navigation satellites provided an average of three fixes per hour with a mean accuracy of approximately 0.5 km.

C. DATA REDUCTION AND ANALYSIS

Single spurious data points, or spikes, were occasionally noted in the CTD data as temperature and salinity profiles were generated on the X-Y plotter. The causes of these spikes are thought to be due to a combination of plankton or ice particles passing through the conductivity cell, power surges, slip ring noise, or instrument noise (Tunnicliffe, 1985). Upon completion of the cruise the data were transferred to 9-track tape for further processing with the NPS IBM 3033 computer. The data were then edited to remove these spikes and to remove mis-sequenced data points caused by the roll of the ship during a cast. The temperature and salinity were then corrected for dynamic response errors as described by Bourke et al. (1986). In addition, the CTD fast-response thermistor experienced intermittent failure throughout the cruise causing voltage fluctions which overflowed into the depth and conductivity circuitry. This resulted in abnormal spiking which was removed during the editing process (Bourke et al., 1986).

The HP 9835B computer was programmed to sample three times per second providing a vertical resolution of approximately three data points per meter of depth.

The profiles were sub-sampled every 5 m and the resulting subset used to produce vertical baroclinic velocity profiles and volume transport estimates.

Surface dynamic heights, based on the geostrophic approximation, were calculated with reference to the 500 dbar level. This level was chosen primarily to allow comparison with earlier work (for example, Paquette et al., 1985; Bourke et al., in press, a). Additionally, Tunnicliffe (1985, p. 98) showed that there was a seven-fold reduction in the resulting current when the dynamic topography was computed at 150 dbar referenced to 500 dbar, indicating that a large fraction of the flow occurs above 150 dbar. Therefore, neglecting data below 500 dbar probably introduces little error in dynamic height and baroclinic transport calculations.

In areas where the bottom was shallower than the selected reference level the isosteres from the nearest deep-water station were projected horizontally into the sea bottom using the technique of Helland-Hansen (1934). This method assumes that the gradient current velocity and, thus, the horizontal pressure gradient at the bottom are zero (Fomin, 1964, p. 153). This method gives identical velocities for the extrapolated depths. However, the regions of greatest velocity are over deep water and not subject to uncertainty from this procedure (Paquette et al., 1985)

The baroclinic velocity cross sections and volume transports were also referenced to 500 dbar, with the Helland-Hansen (1934) technique applied when appropriate. The transports were calculated with a 5 m vertical spacing using a vertical trapizoidal integration of the baroclinic velocity between each pair of stations.

III. TEMPERATURE-SALINITY DISTRIBUTION

A. INTRODUCTION

The distribution of water mass properties in Fram Strait will be described using temperature-salinity (T/S) plots and vertical cross sections, or transects, of temperature and salinity. Ten transects were made in Fram Strait (Figure 3.1); these are shown at the end of this chapter. They will be used to trace the WSC and its interaction with bathymetry, the ice edge, and the EGC. The transects are numbered consecutively from south to north and from east to west, although this does not necessarily reflect the order in which they were made. The transects were made between 6 and 26 September 1985 and with the exception of three were completed in a synoptic time frame ranging from 12 to 96 hours. The three exceptions were constructed by joining adjacent sections.

B. WEST SPITSBERGEN CURRENT

1. Water Mass Characteristics

Figure 3.2 is a T/S plot of ten stations taken along the west coast of Spitsbergen. These stations show warm, saline AW overlaying colder GSDW. The ten stations in Figure 3.2 were taken from a 50 km wide band between 78°N and 82°N. Close agreement in water properties exists between the stations in this region, showing the surface and bottom layers to be composed of two relatively uniform water masses. A temperature maximum occurs in the AW between 30 and 50 m at all stations except Station 22. Station 22 shows instead, an isothermal layer, characteristic of well mixed surface layers in more temperate latitudes. The temperature maximum ranges from slightly warmer than 5°C (5.04°C at Station 118) to almost 6.3°C at Station 26. The salinity at the temperature maximum has a narrow range, from 34.97 to 35.12. A much wider range of salinity is found in the surface layer (34.61 to 35.12). However, below the 3°C isotherm the salinity range is much smaller in this transition region from the surface AW to the more nearly isohaline GSDW. As previously discussed, the lower temperature limit for AW was earlier taken to be 0°C, but more recently was modified by Swift and Aagaard (1981) who define its lower limit as the 3°C isotherm. In the following transects the AW core of the WSC will be traced with the 3°C isotherm, in order to distinguish AW from colder (< 3°C) AIW. The lower salinity

Figure 3.1 A chart showing the locations of transects made in Fram Strait. The dashed line is the location of the ice edge.

limit for AW was earlier defined as 34.9 which is also the upper limit for AIW. To further distinguish it from AIWin the following transects AW will also be traced using water more saline than 35.0.

Transects 1, 2, and 3 show the structure of the northward flow of the WSC along the west coast of Spitsbergen. In Transect 1 (Fig. 3.13), along 78°N, the AW can be seen as a wedge-shaped core along the coast, extending seaward to a distance of 60 km (near Station 22) and to a depth of almost 275 m near the coast. Associated with the warm wedge is a core of saline (> 35.1) water between 50 and 100 m. Seaward of the wedge the warm water spreads out, for almost 200 km, into a surface layer 50-75 m deep. The saline water defined by the 35 isohaline is also found as a tongue spreading out almost halfway across Fram Strait, but generally deeper than the 3°C isotherm, at 100 to 400 m. At the western end of the wedge the surface salinity decreases to less than 34.9 as the AW mixes with PW and becomes diluted. Farther northward Transect 2 (Fig. 3.14), along 79°N, shows the 3°C AW wedge to be wider (140 km) and shallower (210 m), with the 35.1 isohaline still found in the core of the wedge between 50 and 100 m. Seaward of the wedge the surface layer is still present, but it is thicker and narrower with a second stream of 35.1 salinity water found at Station 31. The 35 isohaline tongue is again found to extend almost halfway across Fram Strait, with a large portion below the 3°C isotherm. Along the coast the isotherms slope upward, in contrast to Transect 1 where they slope downward. In Transect 3 (Fig. 3.15), along 79°30'N, the warm wedge extends seaward 100 km and the isotherms again slope downward along the coast to a depth of 360 km. A single 35.1 saline core is found at Station 119. In both Transects 2 and 3 a "tongue" of warm water extends under an "eddy-like" surface feature. In Transect 2 this feature is located between Stations 127 and 123; in Transect 3 it is located between Stations 132 and 136. The characteristics of this feature will be discussed in more detail later.

The distribution of AW in Transects 1, 2, and 3 appears to be controlled, at least in part, by bathymetry. In Transect 1, the isotherms and isohalines appear to be pushed up by the 2000 m isobath defining the Kipnovich Ridge. The core of the WSC is located to the west of the shelf break, while the largest part of the 35.0 isohaline tongue is located over the western slope of the ridge. In Transects 2 and 3 the isotherms and isohalines also appear to be pushed up by the ridge, with a warm saline stream located over the shelf break. In each of these transects the western slope of the ridge appears to control the western limit of AW, with the steeper bathymetry in Fig. 3.14 and 3.15 exerting a larger influence.

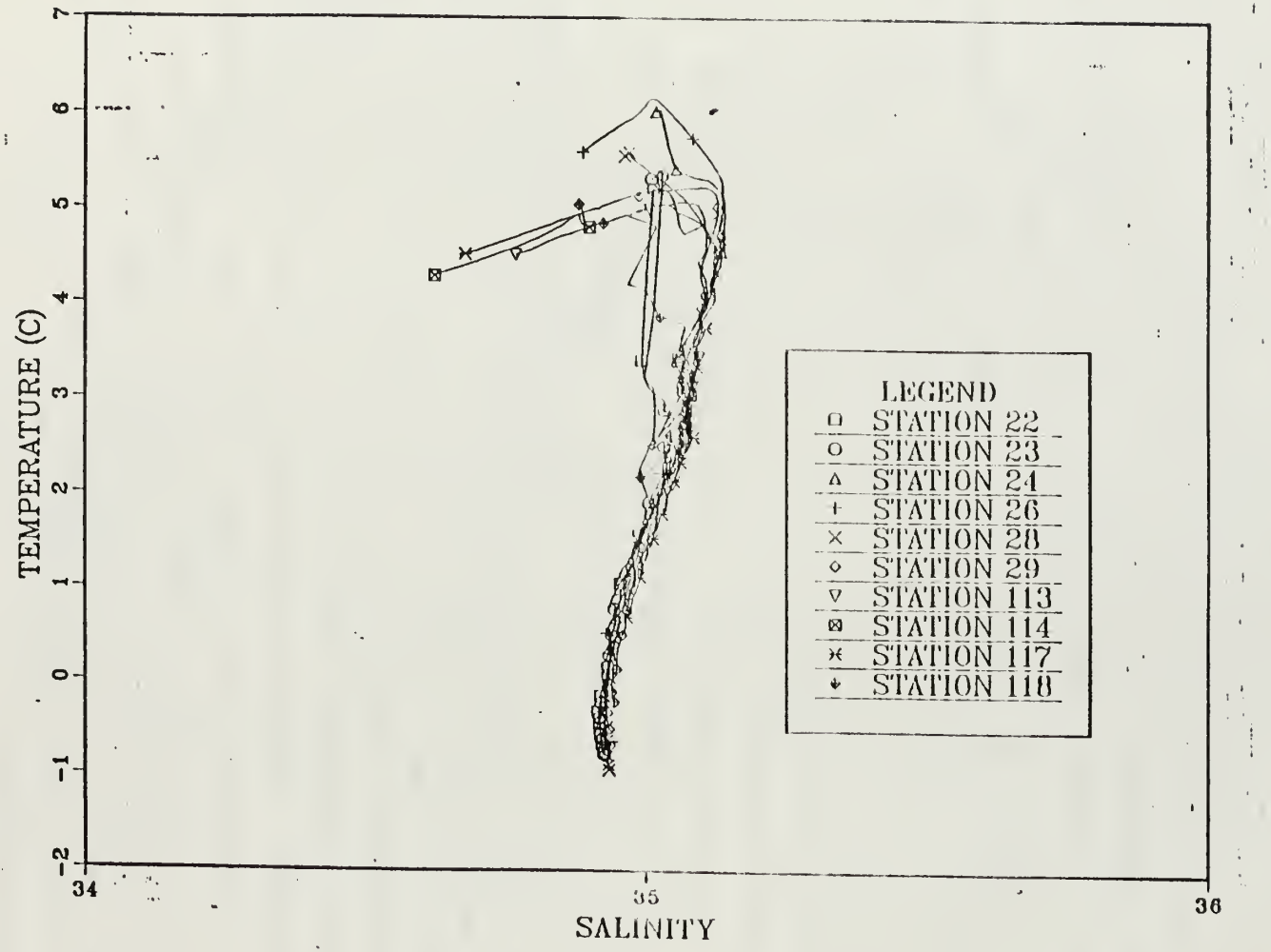

Figure 3.2 A temperature/salinity plot for stations in the core of the WSC. Symbols are at 50 m intervals.

2. East Branch

Starting near 80°10'N, the WSC branches into two streams. The left branch turns westward and appears to sink below the cold surface water. The right branch turns eastward and flows along the north coast of Spitsbergen and into the Arctic Basin. The branching appears to be controlled in part by bathymetry. Transect 5 (Fig. 3.16), along 80°N, is located just south of the branching where the Yermak Plateau shoals into the Spitsbergen continental shelf. Here the AW has spread out into a 160 km wide, 200 m deep, warm, saline core. The 3°C isotherm extends from the shallow water near the Spitsbergen coast to just seaward of the 2000 m isobath, while the 35 isohaline extends, from 100 to 600 m, across the 2000 m isobath into the deeper portion of Fram Strait. Transect 4 (Fig. 3.17) extends northwestward along the ridge of the Yermak Plateau and shows the warm saline core, defined by the 3°C isotherm and the 35.1 isohaline, positioned along the northwest coast of Spitsbergen. A second warm saline core located just behind the ice edge, similarly defined by the 3°C isotherm but the 35.0 isohaline, appears to be detached from the main core of the WSC beneath Station 107. As in Transect 5, the 35.0 isohaline extends beyond the 1000 m isobath into deep water, while the 3°C isotherm is found extending to the slope of a 700 m deep ridge. Transect 6 (Fig. 3.18) extends northwestward from the continental shelf north of Spitsbergen into the Arctic Basin. AW is found here as a narrow stream, within 40 km of the coast and in shallow water. The 35.0 isohaline, however, is found to extend well away from the coast and is evidence of the broad thrust of AW, now cooled to form AIW, propagating north and eastward into the Arctic basin to form the Atlantic layer.

In each of the transects discussed, the isotherms, starting near the surface with the 4°C isotherm, and extending downward to the 0°C isotherm of the GSDW layer, exhibit wave-like features in both the zonal and meridional directions. This wave-like structure was first noted by Helland-Hansen and Nansen (1909) in the Norwegian Sea. They called them "puzzling 'waves'", and theorized that the structure was caused by large cyclonic eddies in the Norwegian Atlantic Current. Dickson (1972) presented a detailed analysis of 17 consecutive hydrographic sections along 66°N in which he identified both standing and travelling "waves". He suggested that the wave patterns, which tended to be stable, were associated with separate northward streams, or filaments, of the Norwegian Atlantic Current. Hanzlick (1983) showed that these separate streams extended into the WSC as well, to at least 80°N.

3. Westward Turning

South of 80°10′N AW is found along the coast close to the 1000 m isobath. North of 80°10′N the left branch of the WSC leaves the shallow water along the west slope of the Yermack Plateau, turns westward into deep water, and joins the southward flowing EGC. The westward turning of the WSC will be traced by following the AW where most of the baroclinicity occurs. As will be seen in the following transects, beginning with Fig. 3.19, there is a large portion of AIW (> 0°C) flowing northward under the ice, over and on both sides of the Yermak Plateau. It is this water that provides the body of Atlantic layer water in the Arctic Ocean. The northward extent of the westward turning is found just north of 81°N. Transect 7 (Fig. 3.19), along 81°N, shows a very small trace of AW at 100 m at Station 63. Transects 8 and 9 cross through the center of the westward turning, in the zonal and meridional directions, respectively. Transect 8 (Fig. 3.20), at 80°30′N, shows a narrow surface layer of warm water between Stations 102 and 104. West of Station 102 the AW is found projecting under the PW of the EGC. The western limit of AW in this transect appears closely tied to the 2200 m deep ridge located near the center of Fram Strait. In Transect 9 (Fig. 3.21), at 2°E, the core of the warm westward turning is seen centered at 100 m between Stations 101 and 99, just at the ice edge, and well to the north of the seamounts between Stations 34 and 36. This is the farthest north that warm AW is found. Also in this transect are smaller "lenses" or "filaments" of warm water to the south seen in the earlier transects. The locations of these "filaments" appear also to be controlled by bathymetry. One "filament" is found at Station 35, between the seamounts, while the others are found well to the south.

The core of the warm westward turning is found below the surface in Transects 4, 7, 8 and 9. This can be accounted for in two possible ways. The warm, saline AW may have submerged under the cold, fresh PW. This could occur if the salinity of the AW were high enough to offset the density of the cold PW. The AW would then sink as it turned westward into the EGC. Another possibility is that the AW is cooled and freshened by the presence of the ice edge as it turns westward. This would then result in finding a temperature maximum below the cold surface layer.

Horizontal plots of water mass properties may also be used to describe the branching and westward turning of warm AW. The distribution of various water properties in Fram Strait shows the influence of bathymetry and, especially in the case of surface properties, the presence of the ice edge. Plots of the surface temperature and

salinity show warm, saline water along the west and north coast of Spitsbergen, corresponding closely to the 1000 m isobath. The plot of surface temperature (Fig. 3.3) shows a wide, warm surface layer in the southern part of Fram Strait. The EGPF, occuring where the isotherms are closely packed together, runs in a generally northeastward direction from the southern end of Fram Strait. North of 80°10′N the surface manifestation of the west branch of the WSC as defined by its AW content can be seen where the 3°C isotherm pushes west against the EGPF. The plot of surface salinity (Fig. 3.4), although less detailed, shows the same general pattern of water mass distribution. There is a wide surface layer more saline than 34.0 across much of Fram Strait. Along the west coast of Spitsbergen there is a surface manifestation of AW more saline than 35.0 that corresponds well to the 6°C isotherm in Fig. 3.3 and the 1000 m isobath. In Fig. 3.4 the 33.0 isohaline corresponds closely to the ice edge except near 80°30′N where the 34.0 isohaline pushes to the west in a surface manifestation of the westward turning.

The distribution of surface properties is strongly influenced by the presence of the ice edge. Thus, other properties must be used to demonstrate the westward turning of warm, saline AW without the contamination by surface processes. One such property to be considered is the maximum temperature at each station, which will be referred to as Tmax (Fig. 3.5). The narrow warm core of the WSC, defined in this figure by the 5° and 6°C isotherms, is confined to the Spitsbergen continental shelf and slope. The detached area warmer than 5°C, to the west of the core, may be evidence of a separate filament of the WSC. To the north of Spitsbergen the 5°C isotherm moves up onto the continental shelf. The westward turning of the western edge of AW shows up well in the 4°C isotherm. A cool area, defined by the 3°C isotherm, is located near the prime meridian between 79° and 80°N. It appears to be detached from the colder water over the Greenland continental slope. A comparison with Fig. 3.3 shows that this cool area is a sub-surface feature with surface temperatures colder than 0°C and, thus, mostly ice covered. The presence of this detached lens suggests a sub-surface cyclonic flow along 0°E between 79°N and 80°N.

An analysis of the property profiles at each station revealed that the maximum temperature in the water column was nearly coincident with the maximum salinity at over 110 of the 156 stations occupied. Those stations where the correlation was closest occurred in the core of the WSC. The density of these stations, expressed as sigma-t, has a mean between 27.9 and 28.0. For this reason, and to compare with historical

data presented by Aagaard and Coachman (1968b), the temperature of the 28.0 sigma-t surface (Fig. 3.6) and the depth of the 28.0 sigma-t surface (Fig. 3.7) were plotted.

Fig. 3.6 shows similar features to the plot of Tmax. The westward spread of the 2.0°C isotherm is seen between 80° and 81°N, with 81°N as the maximum extent of the westward flow. The area of water warmer than 2°C corresponds to the detached pool of cool water described above. (Aagaard and Coachman (1968b) presented data from 1965 which showed virtually identical features, although the maximum temperatures were warmer in 1965.) Perhaps the best evidence of westward turning, based on horizontal distributions of temperature and salinity, is seen in the depth of the 28.0 sigma-t surface. This figure indicates that a zone of westward turning takes place north of 78°N with little westward flow north of 81°N. To the north and west, behind the ice edge, the depth of this surface is greater than 500 m.

C. HISTORICAL COMPARISONS

There is a rich body of literature describing the summertime hydrographic conditions in the ice-free waters west of Spitsbergen and south of 80°N. For example, from hydrographic data obtained during 1966-69 west of Spitsbergen along 79°N, Dickson and Doddington (1968, 1970) presented vertical sections of temperature and salinity which showed a warm, saline subsurface core, warmer than 6°C and more saline than 35.1, at a depth between 50 and 200 m. This is to be compared with Transect 2 where the warm core is only 5°C and is found above the subsurface high-salinity core. More recently, based on August 1984 observations Bourke (1984) presented a section across Fram Strait, at 78°N, with a WSC core temperature greater than 6°C at the surface, and a subsurface salinity maximum of 35.1 at 60 m. This is similar to the structure seen in Transect 1 at the same latitude.

In the ice-covered region north and northwest of Spitsbergen few oceanographic studies have been published. Johannessen et al. (1983) conducted CTD sections near the ice edge north of Spitsbergen in September and October 1979. They found the warm core of AW to be located between 100 and 400 m over the Spitsbergen continental shelf break. This is in contrast to Transect 5 where the warm core is located at the surface. Perkin and Lewis (1984) presented three CTD sections obtained north of Spitsbergen in April 1981. They show two filaments of AIW warmer than 2°C, and more saline than 34.5, entering the Arctic basin along the Spitsbergen continental slope. Quadfasel et al. (in press) described the temperature and salinity

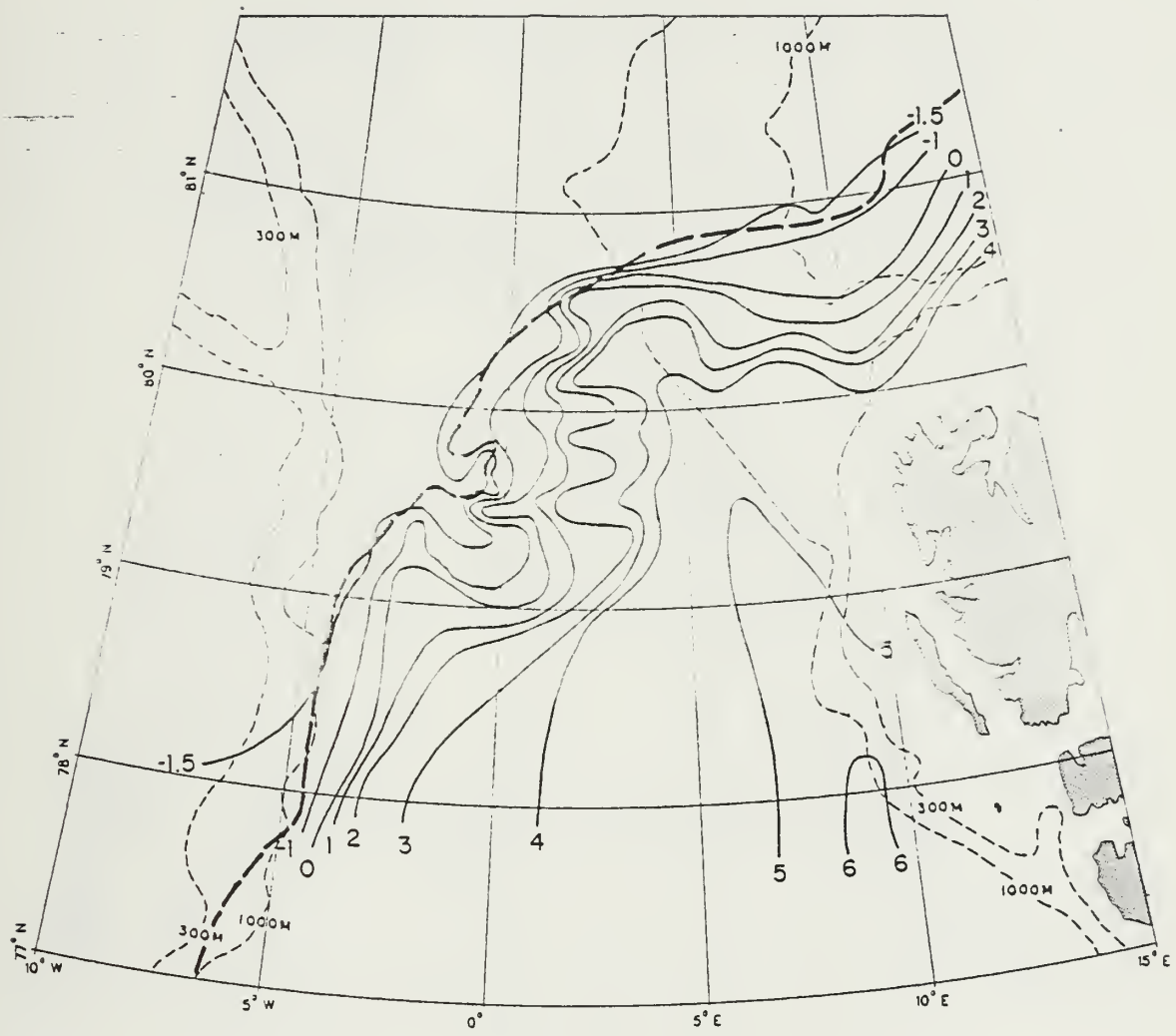

Figure 3.3 Surface temperature (°C) distribution.

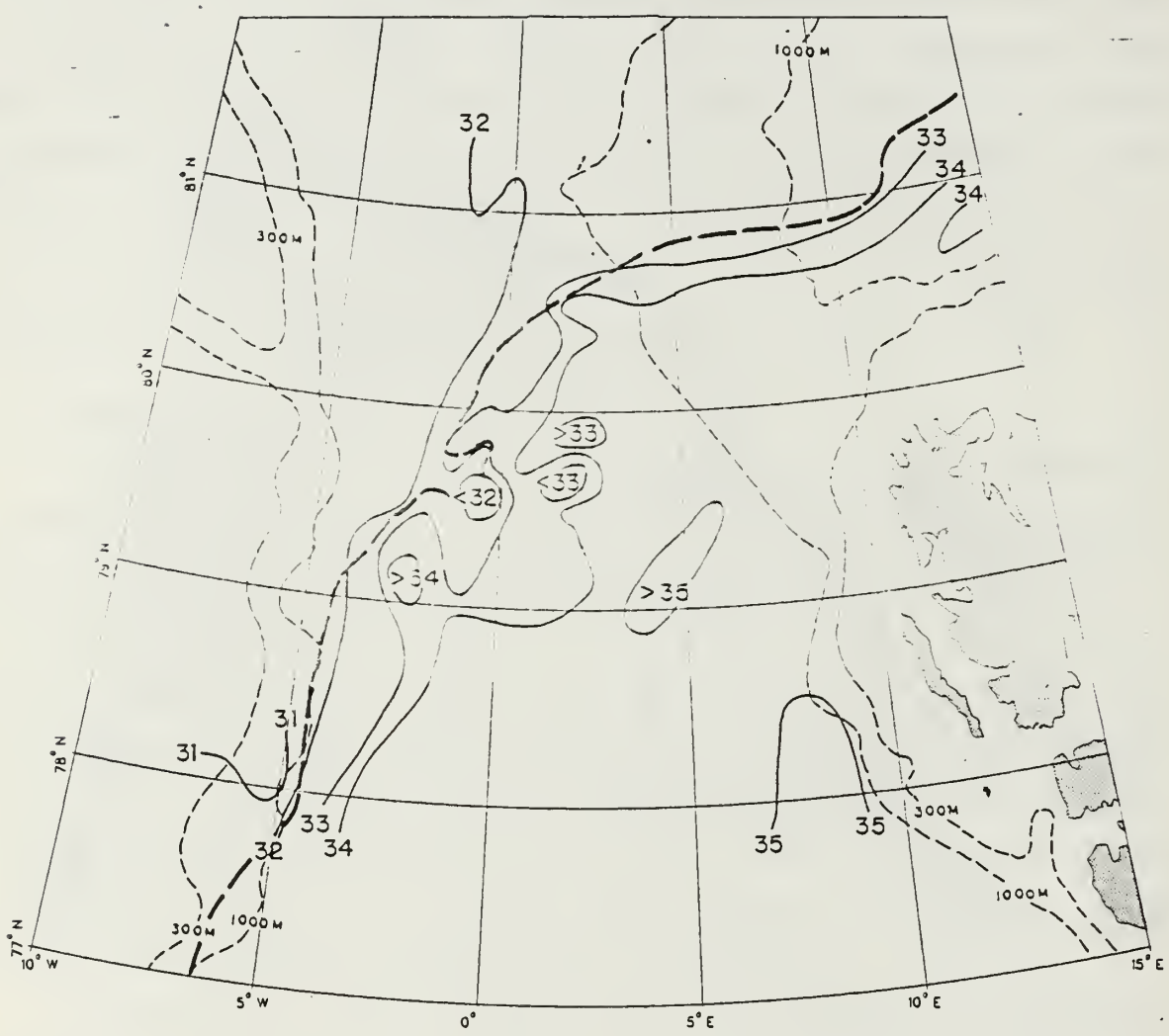

Figure 3.4 Surface salinity distribution.

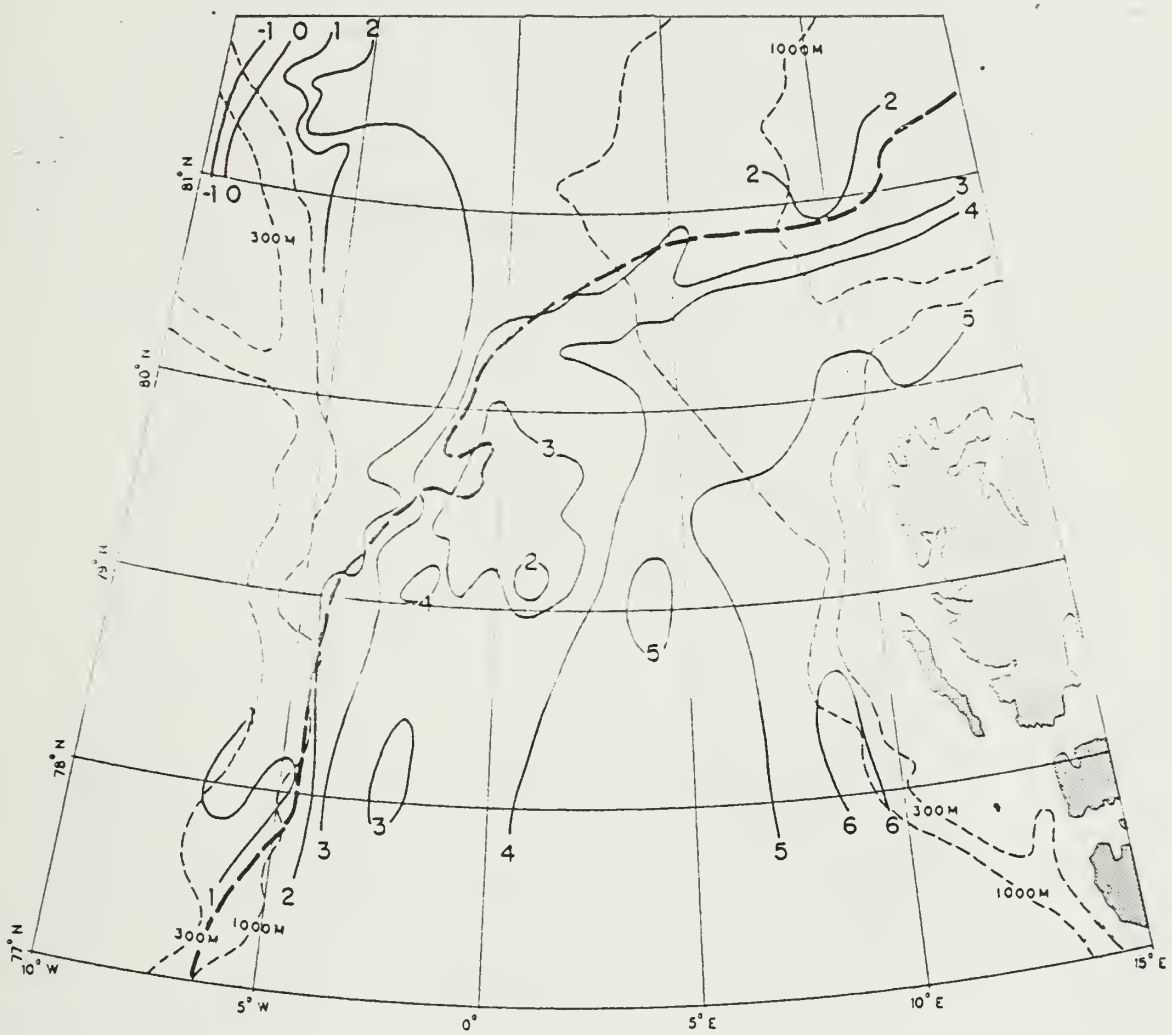

Figure 3.5 The maximum temperature at each station.

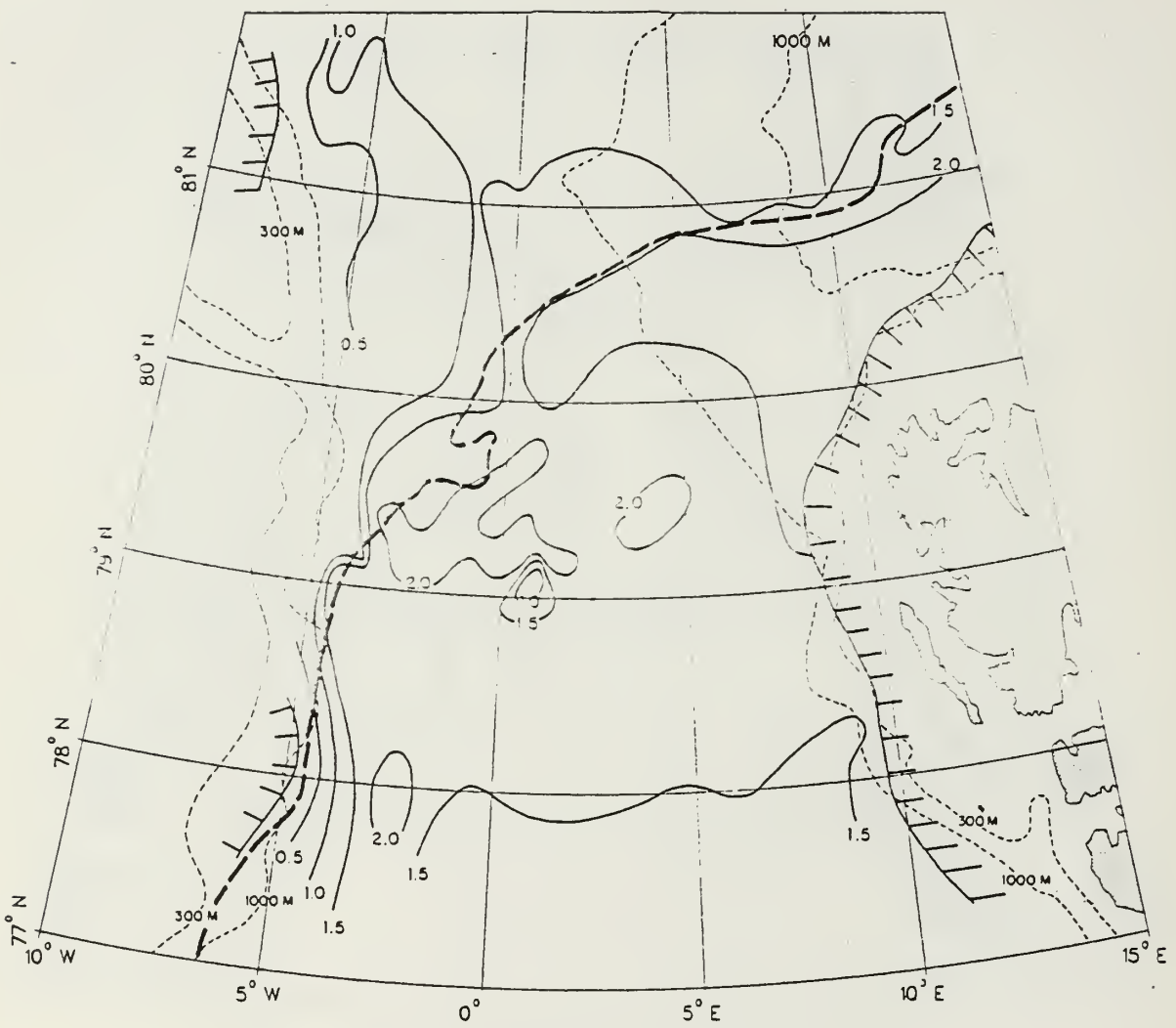

Figure 3.6 The temperature of the 28.0 sigma-t surface.

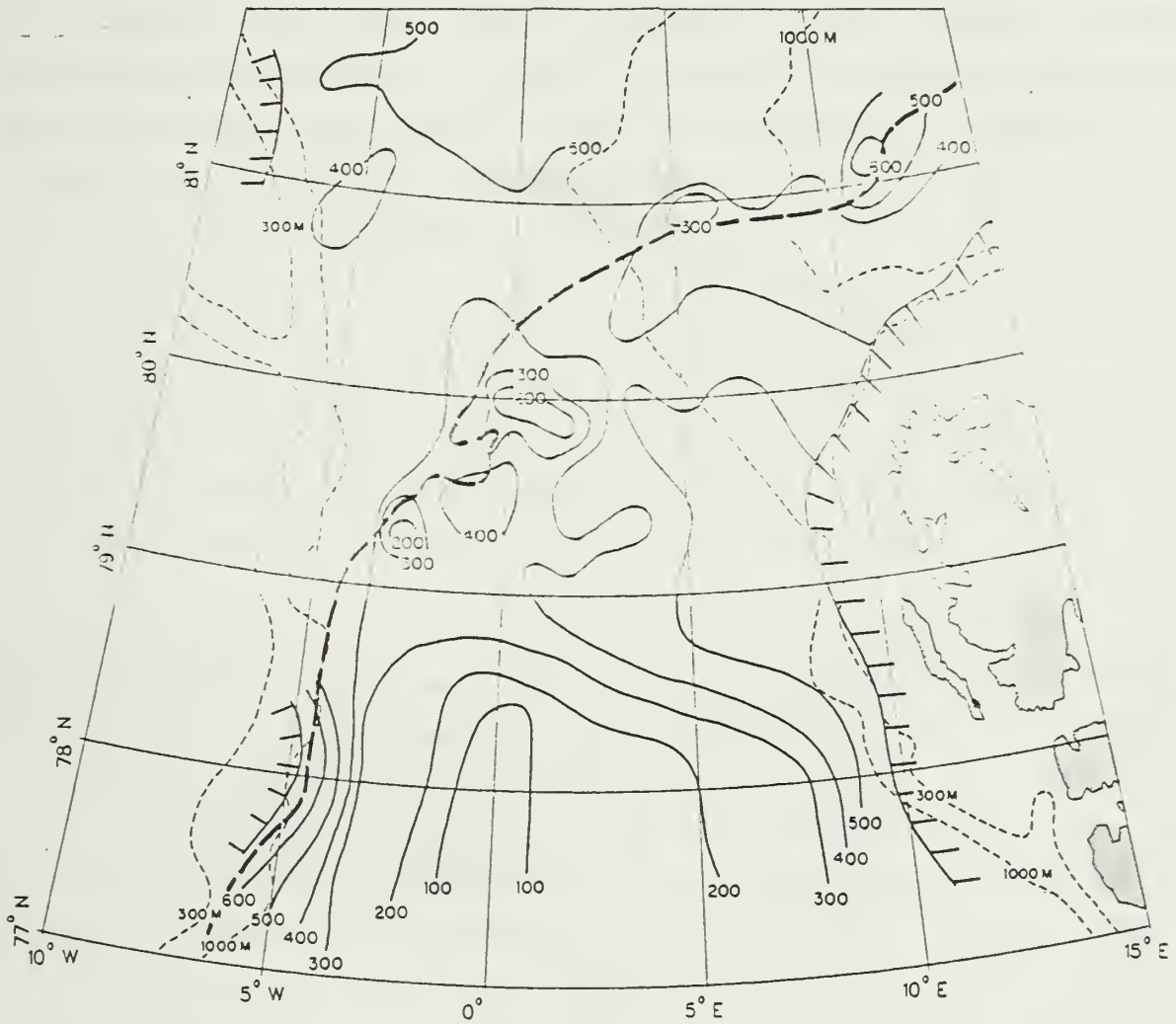

Figure 3.7 The depth of the 28.0 sigma-t surface.

distribution in the upper 600 m of Fram Strait north of 77°N based on CTD and XBT data acquired during the Marginal Ice Zone Experiment (MIZEX) in July 1984. They showed two branches of AW crossing 0°E; one between 78° and 79°N and another between 79°30′ and 80°N. The core of the WSC, warmer than 6°C and more saline than 35.1, was found from the surface to a depth of 200 m along the Spitsbergen continental slope. The warm, saline AW spread across Fram Strait in wave-like structures, some of which are apparently a result of bathymetric forcing by the Kipnovich Ridge similar to Transects 1, 2, 3 and 4. A recent workshop addressed the role of exchanges and dynamics in the circulation in Fram Strait (Aagaard and Reed, in press). There was agreement among the workshop participants that the bathymetry of the Kipnovich Ridge influences, at least in part, the spatial variability of the WSC.

D. EAST GREENLAND CURRENT

1. Water Mass Characteristics

A detailed description of the characteristics of the EGC and the EGPF have already been made (Aagaard and Coachman, 1968a,b; Paquette et al, 1985; Tunnicliffe, 1985; and Bourke, in press, a). They are included here for continuity. In addition, this cruise mapped the course of the EGPF across Fram Strait in greater detail than previous cruises.

Fig. 3.8 is a T/S plot of stations along 78°N near the EGPF. Stations 5 through 11 show the characteristic "double minimum" temperature feature discussed by Paquette et al (1985) and Tunnicliffe (1985). The first minimum is characterized by water colder than -1.5°C and salinities between 32.5 and 33.5. The second minimum occurs at a salinity of between 33.9 and 34.2 at a depth of about 100 m near the bottom of the PW layer. Paquette et al. (1985) suggest that this second minimum is formed when AIW, advected from the east under the PW, is modified by double diffusion. Station 14 is illustrative of stations to the east of the EGPF and shows the warm, saline fraction of AW and AIW often found in the core of the RAC. GSDW is found only in Stations 12 and 14, seaward of the shelf, and generally below 800 m.

A typical distribution of water mass properties in the EGC is seen in Transect 1, along 78°N. Cold, fresh PW, defined by the 0°C isotherm and the 34.5 isohaline, is found over the Greenland continental shelf, to a depth of 180 m. The PW extends seaward of the shelf break, defined by the 400 m isobath, about 40 km and is separated from the warmer water to the east by the EGPF. A warm filament of AW, diluted to a

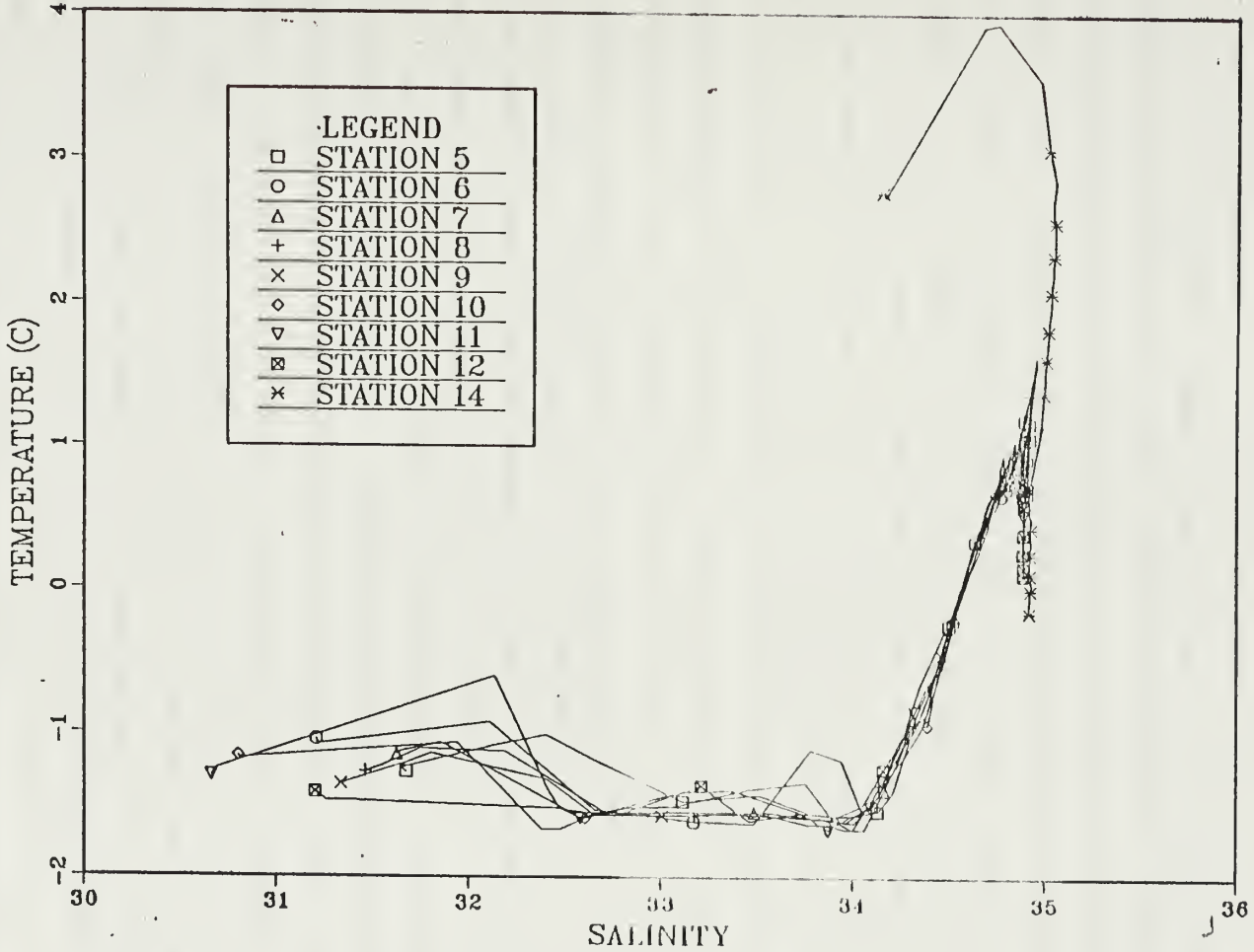

Figure 3.8 A temperature-salinity plot of stations along 78°N in the vicinity of the EGPT

salinity of 34.7, is found along the front between a depth of 25 and 75 m. The AW is found embedded in the large body of AIW which makes up the southward flowing RAC found alongside the front.

2. East Greenland Polar Front

Seven of the ten transects made in Fram Strait cross the EGPF. This series of transects shows the EGPF leaving the Greenland continental shelf break north of 78°N and crossing Fram Strait in a northeastward direction. In Transect 1, along 78°N, the front is concave with respect to the PW and intersects the surface approximately 40 km from the shelf break. This is approximately the same shape and location of the front presented by Tunnicliffe (1985) for a CTD transect made along 78°10'N in September 1984. In Transect 2, along 79°N, and Transect 3, along 79°10'N, the structure of the front is somewhat confused by the presence of the eddy-like feature. In Transect 2 the front is located 50 km from the shelf break and in Transect 3 it is located 63 km from the shelf break. There is a significant fraction of dilute AW located between the front and the eddy. For example, in Transect 2, there is a filament of AW warmer than 4°C with a salinity of 34.7 located between the front and the eddy at Station 127.

North of 79°30'N the front turns away from the shelf break in a northeastward direction. At 80°N, as seen in Transect 5, the front is located over the center of Fram Strait approximately 126 km from the Greenland continental shelf break, also similar to the location found by Tunnicliffe (1985). In addition, in Transect 5 the vertical development of isopleths is minimized because the PW only extends to a depth of 25 m. A dilute AW filament is located under the PW between 40 and 70 m. There is probably a second, deeper front located to the west of this transect, similar to the split front discussed by Tunnicliffe (1985). He hypothesized that the division of the front into a surface and sub-surface portion was due to the dilution of the surface water by melting sea ice. During most of this cruise the wind was from the north or northwest (Bourke et al., 1986) and created a fairly diffuse ice edge. In Transect 5 the ice edge is located about 40 km west of the surface front, thus lending support to the idea that ice, blown into warmer water, has melted and created the surface front.

North of 80°N the front moves up over the Yermak Plateau, as seen in Transect 8, along 80°30'N, and Transect 4, along the top of the Plateau. In both of these transects there is a surface front overlaying AW, which because of the closer proximity to the WSC is less dilute than farther south. Transect 8 clearly shows the split front, with the sub-surface portion located between Stations 95 and 96, just inside the ice edge, and the surface front 50 km farther east in the ice free water.

North of 81°N the front has extended across the Yermak Plateau and into the Arctic Basin. Transect 6, extending northwestward from the Spitsbergen coast, shows a surface front underlaid by AIW. There is probably no strong sub-surface front farther northwest of this transect as the AIW under the front is the basis for the Atlantic layer throughout most of the Arctic Ocean.

3. **Mesoscale Features**

A mesoscale eddy-like feature having a cold, fresh core appears to have detached from the EGPF and is centered at about 79°N and 001°W. Three transects pass through the feature and clearly show its temperature and salinity distribution: Transect 2 (Figure 3.14), at Stations 123 through 126; Transect 3 (Figure 3.15), at Stations 132 through 136; and Transect 10 (Figure 3.22), between Stations 125 and 139. The feature has a diameter of about 60 km, as defined by the 0°C isotherm, and penetrates to a depth of about 180 m. There is also a downward trend to the isotherms and isohalines below the feature, discernible to about 400 m. The plots of surface temperature and salinity also show evidence of this feature. An area of ice appears in these figures to be pulled away from the main pack suggesting an anti-cyclonic rotation around the cold core. As will be seen later, geostrophic velocities calculated for this feature will confirm the anti-cyclonic sense of rotation.

The temperature, salinity, and ice distribution and the flow field of this eddy are similar to those described by Wadhams et al. (1979), Wadhams and Squire (1983) and Bourke et al. (in press, b). Both Wadhams and Squire (1983) and Bourke et al. (in press, b) describe an eddy system near the Molloy Deep composed of a cyclonic and anti-cyclonic couplet. Wadhams and Squire (1983) show the northern limb of the couplet rotating cyclonicly in open water with a warm core enclosed. It is this limb of the couplet which was sampled by NORTHWIND in 1984 and is shown by Bourke et al. (in press, b) in their Figures 2 and 3. The southern limb of the feature has an anticyclonic rotation with a cold core and pulls ice away from the main pack in a shape described by Wadhams and Squire (1983) as a "breaking wave". This anti-cyclonic rotation was also shown by Bourke et al. (in press, b). It is probably this southern limb of the couplet that was sampled by NORTHWIND in 1985 and is shown in Transects 2, 3, and 10.

As discussed in Chapter I, various theories have been suggested concerning the generation of these eddies. Wadhams and Squire (1983) suggested the eddies were generated by baroclinic instabilities along the EGPF. Smith et al. (1984) suggested the

eddies were topographically driven by the interaction between the Molloy Deep and the EGC, although the eddy is often found at a distance from the Molloy Deep which makes direct triggering and steering seem unlikely. As discussed by Bourke et al. (in press, b) the complex bathymetry found in the region (of which the Molloy Deep is only a part) probably does influence the generation and location of these eddies.

E. FINESTRUCTURE

Intermediate scale fluctuations in the temperature, salinity, and flow fields are termed finestructure and are produced by the interaction of the different water masses present in Fram Strait. These fluctuations occur on vertical scales of the order of 1-100 m. They have horizontal scales of 1 m to 10 km and time scales from 1 min to several days. Temperature and salinity finestructure near the ice edge have been reported numerous times. For example, Perkin and Lewis (1984) describe finestructure resulting from intrusive layering in the WSC north of Spitsbergen. Paquette et al. (1985) describe finestructure occuring in the AIW along the EGPF.

Fig. 3.9 is a plot of the stations having notable vertical structure. Small open circles represent stations where there was little or no notable finestructure. Small solid circles indicate temperature finestructure having peak-to-peak variations between 0.5°C and 1.0°C. Large solid circles indicate fine structure having peak-to-peak temperature variations greater than 1.0°C and solid stars indicate peak-to-peak temperature variations greater than 2.0°C. Superimposed on this plot is the location of the EGPF as defined by the 0°C isotherm at the surface (solid line) and the location of the ice edge (dashed line). As can been seen in the figure large temperature variations occur most notably along the ice edge and along the EGPF.

The significant finestructure activity along the EGPF and in the vicinity of the ice edge is due to the mixing of AW from the WSC and PW from the EGC. An example of this mixing is shown in a series of temperature and salinity profiles along 80.5°N (Figs. 3.10 and 3.11). In these figures the temperature and salinity values for Station 90 are shown according to scale, the values for other stations are offset from the previous station by one unit each. The true values of temperature and salinity at the bottom of each station are listed below the profiles.

Station 103 is located in the core of the WSC, over the Yermak Plateau, outside of the ice edge. There is only a small positive thermocline and halocline between warm AW, with surface temperatures greater than 3°C, and cold GSDW below 700 m.

Figure 3.9 Stations exhibiting significant vertical structure.
The solid line is the location of the PGPT and the dashed line is the ice edge.
Other symbols are defined in the text.

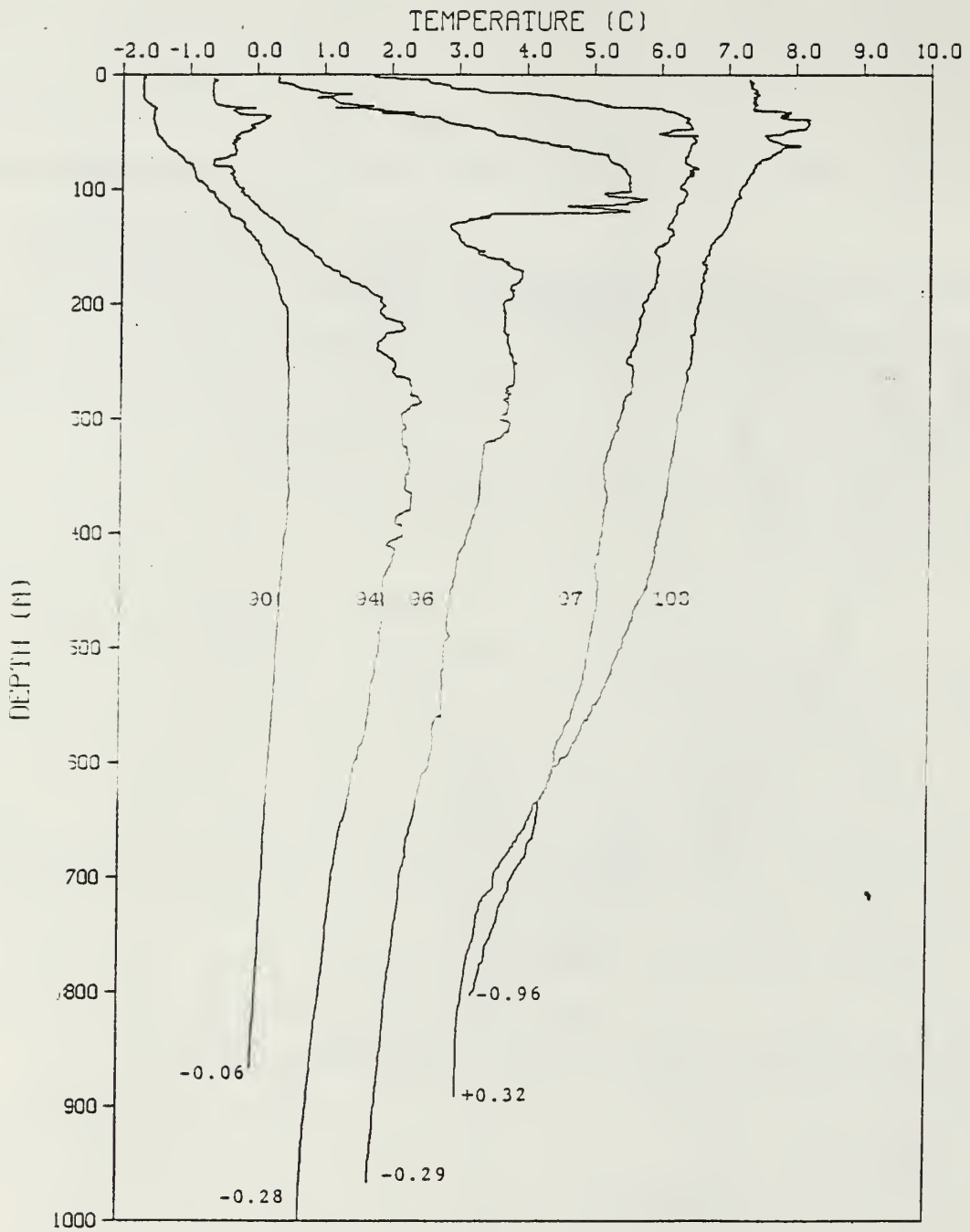

Figure 3.10 Temperature profiles for stations along 80°30′N.

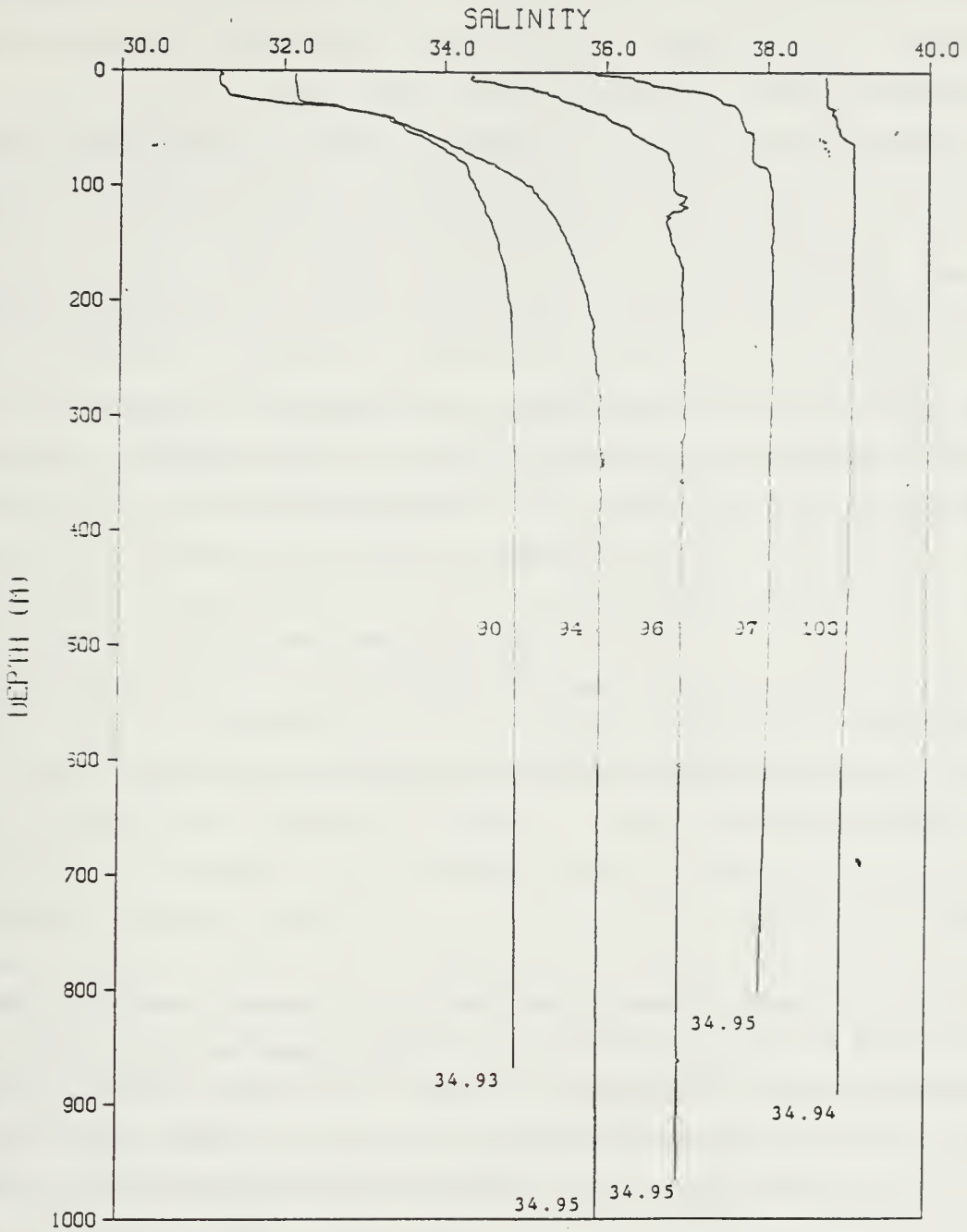

Figure 3.11 Salinity profiles for stations along 80°30′N.

Station 90 is located over the Greenland continental slope. A cold, fresh PW layer is located close to the surface. The temperature maximum at 200 m, of less than 0.5°C and salinity of 34.9, is similar to the Atlantic layer at the end of its cyclonic path in the central Arctic. GSDW is found at this station below 650 m.

Station 97, located just at the ice edge but seaward of the EGPF, shows cooling and dilution at the surface. The maximum temperature at this station is still greater than 3°C but a strong positive thermocline and halocline have developed as a result of ice melt. Station 96 in the center of the front shows more extensive cooling and dilution. Warm AW is still present; however the thermocline and halocline now extend to 75 m, further eroding the AW layer from above. In addition, a lens of cool (< 1°C) water at 150 m is eroding the AW from below. Station 94 is well behind the EGPF; here the cooling and dilution extend to 200 m. No AW is present, the maximum temperature at the station is only 1.5°C. With the exception of the small temperature finestructure above and below the thermocline, this station is characteristic of an EGC water mass distribution. As can be seen in Stations 94, 96, 97, and 103 finestructure is usually associated with the depth zone of the maximum temperature in the water column. A notable example of this type of finestructure is seen in Station 96, located at the EGPF. The cool lens below the AW creates a temperature change of greater than 2°C in 10 m, as well as other interleaving regions above and below the lens.

The density ratio,

$$R_\rho = \alpha \partial T_z / \beta \partial S_z \qquad \text{(eqn 3.1)}$$

where α = the thermal expansion coefficient; β = the salinity expansion coefficient and ∂T_z and ∂S_z are the temperature and salinity gradients, is the single most important parameter in determining the nature and strength of double diffusive activity. Laboratory measurements have shown that $R_\rho > 1.0$ but < 2.0 is unstable to salt-fingering and $R_\rho < 1.0$ is diffusively unstable (Ruddick, 1983). Several disadvantages exist, however, in using the density ratio. The first is that R_ρ has an infinite scale, with the diffusive region smaller than the fingering region. In addition, an indeterminate value exists for R_ρ when $\partial S_z = 0$.

In order to overcome the inadequacies of the density ratio Ruddick (1983) suggests the use of a new quantity: the Turner angle (Tu). The Turner angle is defined as the four quadrant arctangent of

$$(N_T^2 - N_S^2)/(N_T^2 + N_S^2) \qquad \text{(eqn 3.2)}$$

where

$$N_T^2 = \pm g\alpha\partial T/\partial z \qquad \text{(eqn 3.3)}$$

and

$$N_S^2 = \pm g\beta\partial S/\partial z. \qquad \text{(eqn 3.4)}$$

(Note that N_T^2 and N_S^2 can be considered the temperature and salinity contributions to the Brunt-Vaisala frequency.) The Tu is related to the density ratio such that R_ρ = -tan(Tu − 45°). The stability properties of the local stratification are determined by R_ρ and are represented by the four Tu regions in Fig. 3.12 where |Tu| > 90° is gravitationally unstable, 45° < Tu < 90° is unstable to salt-fingering, |Tu| < 45° is stable, and -90 < Tu < -45 is diffusively unstable.

In order to determine the role double diffusion plays in effecting finestructure along the EGPF the Turner angle (Tu) was computed for Station 96 (Fig. 3.12) by smoothing the temperature and salinity profiles with a 5 - point (approximately 1.5 m) running mean and then calculating the gradients. Station 96 shows generally stable conditions in the thermocline. The interleaving between the region of AW > 3°C and the cool lens between 80 m and 120 m is associated with alternating strong fingering and diffusive regions. The cool lens between 120 m and 180 m, however, shows stable conditions. Below the lens are two areas of alternating activity that are associated with regions of finestructure. One, between 180 m and 320 m, is located in AIW resulting from mixing between PW and AW. Another is located between 470 m and 550 m with generally stable contitions between the two regions of activity. Below 550 m the finestructure decreases as does the strength of the double diffusive activity.

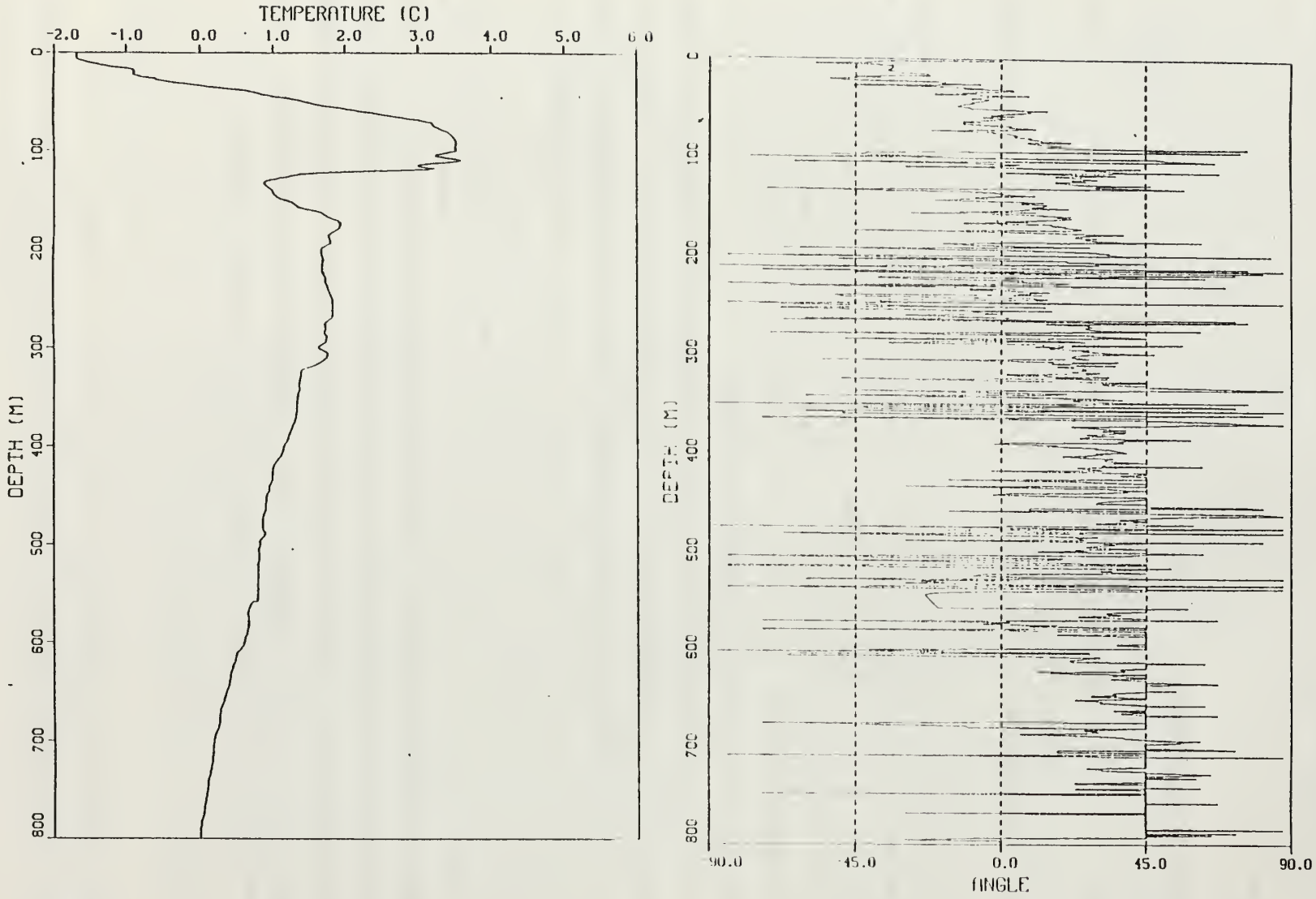

Figure 3.12 The Turner angle for Station 96 in the EGPF.

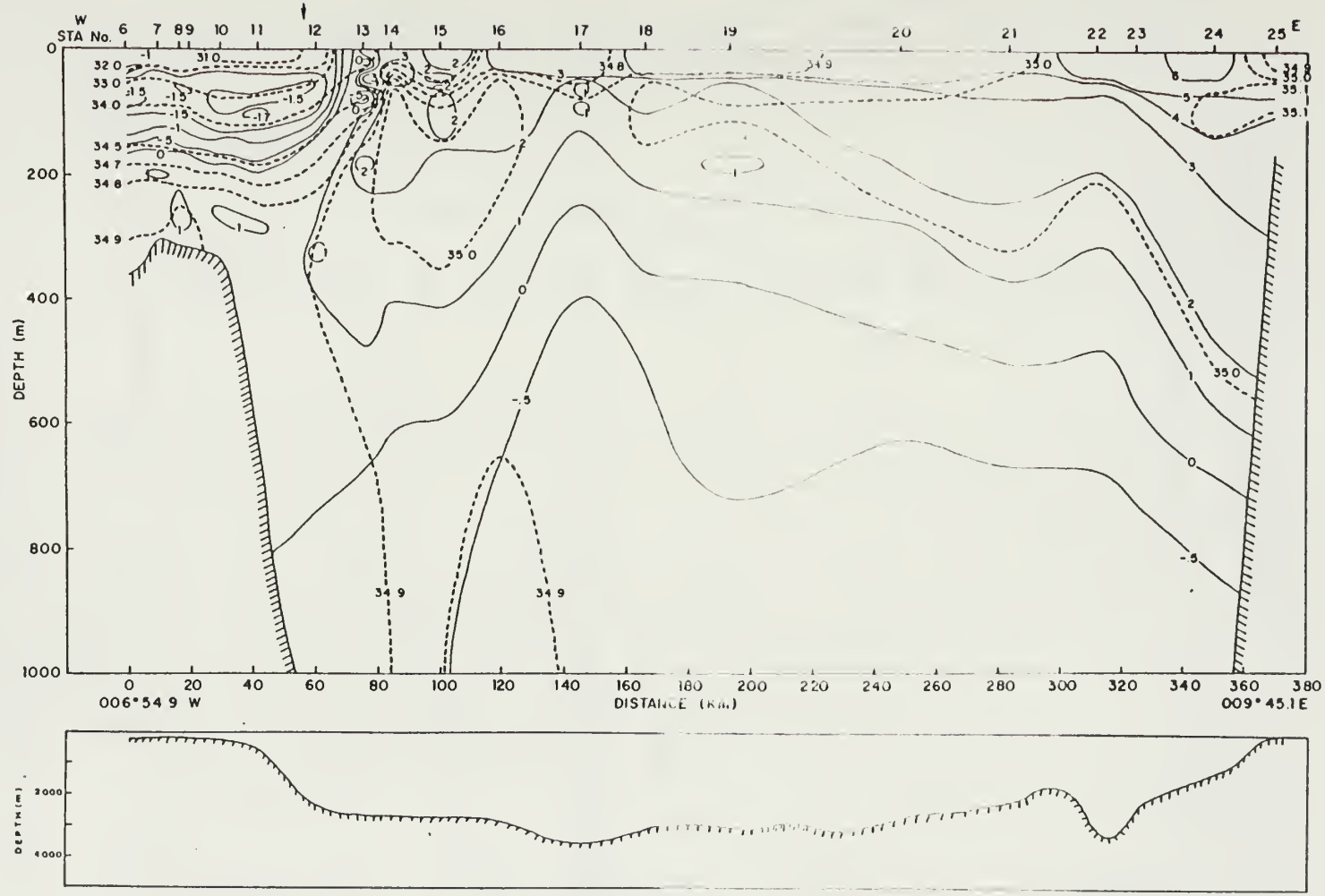

Figure 3.13 Transect 1, along 78°N. The 2000 m feature between Stations 21 and 22 is the Kipnovich Ridge. The arrow at the top indicates the location of the ice edge.

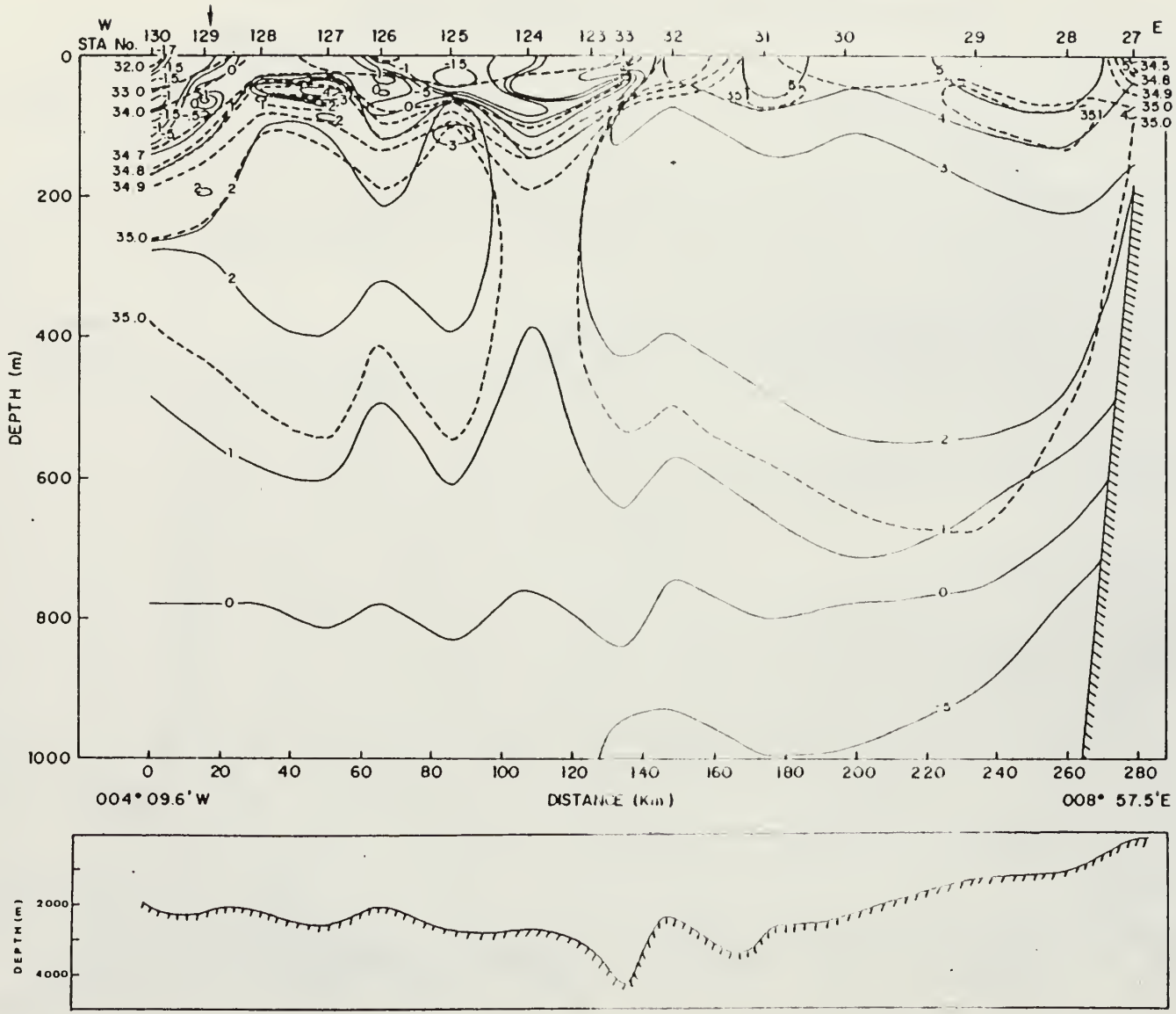

Figure 3.14 Transect 2 along 79°N. Note the effect of the Kipnovich Ridge between Stations 31 and 32 creating a wave-like structure in the isotherms and isohalines.

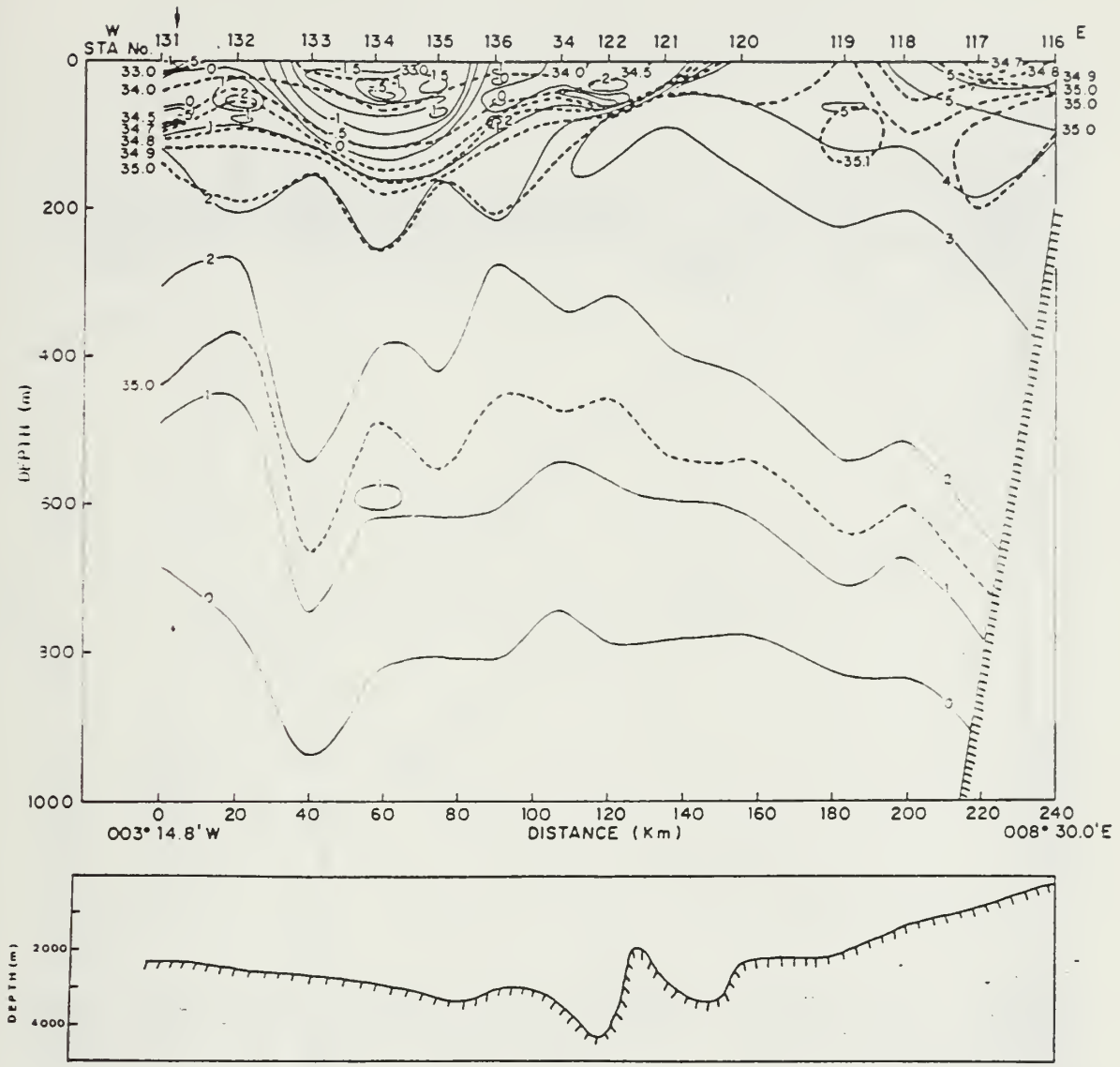

Figure 3.15 Transect 3 along 79°30′N. The Kipnovich Ridge is very pronounced at this latitude..

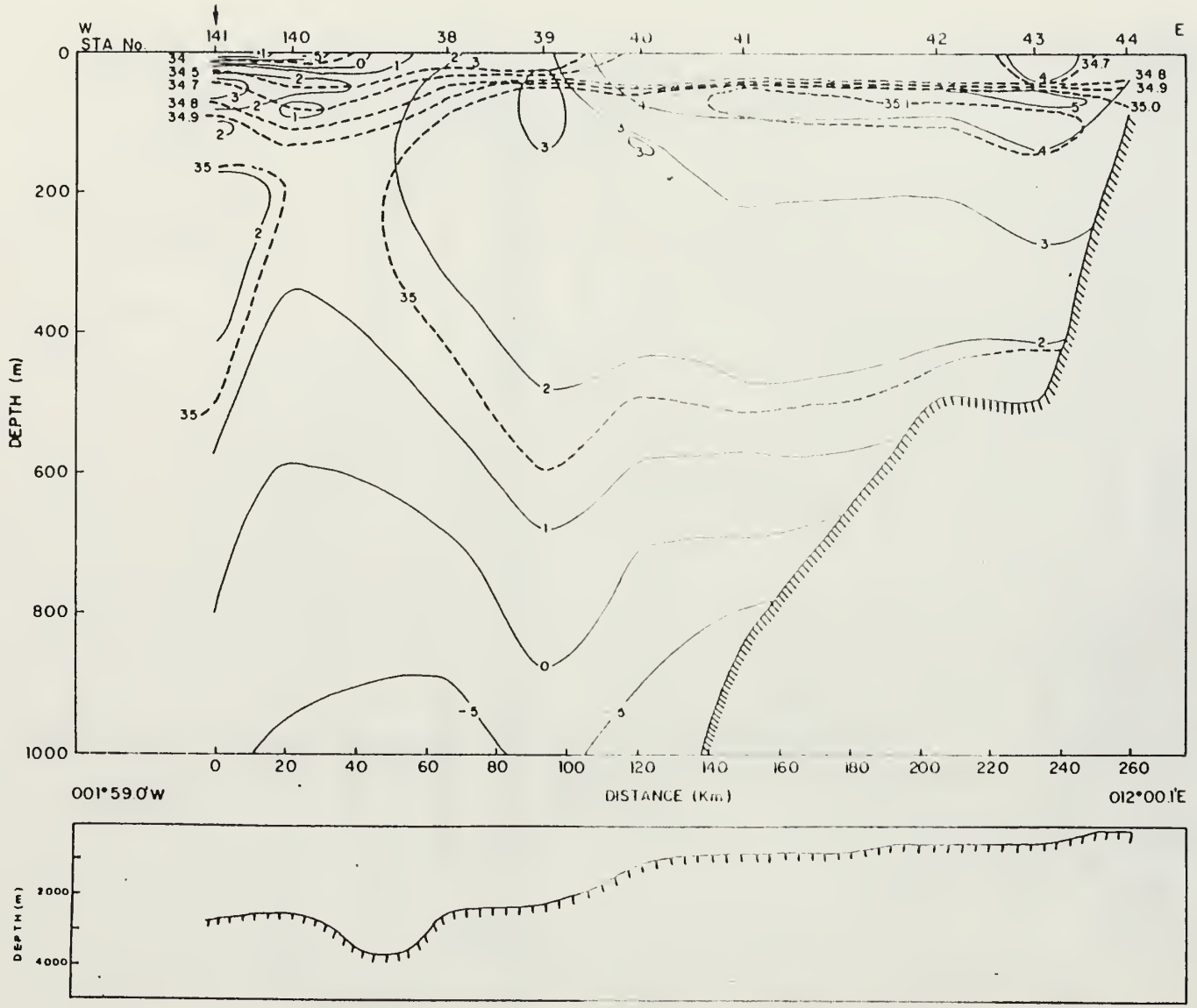

Figure 3.16 Transect 5 along 80°N.

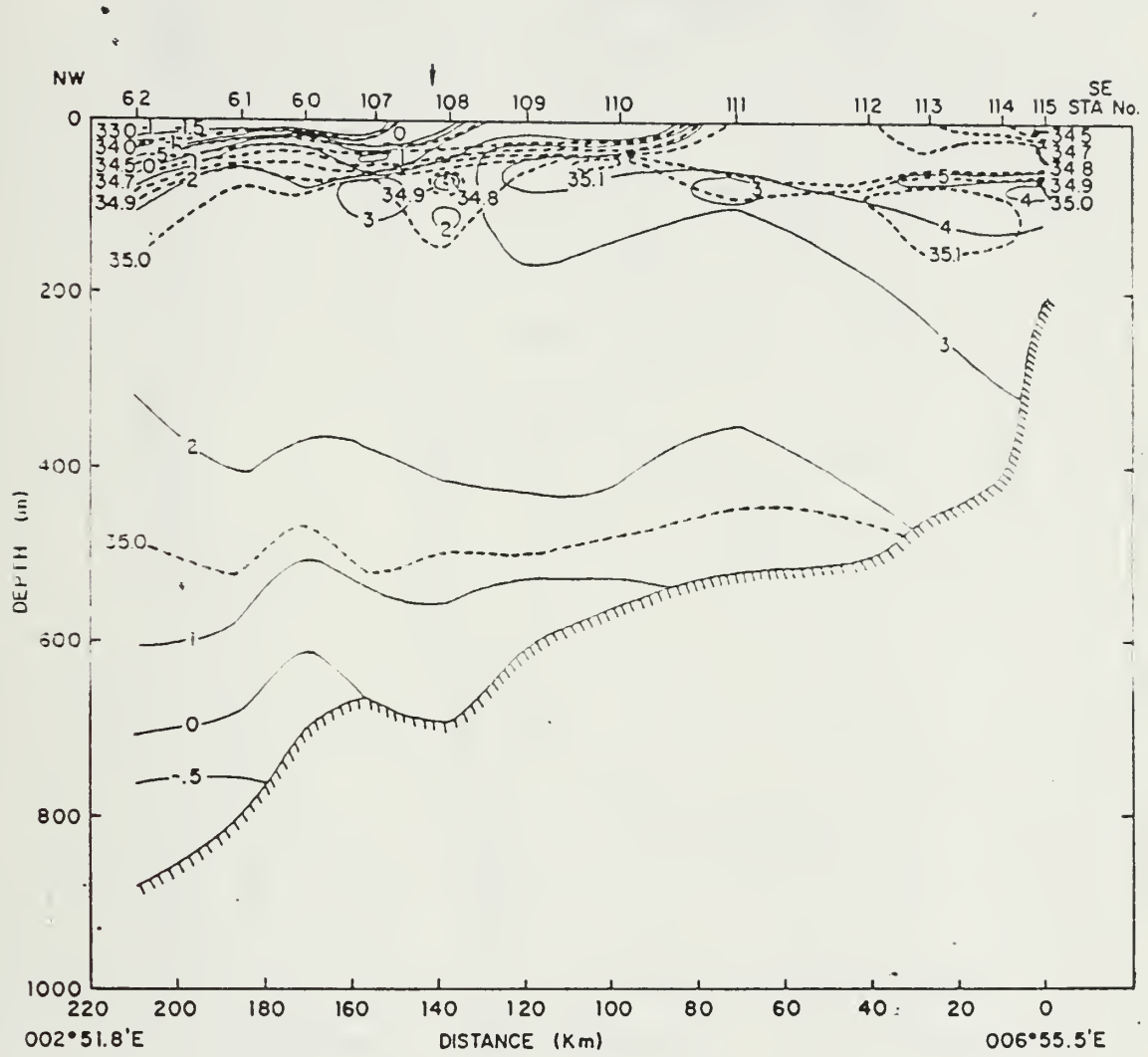

Figure 3.17 Transect 4 along the top of the Yermak Plateau.

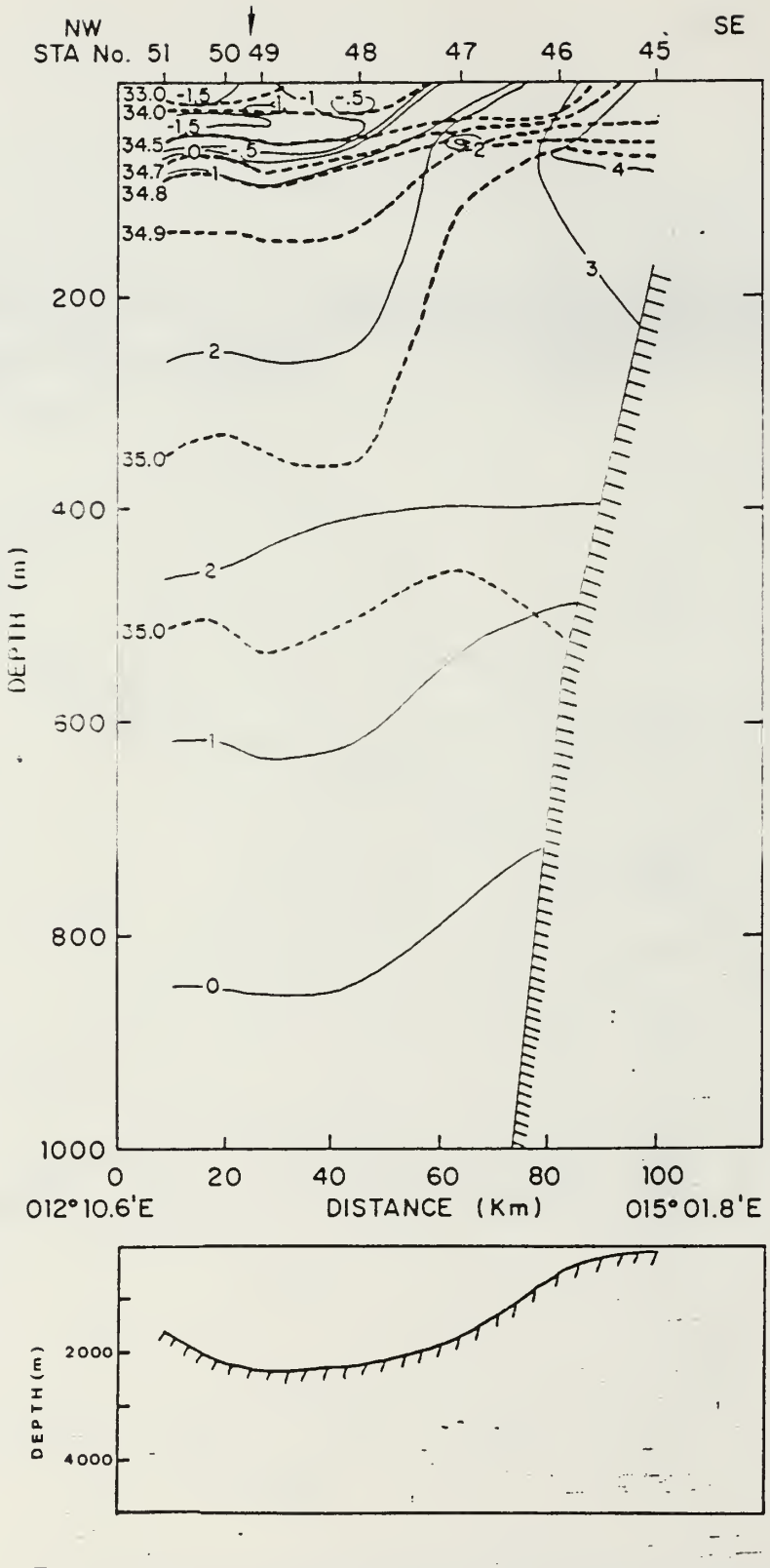

Figure 3.18 Transect 6 north of Spitsbergen.

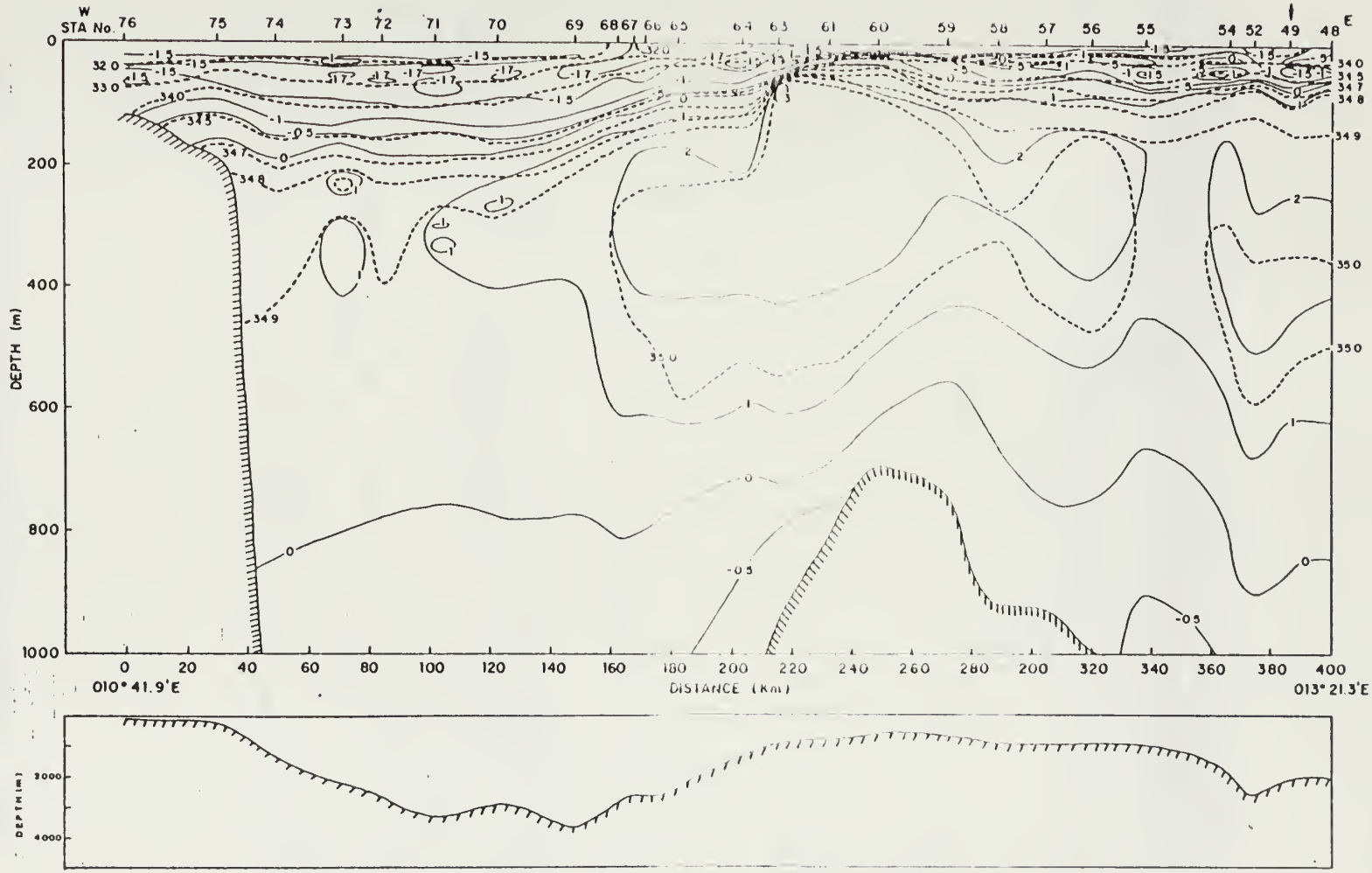

Figure 3.19 Transect 7 along 81°N

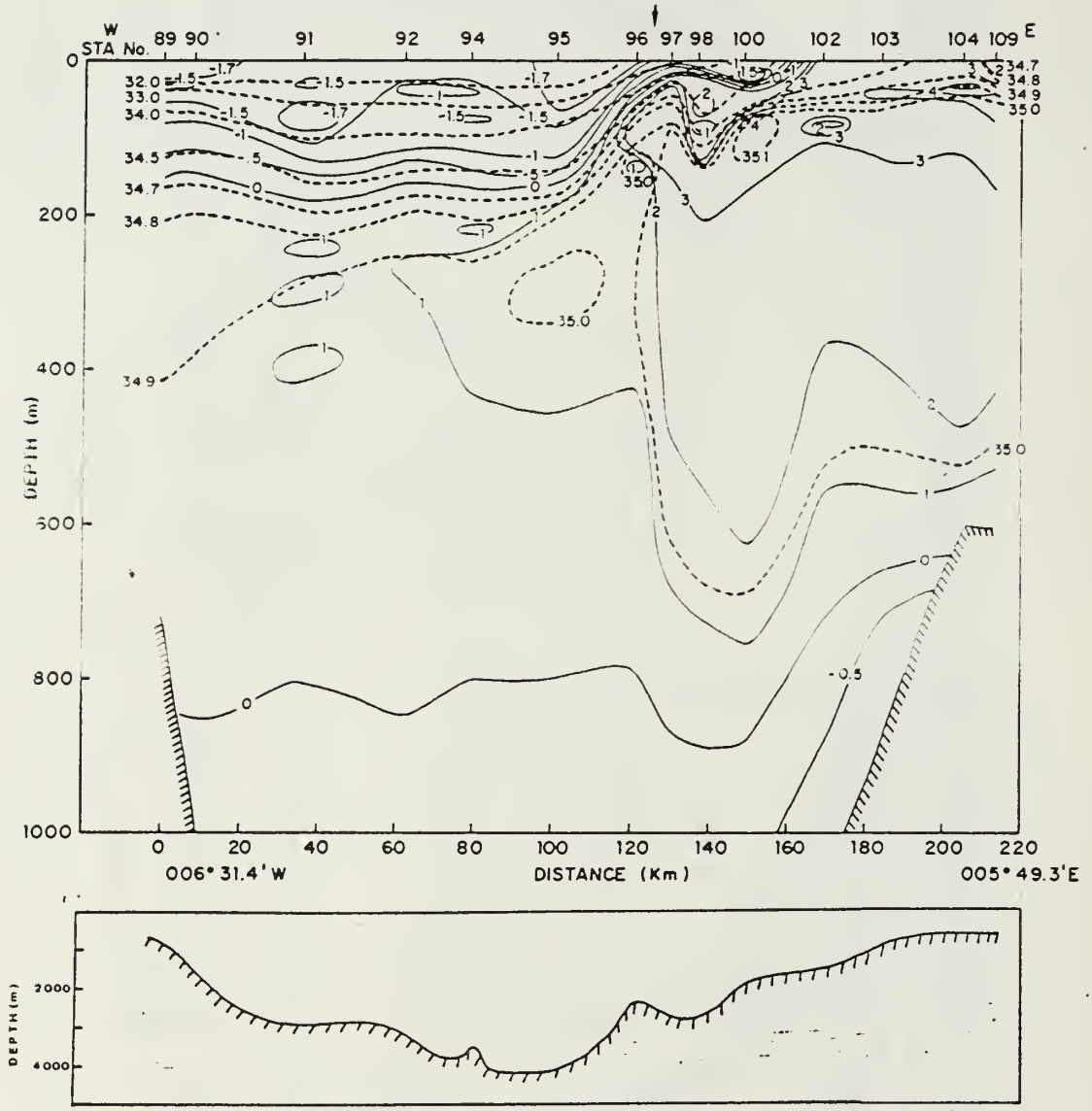

Figure 3.20 Transect 8 along 80°30′N.

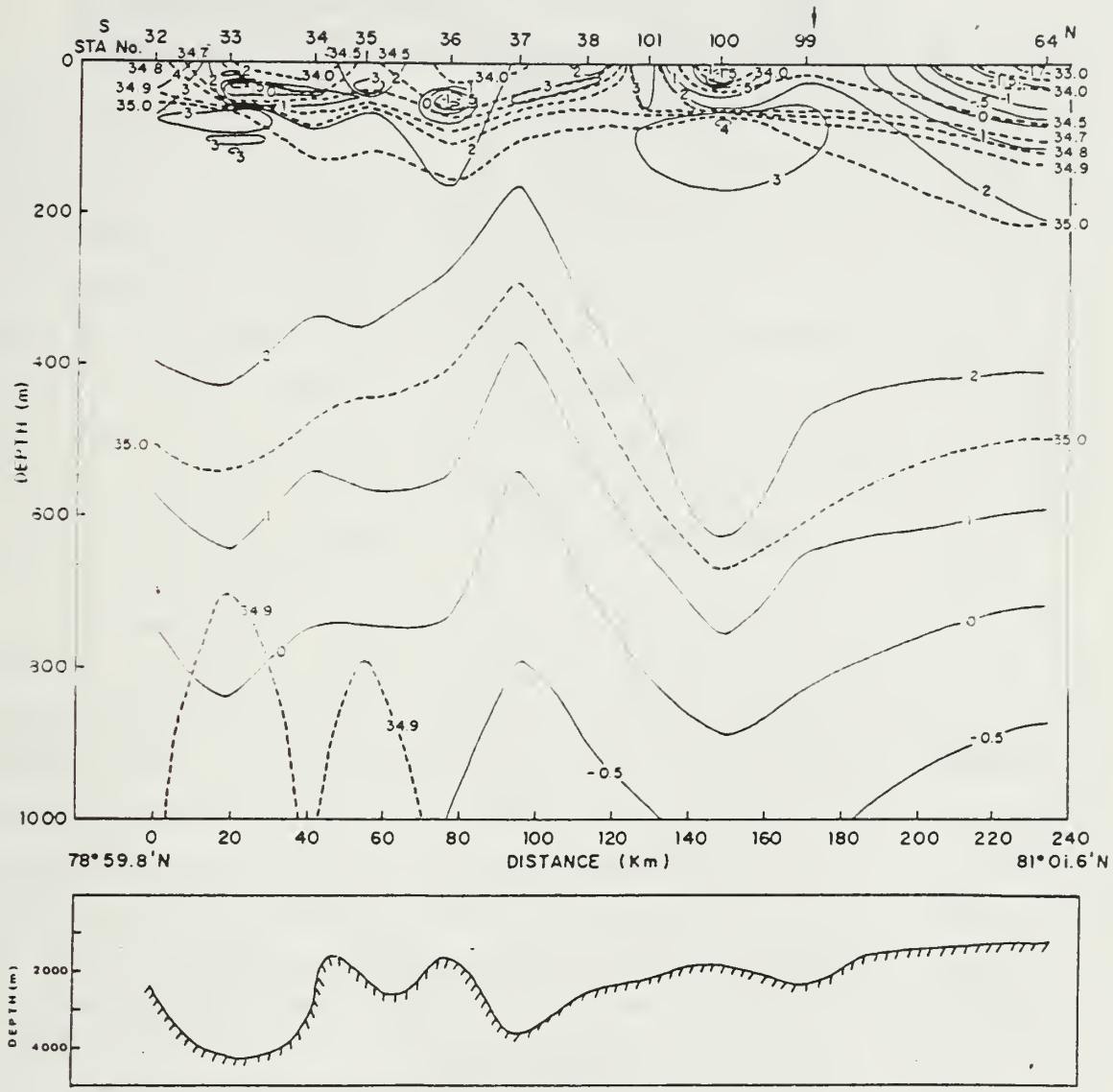

Figure 3.21 Transect 9 along 2°E shows the core of westward turning as the 3° lens between Stations 36 and 99.

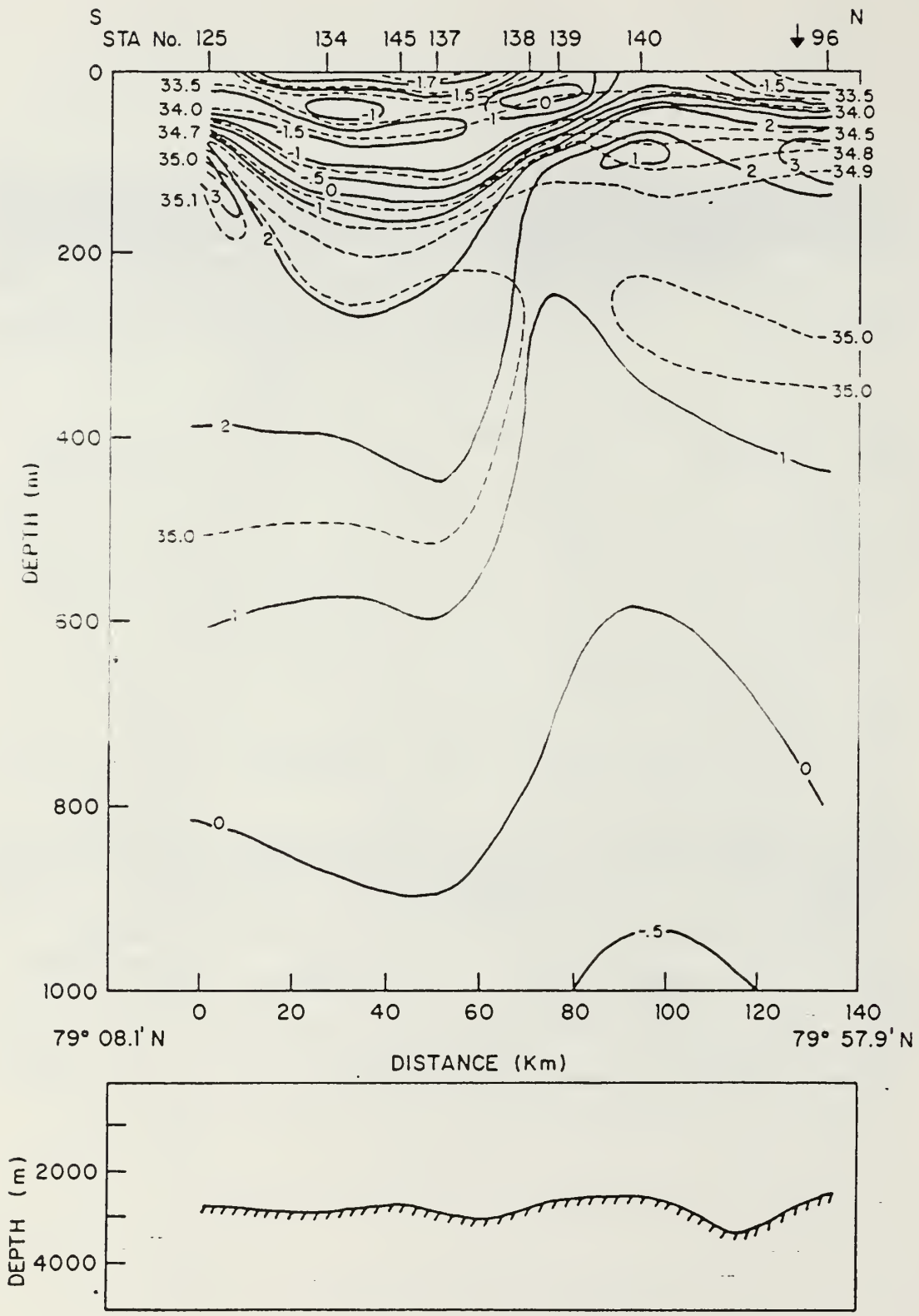

Figure 3.22 Transect 10 along 2°W through the center of the eddy.

IV. CIRCULATION AND TRANSPORT

A. INTRODUCTION

Current meter moorings have been made a number of times in the WSC off the coast of Spitsbergen. The first estimate of the WSC transport using direct, long-term current measurements was made at 79°N by Greisman (1976). From these measurements and hydrographic data obtained during 1971-72 he found that the average baroclinic component of the WSC was approximately one half of the total flow. Based on similar current meter and hydrographic data obtained in 1976-77, Hanzlick (1983) estimated the mean baroclinic component to be much less, only 18% of the total flow. Hanzlick also showed that the degree of baroclinicity varies significantly. Using the vertical shear calculated from direct current measurements obtained during 1976-81, and assuming no baroclinicity in the deep part of the water column, he found that the mean baroclinic contribution to the mean total transport at 79°N varied from 14% to 38%.

During 1984-85 a series of three current meters was deployed across the WSC at 78°45'N (Aagaard et al., 1986a). The total transport for this section for a one week average current taken in August 1984 was calculated using the method outlined by Hanzlick (1983). This time period corresponded to the time when NORTHWIND acquired hydrographic data at the locations of these current meters. This time also corresponded to a period of very strong northward flow in the WSC, resulting in a transport estimate of 16.5 Sv northward. The baroclinic component calculated from the hydrographic data, using the method described in Chapter II, was 1.5 Sv northward, resulting in a baroclinic contribution to the total flow of only 9%. Unfortunately, the series of current meters was removed prior to September 1985. Thus, no direct comparison can be made with the data presented in this thesis.

There are no moored current meter records from locations further north than 79°N. While there is a large body of ice drift data in this region, this provides little indication of the flow within the warm WSC. Recently, Quadfasel et al. (in press) presented direct current observations, using surface and subsurface floats, in the region of the westward turning of the WSC. Satellite-tracked drifters were deployed at 78°N and showed two separate streams of the WSC, one at 6°E and another at 10°E.

Subsurface floats deployed between 79°30′N and 80°N showed westward flow across the prime meridian of about 0.1 m/s. Baroclinic calculations, however, were not presented for this data set so no direct comparison can be made here as well. It can only be assumed that high baroclinic variability also occurs in this region.

Long-term current meter moorings have also recently been made in the EGC over the Greenland continental slope. Muench et al. (1986) presented data obtained from moorings positioned at 100 m and 400 m, within and beneath the core of the core of the frontal jet associated with the EGPF at about 78°35′N and 004°40′W in 1984-85. When compared with the geostrophic data from Tunnicliffe (1985), it is evident that the EGC is strongly baroclinic, especially within the frontal jet but only to a depth of 100 m. Beneath the highly baroclinic zone the baroclinic component in 1984 decreased to about one half of the total flow. As with the series of current meters in the WSC, the current meters in the EGC were also removed prior to September 1985, making direct comparison with the present data difficult.

B. DYNAMIC HEIGHT

The dynamic topography was computed using the methods described in Chapter II. Dynamic heights were computed for the surface referenced to 150 decibars (Fig. 4.1) and 500 decibars (Fig. 4.2) in order to determine the baroclinic structure of the surface flow and to allow comparison with previous work. Dynamic heights were also computed for the 150 decibar surface referenced to 500 decibars (Fig. 4.3) in order to assess the depth variation of the baroclinic current.

The surface dynamic topographies referenced to 150 and 500 decibars show the weak baroclinicity of the WSC in comparison to the EGC. The northern limb of the cyclonic Greenland Sea gyre can be seen in the southern part of Fram Strait. The high gradient region in both figures is the EGPF. A prominent feature along the EGPF is the anticyclonic eddy located at 79°30′N and 001°W. The dynamic height gradient across the EGPF would suggest a baroclinic flow of between 0.20 and 0.30 m/s, while the gradient in the eddy would support a flow of 0.10 to 0.20 m/s. The sluggish WSC flow can be seen along the coast of Spitsbergen. The dynamic height gradient here is much reduced from that in the EGC indicating a baroclinic flow of 0.06 to 0.08 m/s. Fig. 4.2 clearly shows the branching of the WSC just north of 80°10′N. Westward flow is indicated between 79° and 81°N with the core of the westward turning crossing 5°E just north of 80°30′N and merging with the southward flowing EGC. Fig. 4.1 shows

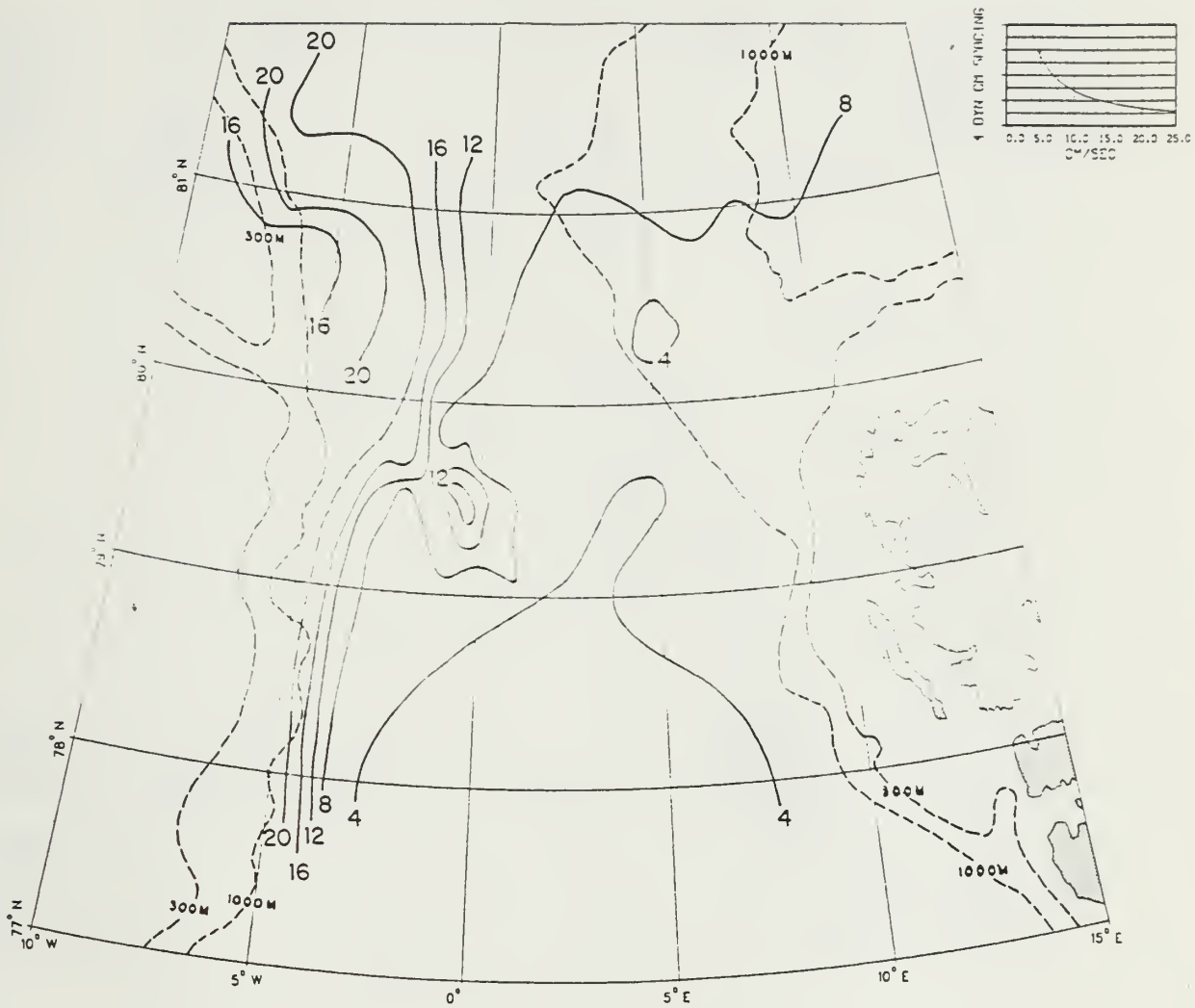

Figure 4.1 Surface dynamic topography referenced to 150 decibars in dynamic centimeters.

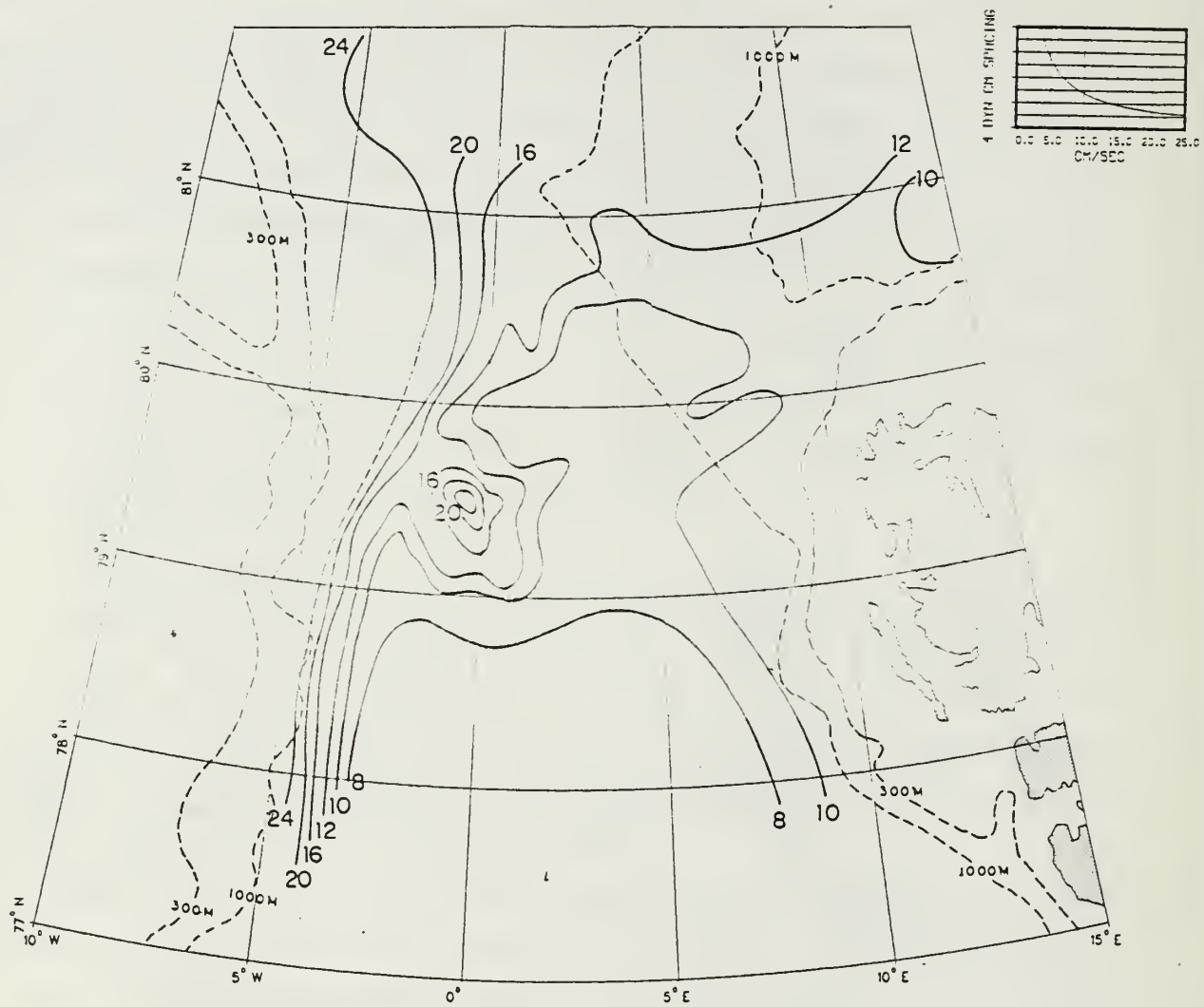

Figure 4.2 Surface dynamic topography referenced to 500 decibars in dynamic centimeters.

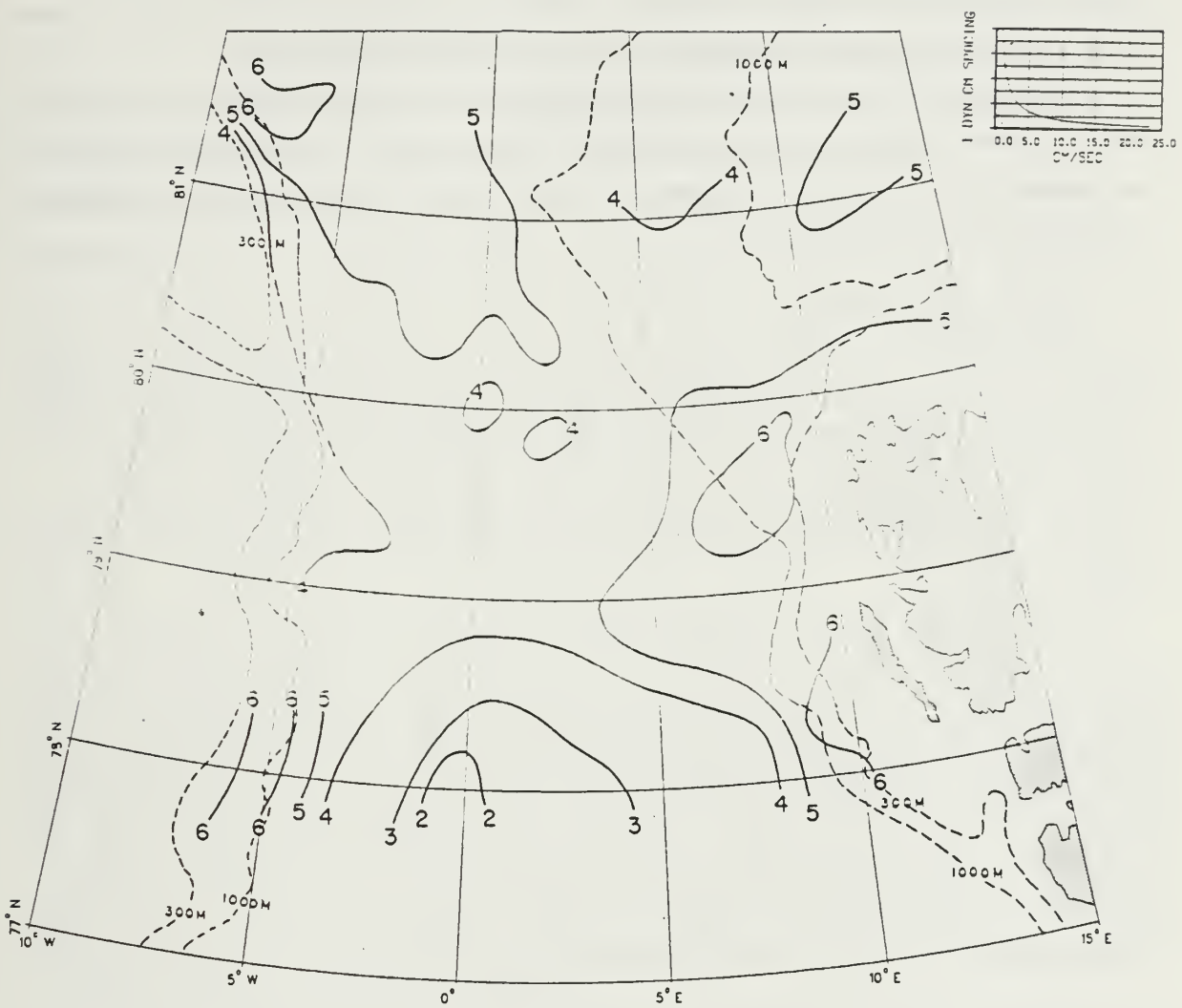

Figure 4.3 150 decibar dynamic topography referenced to 500 decibars in dynamic centimeters.

this westward turning core as a slightly wider flow with the core of the turning occuring across 5°E at 79°30'N. All three figures show that all of the current turns westward at or south of 81°N. Even at 150 decibars there is evidence that the sub-surface portion of the WSC which turns west does so south of 81°N. Fig. 4.2 also shows some evidence of a baroclinic cyclonic flow north of Spitsbergen.

Comparison of surface dynamic topography with 150 m dynamic topography shows westward turning to be a surface layer phenomenon. The WSC flow can be seen along the coast of Spitsbergen. At depth most of the westward turning has occured between 78° and 79°N.

C. BAROCLINIC FLOW

To further investigate the geostrophic velocity and volume transport in Fram Strait, ten vertical baroclinic velocity sections were constructed corresponding to the ten transects of temperature and salinity. Sections 1-10 are presented as Figs. 4.6 - 4.15 at the end of this chapter. As described in Chapter II, a reference level of 500 decibars was selected for the sections, with horizontal extrapolation made for shallower bottom depths.

Section 1 (Fig. 4.6), along 78°N, shows the weakly baroclinic WSC with a core speed of 0.07 m/s located over the center of the Kipnovich Ridge. The filamental nature of the WSC can be seen in a second, much weaker, northward stream between Stations 19 and 20, extending only to a depth of about 80 m. The northward transport resulting from this flow is 1.3 Sv. The EGC shows strong baroclinic flow over the Greenland continental shelf with a speed of almost 0.2 m/s. The core of the RAC is located at a depth of 50 m at Station 16 with a maximum speed of 0.13 m/s. The combined transport for this section for the EGC and the RAC is 3.1 Sv southward.

Section 2 (Fig 4.7), along 79°N, and Section 3 (Fig 4.8), along 79°30'N, also show a weakly baroclinic WSC, with northward speeds of 0.02 to 0.03 m/s. The northward transport for these sections is 0.5 Sv, indicating that some of the flow has turned westward between 78° and 79°N. These sections also clearly show the presence of a baroclinic, anticyclonic eddy extending from the surface to 150 m. The eddy has rotational speeds of between 0.05 and 0.09 m/s, the asymetric character of which may be a result of southward advection of the eddy by the mean flow of the EGC. The EGC is seen in the left hand corner of these figures having a southward flow of greater than 0.16 m/s. Also seen in Figs. 4.7 and 4.8 is a weak southward flow of low salinity

water at the surface near the coast of Spitsbergen, probably the result of glacial run off.

Section 4 (Fig. 4.9), along the ridge of the Yermak Plateau, and Section 5 (Fig. 4.10), along 80°N, show the branching of the WSC into two streams, with one branch flowing north along the Spitsbergen continental shelf and the other along the western slope of the Yermak Plateau. The northward speeds in both branches is 0.02 to 0.03 m/s, while the transport for each section is 0.5 Sv northward. Section 6 (Fig. 4.11), extending northwestward from the coast of Spitsbergen, shows the WSC over the continental slope with a speed of 0.02 m/s. The orientation of this section results in a transport of 0.1 Sv toward the northeast, indicating that approximately 20% of the baroclinic flow of the WSC has turned into the Arctic around the northern coast of Spitsbergen. Fig. 4.11 also shows a southward flow of 0.05 m/s; this is part of the cyclonic flow north of the Spitsbergen continental slope discussed earlier in Fig. 4.2.

Section 7 (Fig. 4.12), along 81°N, all of which is behind the ice edge, shows that at this latitude the flow is dominated by the southward flowing EGC with a speed of 0.14 m/s. The speed of the WSC in this section is at most 0.01 m/s. Section 8 (Fig. 4.13), along 80°30'N, is also dominated by the southward flow of the EGC. A much stronger jet than in Fig 4.12 is located between Stations 95 and 100 with a speed of 0.2 m/s. The maximum speed of the WSC in this section is 0.05 m/s and centered over the western slope of the Yermak Plateau near Station 104. The southward transport for Fig. 4.12 is 1.2 Sv and for Fig. 4.13 is 1.1 Sv. The northward transport in the WSC for Fig. 4.12 is less than 0.1 Sv, while for Fig. 4.13 it is 0.4 Sv. Also present in these two sections is a shallow northward flowing current over the Greenland continental slope between 5° and 7°W. The cause for this northward flow is probably a meander in the EGC that is not fully resolved by the data.

Section 9 (Fig. 4.14), along 2°E between 79° and 81°N, shows the core of the westward turning is predominantly north of 80°N, between Stations 38 and 99, with a speed of 0.03 m/s. There is also a westward flow south of Station 34, indicating that some westward turning is taking place south of 79°N. The transport for the northern core of westward turning is 0.4 Sv, while that south of Station 34 is about 0.1 Sv westward. Section 10 (Fig. 4.15) extends through the eddy along 2°W. This section shows a much more symetric pattern to the anti-cyclonic rotation, although the rotational speed of 0.15 m/s is somewhat in contrast to the slower speeds discussed earlier. The swirl transport calculated from these velocities is about 0.4 Sv.

Fig. 4.4 shows a plan view of Fram Strait and summarizes the transport measurements just disscussed. The solid arrows indicate the transports calculated from the present data. The dashed-dot line indicates the latitude band where there is little or no westward flow. Assuming continuity of the flow, 0.8 Sv must turn westward south of 79°N. This is indicated by the dashed arrow with the transport value in parenthesis. The splitting of the WSC is indicated by the arrow pointing westward at 80°N and the second arrow pointing northeastward north of Spitsbergen. Included for comparison are transport calculations from data obtained in 1984 (Tunnicliffe, 1985) shown as open arrows. The 1.5 Sv southward found in 1984 included contributions from the flow over the sheif and out to the EGPF but little. if any. of the RAC. The 3.1 Sv southward found in 1985 included the EGPF and the RAC. Assuming the flow is the same in both years, an uncertain assumption at best, then the RAC carries at least 1.5 Sv southward, which is similar in magnitude to the transport of the EGPF jet.

D. CIRCULATION

The surface circulation pattern suggested by the dynamic height and geostrophic velocity calculations is shown in Fig. 4.5. The arrow lengths and widths are representitive of the magnitude of the flow as shown in the accompanying scale. A weakly baroclinic WSC flows north in several streams controlled in part by bathymetry. Some westward turning takes place south of 79°N, with a second core of westward turning between 80° and 81°N.

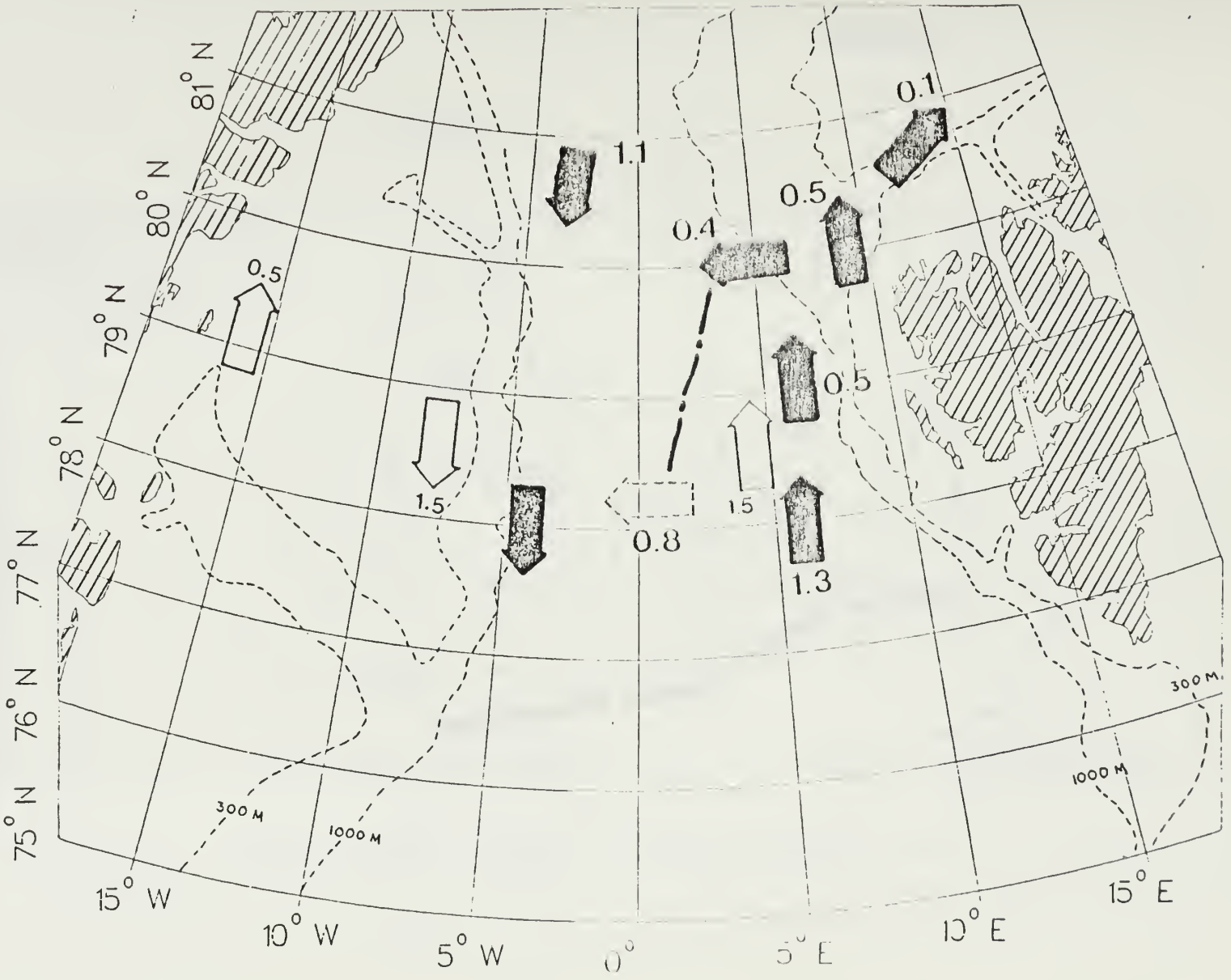

Figure 4.4 A plan view of Fram Strait summarizing the transport calculations..

Figure 4.5 A plot of the surface circulation suggested by the dynamic topography and geostrophic velocities.

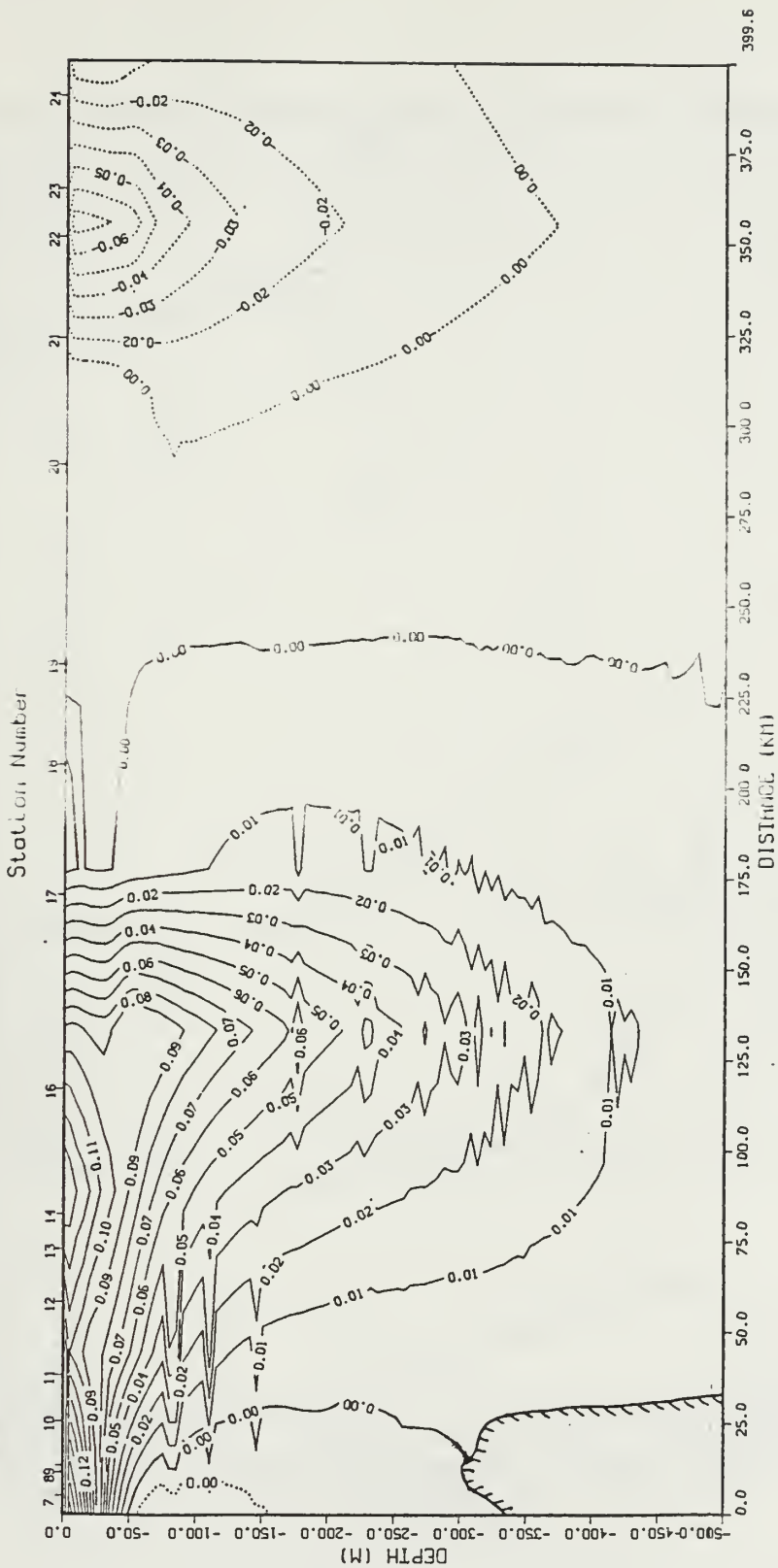

Figure 4.6 Section 1, along 78°N. Southward flow is indicated by postive isotachs spaced at 0.01 m/s intervals.

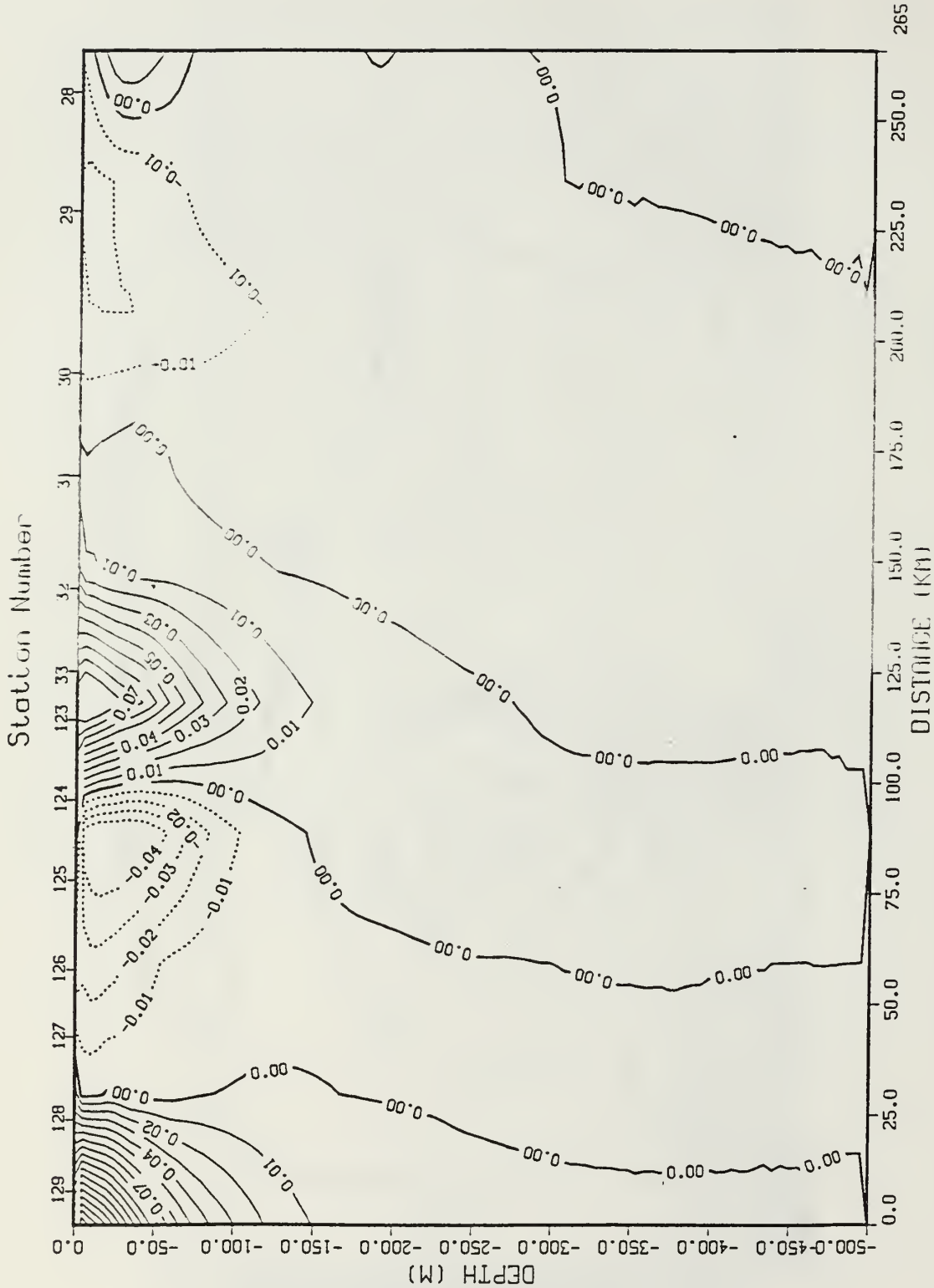

Figure 4.7 Section 2, along 79°N

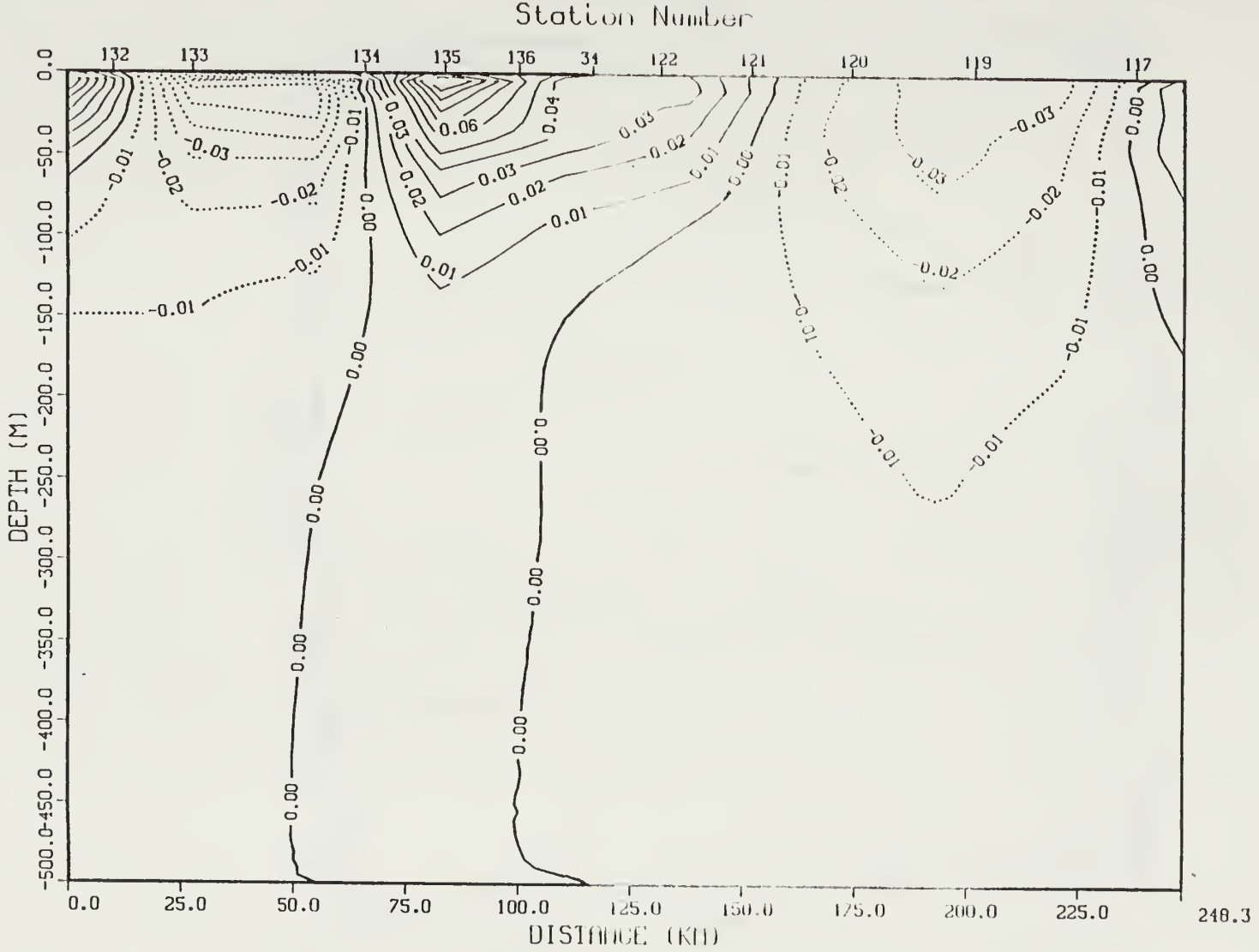

Figure 4.8 Section 3, along 79°30 N.

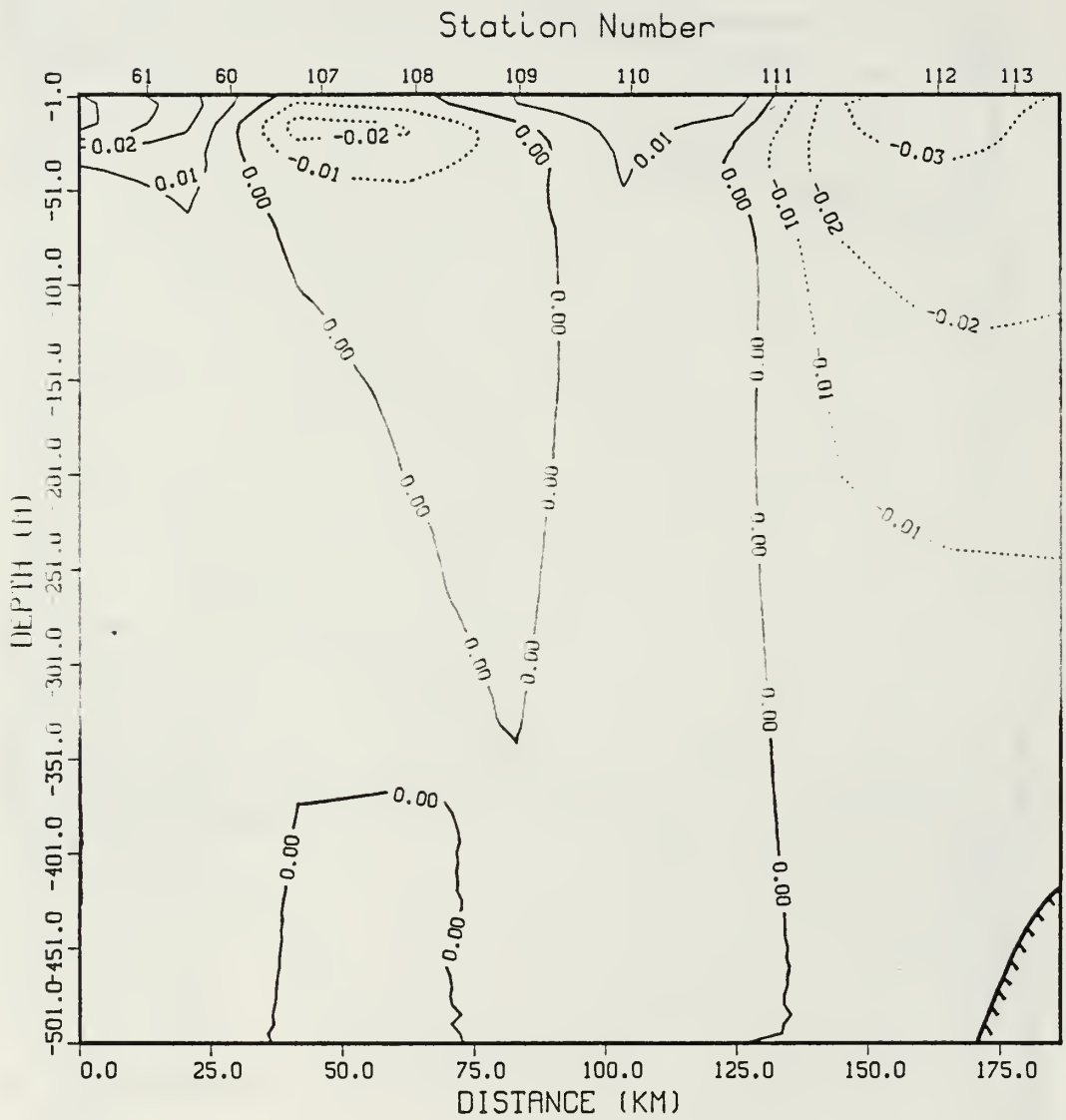

Figure 4.9 Section 4, along the top of the Yermak Plateau.

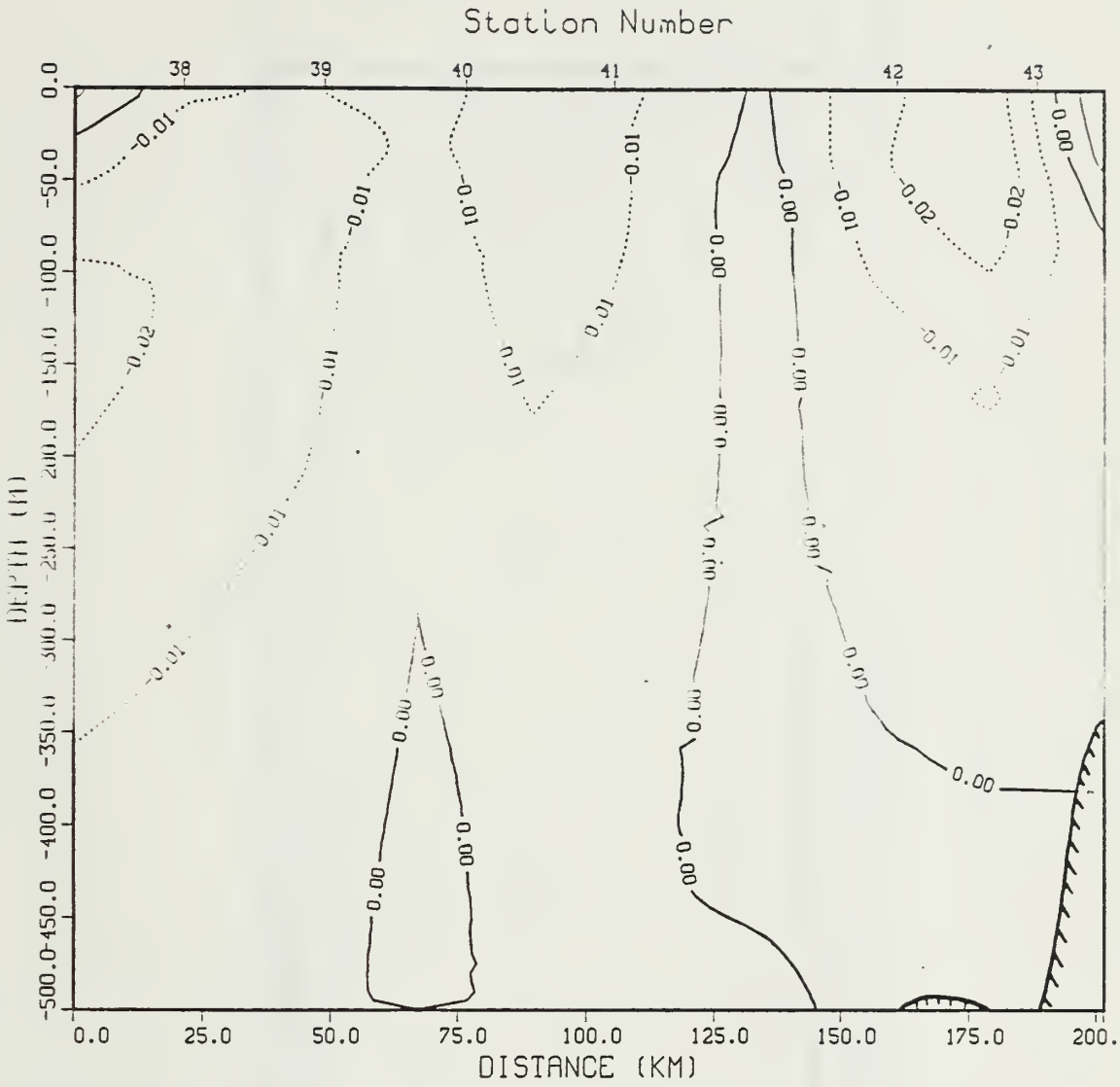

Figure 4.10 Section 5, along 80°N.

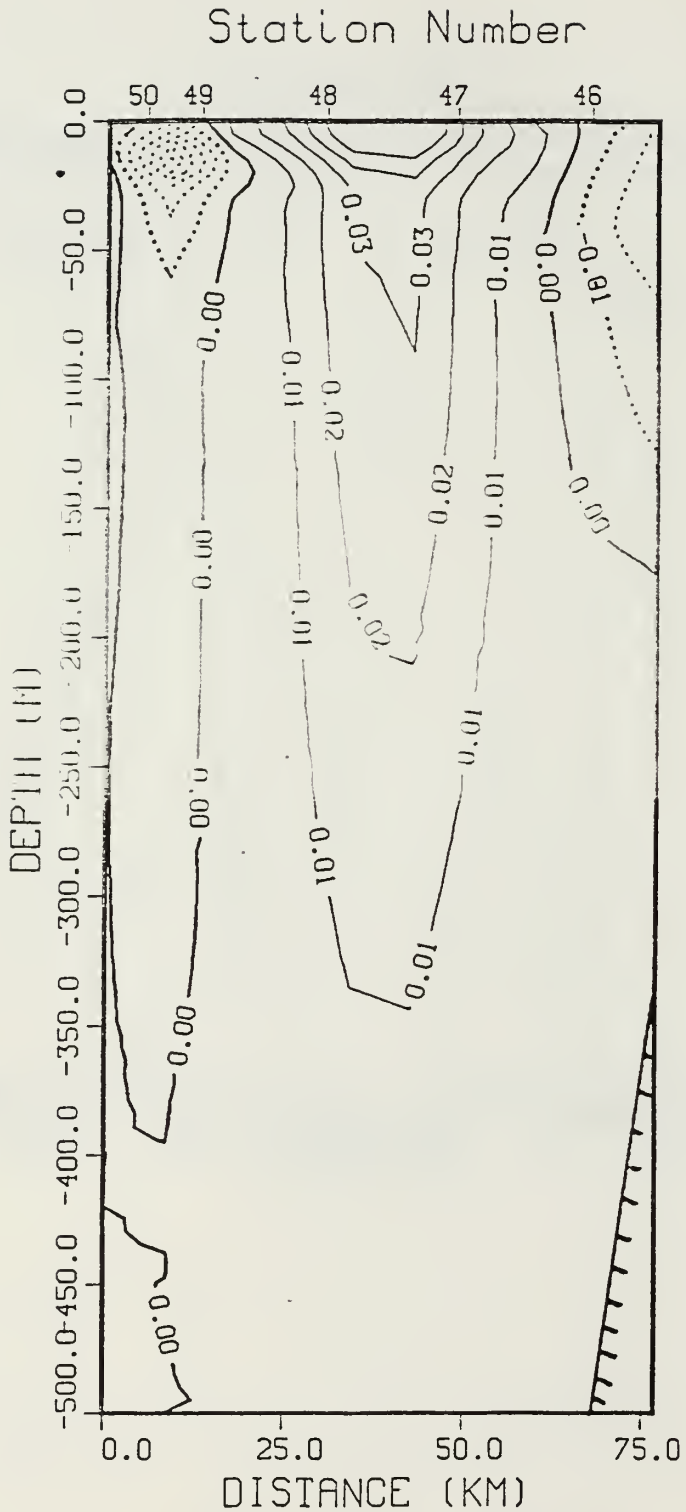

Figure 4.11 Section 6, extending northwestward from the Spitsbergen coast.

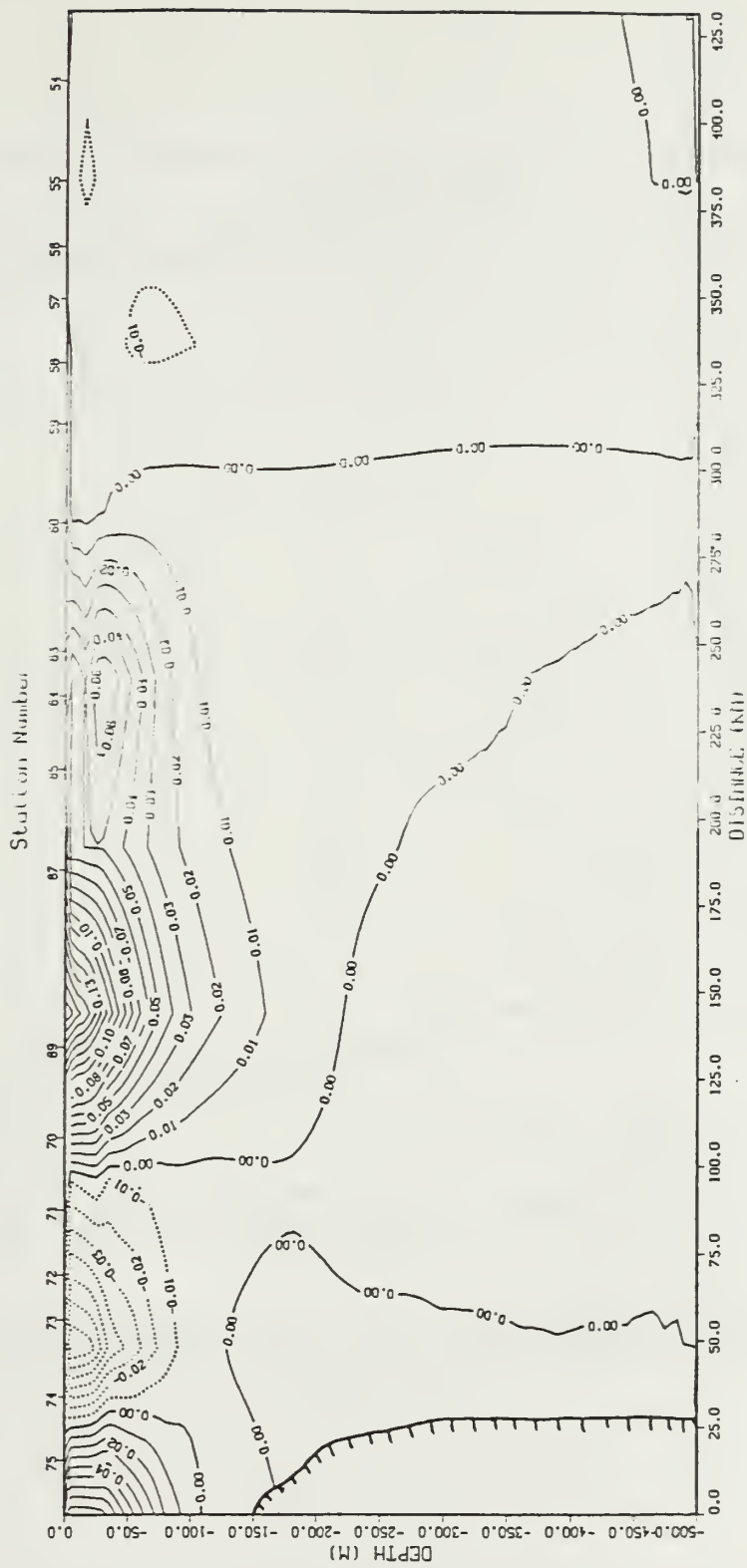

Figure 4.12 Section 7, along 81°N

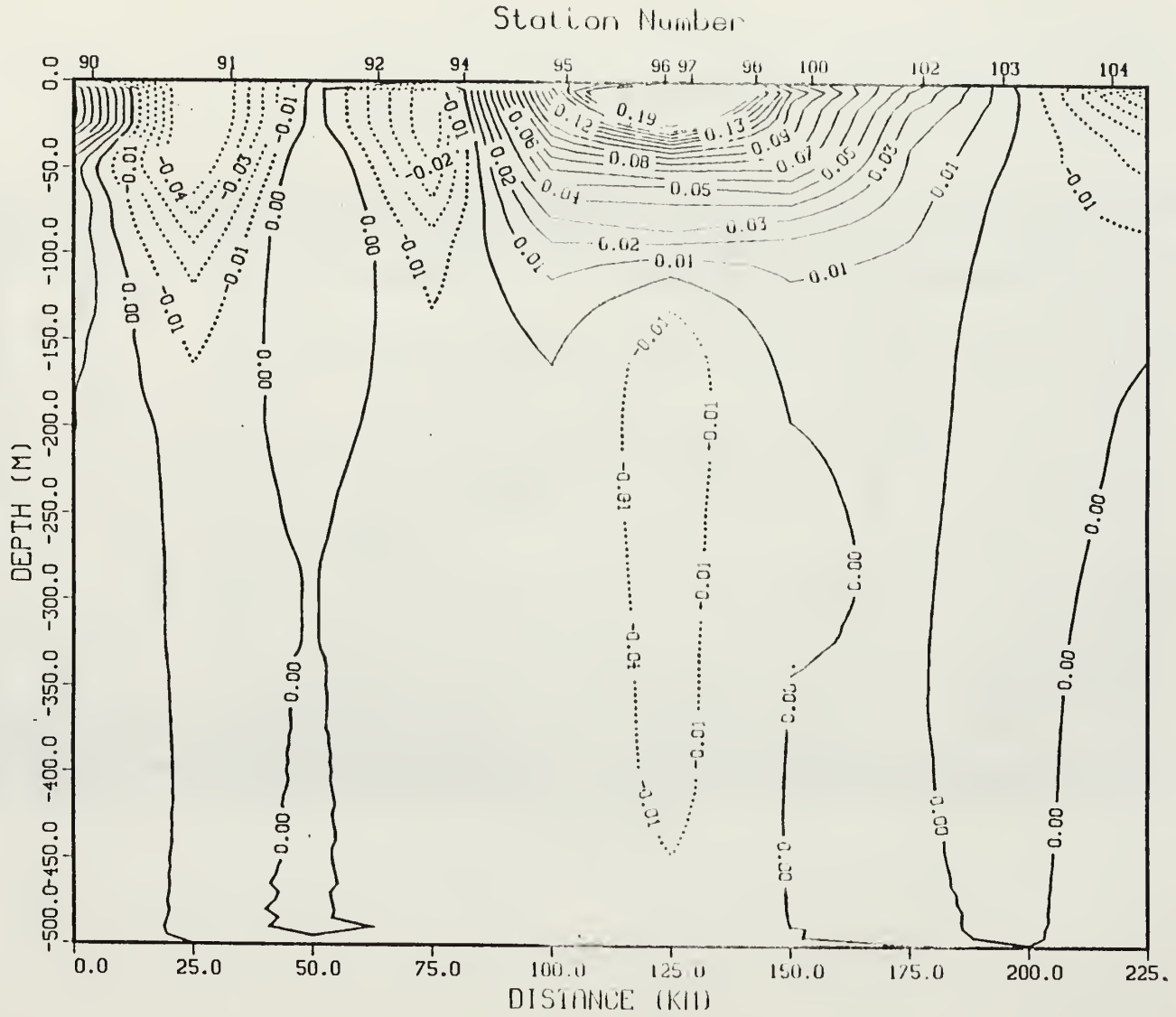

Figure 4.13 Section 8, along 80°30'N.

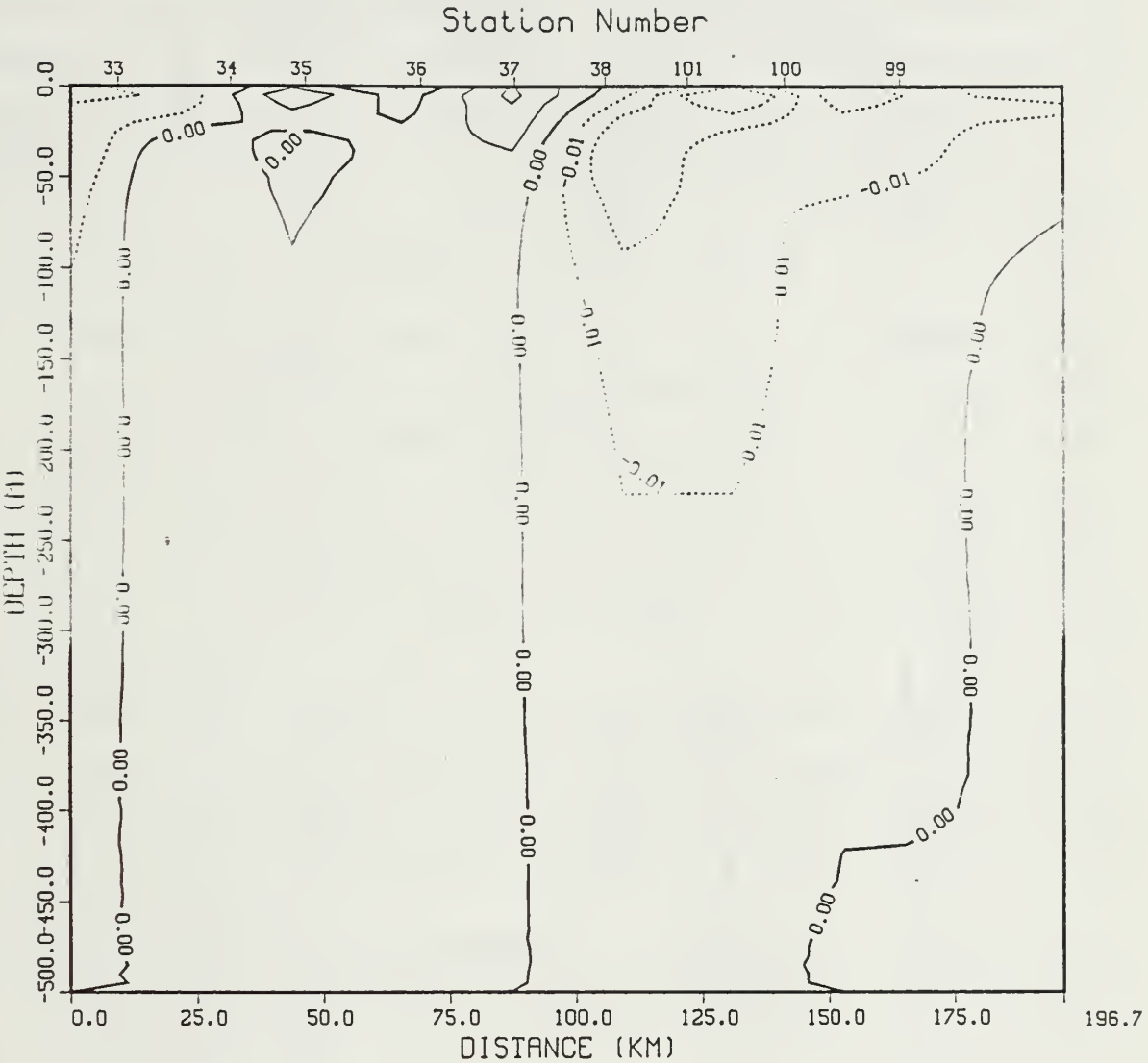

Figure 4.14 Section 9, along 2°E, showing the core of the westward turning.

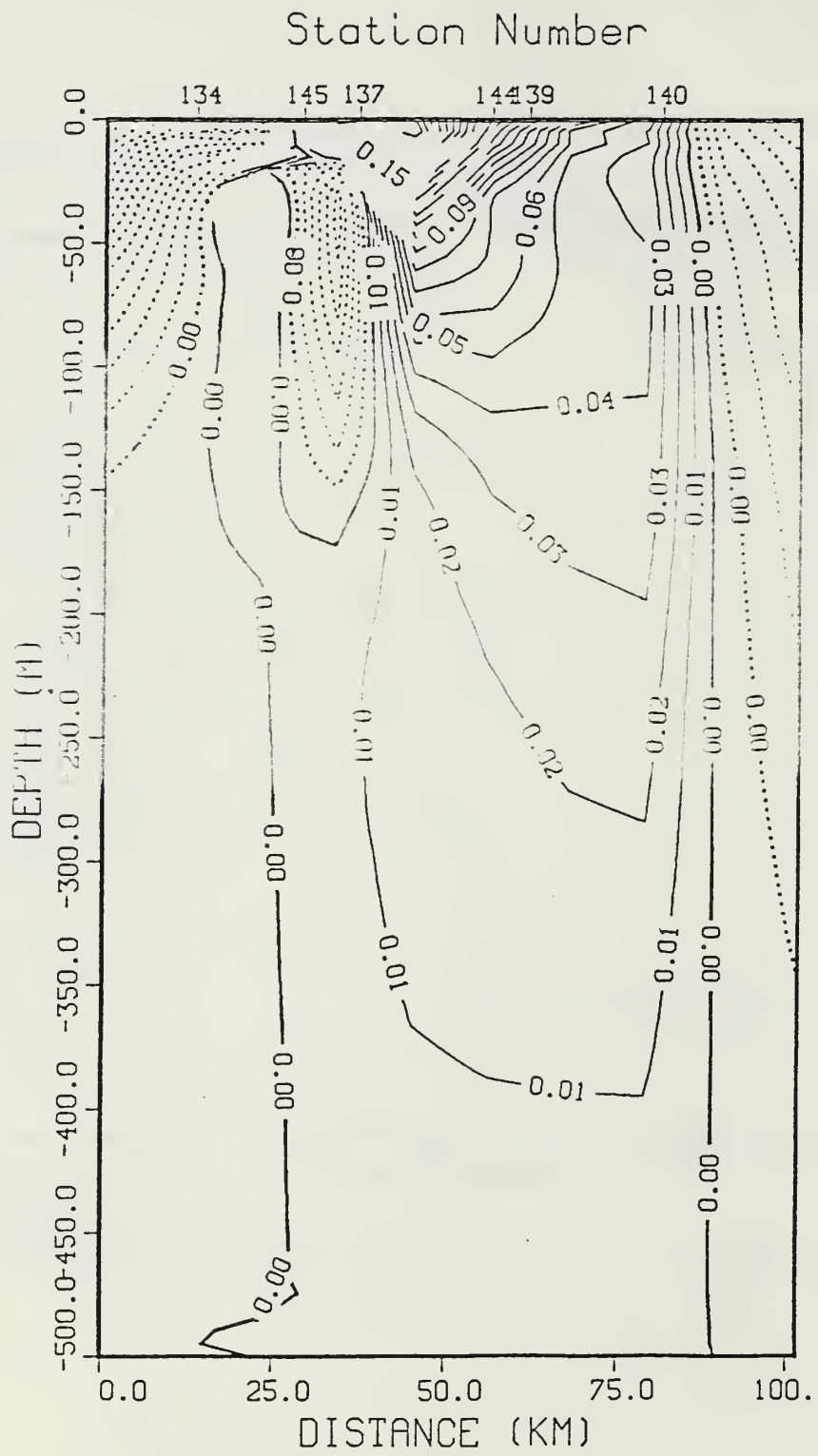

Figure 4.15 Section 10 along 2°W, through the center of the eddy.

V. CONCLUSIONS

The West Spitsbergen Current and adjacent waters in Fram Strait have been examined using a dense network of CTD stations occupied by NORTHWIND in September 1985. The distribution of water masses in Fram Strait was examined in detail. Baroclinic transports were calculated from geostrophic velocities based on the distribution of these water properties. The following conclusions can be drawn:

- The WSC was found as a weakly baroclinic flow in several streams along the Spitsbergen continental slope. Northward geostrophic velocity at the surface along 78°N was found to be 0.07 m/s.
- Bathymetric steering appears to play an important role in the location of the separate streams of the WSC. The Kipnovich Ridge, a 2000 m deep feature to the west of the Spitsbergen continental shelf, exerts an influence on the distribution of water mass properties, especially north of 78°N.
- North of 80°N the WSC splits into two branches, with approximately 20% of the baroclinic flow following the Spitsbergen continental shelf into the Arctic Basin and 80% of the flow turning westward over the western slope of the Yermak Plateau.
- Some westward turning of the WSC takes place south of 79°N. A core of westward turning was located between 80° and 81°N along the prime meridian with baroclinic speeds of 0.03 m/s. Several filaments of AW were found turning westward between 79° and 80°N, although these contributed little to the net westward transport.
- South of 79°N the EGPF is found close to the 400 m isobath. North of 79°N the front turns northeastward and crosses the Yermak Pleateau into the Arctic Ocean.
- North of 79°N the EGPF was found split into surface and subsurface sections, probably as a result of the cooling and dilution of AW by melting sea ice.
- An anti-cyclonic, cold core eddy with a diameter of approximately 60 km and a depth of 180 m was found along the EGPF. This eddy had geostrophic velocities of up to 0.15 m/s resulting in a swirl transport of 0.4 Sv.

- Notable temperature and salinity finestructure was found along the EGPF and in the vicinity of the ice edge, with the temperature signal often varying by more than 2°C peak-to-peak. Strong interleaving of water masses was often found to occur resulting in alternating regions of strongly diffusive and fingering activity.

LIST OF REFERENCES

Aagaard, K., Wind-driven transports in the Greenland and Norwegian seas, *Deep-Sea Res.*, *17*, 281-291, 1970.

Aagaard, K., and L.K. Coachman, The East Greenland Current north of the Denmark Strait,I, *Arctic*, *21*, 181-200, 1968a.

Aagaard, K., and L.K. Coachman, The East Greenland Current north of the Denmark Strait,II, *Arctic*, *21*, 267-290, 1968b.

Aagaard, K., and A. Foldvik, The West Spitsbergen Current in Fram Strait: what happens to the water, *EOS*, *66*, 1262, 1985.

Aagaard, K., and P. Greisman, Toward new mass and heat budgets for the Arctic Ocean, *J. Geophys. Res.*, *80*, 3821-3827, 1975.

Aagaard, K., and R. Reed, Fram Strait: exchange and dynamics, report on a workshop, *EOS*, in press.

Aagaard, K., C. Darnall, A. Foldvik, and T. Torresen, Fram Strait current measurements 1984-1985, Report No. 63, Dept. of Oceanography, Geophysical Institute, University of Bergen, Bergen, Norway, 1985a.

Aagaard, K., J.H. Swift, and E. Carmack, Thermohaline circulation in the Arctic mediterranean seas, *J. Geophys. Res.*, *90*, 4833-4846, 1985b.

Bourke, R.H., Preliminary results of the oceanographic cruise of the USCGC Northwind to the Greenland Sea: August - September, 1984, Tech. Rep. NPS 68-84-019, Dept. of Oceanography, Naval Postgraduate School, Monterey, California, 1984.

Bourke, R.H., J.L. Newton, R.G. Paquette, and M.D. Tunnicliffe, Circulation and water masses of the East Greenland shelf, *J. Geophys. Res.*, in press a.

Bourke, R.H., M.D. Tunnicliffe, J.L. Newton, R.G. Paquette, and T.O. Manley, Eddy near the Molloy Deep revisited, *J. Geophys. Res.*, in press b.

Bourke, R.H., R.G. Paquette, and A.M.Weigel, MIZLANT 85 data report: results of an oceanographic cruise to the Greenland Sea, September, 1985, Tech. Rep. NPS 68-86-007, Dept. of Oceanography, Naval Postgraduate School, Monterey, California, 1986.

Carmack, E., On the hydrography of the Greenland Sea, Ph.D Thesis, University of Washinton, Seattle, Washington, 1972.

Carmack, E., and K. Aagaard, On the deep water of the Greenland Sea, *Deep-Sea Res.*, *20*, 687-715, 1973.

Coachman, L.K., and K. Aagaard, Physical oceanography of Arctic and Subarctic seas, in *Arctic Geology and Oceanography*, edited by Y. Herman, pp. 1-72, Springer-Verlag, New York, 1974.

Davidson, K., and others, MIZEX Bulletin VIII: A science plan for a winter marginal ice zone experiment in the Fram Strait/Greenland Sea: 1987/89, CRREL Special Report 86-9, U.S. Army Cold Regions Research and Engineering Laboratory, Hanover, New Hampshire, 1986.

Dickson, R.R., Variability and continuitity within the Atlantic Current of the Norwegian Sea, *Rapp. Cons. Explor. Mer*, *162*, 167-183, 1972.

Dickson, R.R., and T.C. Doddington, Hydrographic conditions off Spitsbergen in the summers of 1966 and 1967, *Ann. Biol.*, *24*, 24-29, 1968.

Dickson, R.R., and T.C. Doddington, Hydrographic conditions off Spitsbergen in the summers of 1968 and 1969, *Ann. Biol.*, *26*, 26-32, 1970.

Fomin, L.M., *The Dynamic Method in Oceanography*, Elsevier Publishing Company, New York, 1964.

Greisman, P., Current measurements in the eastern Greenland Sea, Ph.D. Thesis, University of Washington, Seattle, Washington, 1976.

Greisman, P., and K. Aagaard, Seasonal variability of the West Spitsbergen Current, *Ocean Modelling*, *19*, 3-5, 1979.

Griffiths, R.W., and P.F. Linden, The stability of buoyancy-driven coastal currents, *Dyn. Atmos. Oceans*, *5*, 281-306, 1981.

Hakkinen, S., Coupled ice-ocean dynamics in the marginal ice zones: upwelling, downwelling, and eddy generation, *J. Geophys Res.*, *91*, 819-832, 1986.

Hanzlick, D.J., The West Spitsbergen Current: transport, forcing and variability, Ph.D. Thesis, University of Washington, Seattle, Washington, 1983.

Helland-Hansen, B., The Sognefjord Section - oceanographic observations in the northernmost part of the North Sea and the southern part of the Norwegian Sea. James Johnstone Memorial Volume, Lancashire Sea - Fish. Lab., Liverpool, 1934.

Helland-Hansen, B. and F. Nansen, The Norwegian Sea, *Report on Norwegian Fishery and Marine Investigations*, vol. 2, part 1, no. 2, Bergen, Norway, 1909.

Hill, H.W. and A.J. Lee, The effect of wind on water transport in the region of the Bear Island fishery, *Proc. Roy. Soc., B, 148*, 104-116, 1957.

Johannessen, O.M., J.A. Johannessen, J. Morison, B.A. Farrelly, and E.A.S. Svendsen, Oceanographic conditions in the marginal ice zone north of Svalbard in early fall 1979 with an emphasis on mesoscale processes, *J. Geophys. Res.*, *88*, 2755-2769, 1983.

Kiilerich, A.B., On the hydrography of the Greenland Sea, *Meddelser om Gronland*, *144*, 63 pp., 1945.

Kislyskov, A.G., Fluctuations in the regime of the Spitsbergen Current, Translation: *Soviet Fisheries Investigations in North European Seas*, 39-49, 1960.

Lee, A., The hydrography of the European Artic and Subartic Seas, *Oceanogr. Mar. Biol. Ann. Rev.*, *1*, 47-76, 1963.

Muench, R.D., G.S.E. Laagerloef, and J.T. Gunn, 1984-85 Current observations in the East Greenland Current: A preliminary description, MIZEX Bulletin VII, CRREL Special Report 86-3, U.S. Army Cold Regions Research and Engineering Laboratory, Hanover, New Hampshire, 1986.

Paquette, R.G., R.H. Bourke, J.L. Newton, and W.F. Perdue, The East Greenland Polar Front in Autumn, *J. Geophys. Res*, *90*, 48866-4882, 1985.

Perdue, W.F., Oceanographic investigation of the East Greenland Polar Front, Master's Thesis, Naval Postgraduate school, Monterey, California, March,1982.

Perkin, R.G. and E.L. Lewis, Mixing in the West Spitsbergen Current, *J.Phys. Oceanogr.*, *14*, 1315-1325, 1984.

Perry, R.K., Bathymetry, in: *The Nordic Seas*, edited by B.G. Hurdle, pp. 211-234, Springer-Verlag, 1986.

Quadfasel, D., J.C. Gascard, and K.P. Koltermann, Large scale oceanography in Fram Strait during MIZEX 84, *J. Geophys. Res.*, in press.

Ruddick, B., A practical indicator of the stability of the water column to double-diffusive activity, *Deep-Sea Res.*, *30*, 1105-1107, 1983

Smith, D.C., J.H. Morison, J.A. Johannessen, and N. Untersteiner, Topographic generation of an eddy at the edge of the East Greenland Current, *J. Geophys. Res.*, *89*, 8205-8208, 1984.

Swift, J.H., and K. Aagaard, Seasonal transitions and water mass formation in the Iceland and Greenland Seas, *Deep Sea Res.*, *28A*, 1107-1129, 1981.

Timofeyev, V.T., The movement of Atlantic water and heat into the Artic Basin, *Deep-Sea Res.*, *9*, 358-361. 1962.

Trangeled, S., Oceanography of the Norwegian and Greenland Seas and adjacent areas, NATO SACLANTCEN memorandum SM-47, 1974.

Tunnicliffe, M.D., An investigation of the waters of the East Greenland Current, Master's Thesis, Naval Postgraduate School, Monterey, California, September, 1985.

Turner, J.S., *Buoyancy Effects in Fluids*, Cambridge University Press, New York, 1973.

UNESCO, Background papers and supporting data on the practical salinity scale, 1978, UNESCO Tech. Pap. in Mar. Sci., No. 37, 1981.

Wadhams, P., and V.A. Squire, An ice-water vortex at the edge of the East Greenland Current, *J. Geophys. Res.*, *88*, 2770-2780, 1983.

Wadhams, P., A.E. Gill, and P.F. Linden, Transects by submarine of the East Greenland Polar Front, *Deep-Sea Res.*, *26*, 1311-1329, 1979.

INITIAL DISTRIBUTION LIST

		No. Copies
1.	Director Applied Physics Laboratory Attn: Mr. Robert E. Francois Mr. E.A. Pence Mr. G.R. Garrison Library University of Washington 1013 Northeast 40th Street Seattle, Washington 98105	 1 1 1 1
2.	Director Arctic Submarine Laboratory Code 19, Building 371 Naval Ocean Systems Center San Diego, California 92152	5
3.	Superintendent Naval Postgraduate School Attn: Dr. R.H. Bourke, Code 68Bf Dr. R.G. Paquette, Code 68Pa Dr. D.C. Smith IV, Code 68Si Monterey, California 93943	 5 5 1
4.	Polar Research Laboratory, Inc. 6309 Carpinteria Ave. Carpinteria, California 93103	1
5.	Chief of Naval Operations Department of the Navy Attn: NOP-02 NOP-22 NOP-964D2 NOP-095 NOP-098 Washington, District of Columbia 20350	 1 1 1 1 1
6.	Commander Submarine Squadron THREE Fleet Station Post Office San Diego, California 92132	1
7.	Commander Submarine Group FIVE Fleet Station Post Office San Diego, California 92132	1
8.	Dr. John L. Newton 10211 Rookwood Drive San Diego, California 92131	2

9. Director — 1
Marine Physical Laboratory
Scripps Institution of Oceanography
San Diego, California 92132

10. Commanding Officer — 1
Naval Intelligence Support Center
4301 Suitland Road
Washington, District of Columbia 20390

11. Commander — 1
Space and Naval Warfare Systems Command
Department of the Navy
Washington, District of Columbia 20360

12. Director — 1
Woods Hole Oceanographic Institution
Woods Hole, Massachusetts 02543

13. Commanding Officer — 1
Naval Coastal Systems Laboratory
Panama City, Florida 32401

14. Commanding Officer — 1
Naval Submarine School
Naval Submarine Base, New London
Groton, Connecticut 06349-5700

15. Assistant Secretary of the Navy — 1
(Research and Development)
Department of the Navy
Washington, District of Columbia 20350

16. Director of Defense Research and Engineering — 1
Office of Assistant Director (Ocean Control)
The Pentagon
Washington, District of Columbia 20301

17. Commander, Naval Sea Systems Command — 1
Department of the Navy
Washington, District of Columbia 20362

18. Chief of Naval Research
Department of the Navy
Attn: Code 102-OS — 1
Code 220 — 1
Code 1125 Arctic — 1
800 N. Quincy Street
Arlington, Virginia 22217

19. Project Manager — 1
Anti-Submarine Warfare Systems Project
Office (PM4)
Department of the Navy
Washington, District of Columbia 20360

20. Commanding Officer — 1
Naval Underwater Systems Center
Newport, Rhode Island 02840

21. Commander — 1
Naval Air Systems Command
Headquarters
Department of the Navy
Washington, District of Columbia 20361

22. Commander
Naval Oceanographic Office
Attn: Library Code 3330 — 1
Washington, District of Columbia 20373

23. Director — 1
Advanced Research Project Agency
1400 Wilson Boulevard
Arlington, Virginia 22209

24. Commander SECOND Fleet — 1
Fleet Post Office
New York, New York 09501

25. Commander THIRD Fleet — 1
Fleet Post Office
San Francisco, California 96601

26. Commander
Naval Surface Weapons Center
White Oak
Attn: Mr. M.M. Kleinerman — 1
Library — 1
Silver Springs, Maryland 20910

27. Officer-in-Charge — 1
New London Laboratory
Naval Underwater Systems Center
New London, Connecticut 06320

28. Commander
Submarine Development Squadron TWELVE — 1
Naval Submarine Base
New London
Groton, Connecticut 06349

29. Commander
Naval Weapons Center
Attn: Library 1
China Lake, California 93555

30. Commander
Naval Electronics Laboratory Center
Attn: Library 1
271 Catalina Boulevard
San Diego, California 92152

31. Director 1
Naval Research Laboratory
Attn: Technical Information Division
Washington, District of Columbia 20375

32. Director 1
Ordnance Research Laboratory
Pennsylvania State University
State College, Pennsylvania 16801

33. Commander Submarine Force 1
U.S. Atlantic Fleet
Norfolk, Virginia 23511

34. Commander Submarine Force
U.S. Pacific Fleet 1
Attn: N-21
Pearl Harbor, Hawaii 96860-6550

35. Commander 1
Naval Air Development Center
Warminster, Pennsylvania 18974

36. Commander 1
Naval Ship Research and Development Center
Bethesda, Maryland 20084

37. Commandant 1
U.S. Coast Guard Headquarters
400 Seventh Street, S.W.
Washington, District of Columbia 20590

38. Commander 1
Pacific Area, U.S. Coast Guard
630 Sansome Street
San Francisco, California 94126

39. Commander 1
Atlantic Area, U.S. Coast Guard
159E, Navy Yard Annex
Washington, District of Columbia 20590

40. Commanding Officer — 1
U.S. Coast Guard Oceanographic Unit
Building 159E, Navy Yard Annex
Washington, District of Columbia 20590

41. Scientific Liaison Office — 1
Office of Naval Research
Scripps Institute of Oceanography
La Jolla, California 92037

42. Scripps Institution of Oceanography — 1
Attn: Library
P.O. Box 2367
La Jolla, California 92037

43. School of Oceanography
University of Washington
Attn: Dr. L.K. Coachman — 1
Dr. S. Martin — 1
Dr. J. Swift — 1
Library — 1
Seattle, Washington 98195

44. School of Oceanography — 1
Oregon State University
Attn: Library
Corvallis, Oregon 97331

45. CRREL
U.S. Army Corps of Engineers
Attn: Library — 1
Hanover, New Hampshire 03755-1290

46. Commanding Officer — 1
Fleet Numerical Oceanography Center
Monterey, California 93943

47. Commanding Officer — 1
Naval Environmental Prediction Research Facility
Monterey, California 93943

48. Defense Technical Information Center — 2
Cameron Station
Alexandria, Virginia 22304-6145

49. Commander — 1
Naval Oceanography Command
NSTL Station
Bay St. Louis, Mississippi 39529

50. Commanding Officer
Naval Ocean Research and Development Activity
Attn: Technical Director 1
NSTL Station
Bay St. Louis, Mississippi 39529

51. Commanding Officer 1
Naval Polar Oceanography Center, Suitland
Washington, District of Columbia 20373

52. Director 1
Naval Oceanography Division
Naval Observatory
34th and Massachussetts Ave. NW
Washington, District of Columbia 20390

53. Commanding Officer
Naval Oceanographic Command 1
NSTL Station
Bay St. Louis, Mississippi 39522

54. Scott Polar Research Institute
University of Cambridge
Attn: Library 1
Sea Ice Group 1
Cambridge, ENGLAND
CB2 1ER

55. Chairman 1
Department of Oceanography
U.S. Naval Academy
Annapolis, Maryland 21402

56. Dr. James Morison 1
Polar Science Center
4057 Roosevelt Way, NE
Seattle, Washington 98105

57. Dr. Kenneth Hunkins 1
Lamont-Doherty Geological Observatory
Palisades, New York 10964

58. Dr. David Paskowsky, Chief 1
Oceanography Branch
U.S. Department of the Coast Guard
Research and Development Center
Avery Point, Connecticut 06340

59. Science Applications, Inc.
Attn: Dr. Robin Muench 1
13400B Northrup Way
Suite 36
Bellevue, Washington 98005

60. Institute of Polar Studies
Attn: Library 1
103 Mendenhall
125 South Oval Mall
Columbus, Ohio 43210

61. Institute of Marine Science
University of Alaska
Attn: Library 1
Fairbanks, Alaska 99701

62. Department of Oceanography
University of British Columbia
Attn: Library 1
Vancouver, British Columbia
CANADA
V6T 1W5

63. Institute of Marine Science
University of Alaska
Attn: Dr. H.J. Niebauer 1
Fairbanks, Alaska 99701

64. Bedford Institute of Oceanography
Attn: Dr. P. Jones 1
Library 1
P.O. Box 1006
Dartmouth, Nova Scotia
CANADA
B2Y 4A2

65. Carol Pease 1
Pacific Marine Environmental Lab/NOAA
7600 Sand Point Way N.E.
Seattle, Washington 98115

66. Department of Oceanography 1
Dalhousie University
Halifax, Nova Scotia
CANADA
B3H 4J1

67. Dr. Richard Armstrong 2
MIZEX Data Manager
National Snow and Ice Data Center
Cooperative Institute for Research
in Environmental Sciences
Boulder, Colorado 80309

68. Dr. Eddy Carmack 1
Institute of Ocean Sciences
P.O. Box 6000
Sidney, British Columbia
CANADA
V8L 4B2

70. Dr. Knut Aagaard 1
NOAA/PMEL
NOAA Bldg. #3
7600 Sand Point Way, N.E.
Seattle, Washington 98115

71. Department of Ocean Engineering 1
Attn: Library
Mass. Institute of Technology
Cambridge, Massachusetts 02139

72. Dr. Theodore D. Foster 1
Center for Coastal Marine Studies
University of California
Santa Cruz, California 95064

73. Research Administration 1
Code 012
Naval Postgraduate School
Monterey, California 93943-5000

74. Dr. Hugh D. Livingston 1
Woods Hole Oceanographic Institution
Woods Hole, Massachusetts 02543

75. Dr. T.O. Manley 1
Lamont-Doherty Geological Observatory
Palisades, New York 10964

76. Dr. A. Foldvik 1
Geophysical Institute
University of Bergen
Bergen, NORWAY

77. Dr. Preben Gudmandsen 1
Electromagnetics Institute
Technical University of Denmark
Building 349
DK-2800 Lyngby, DENMARK

78. Dr. D. Hanzlick 1
Flow Industries, Inc.
Kent, Washington 98064

79. Dr. W.D. Hibler 1
Thayer School of Engineering
Dartmouth College
Hanover, New Hamsphire 03755

80. Dr. J. Meincke 1
Inst. fur Meereskunde
Universistat Hamburg
Heimhunder Strasse 71
2000 Hamburg 13
WEST GERMANY

81. Dr. B. Rudels 1
Norwegian Polar Research Institute
P.O. Box 158
1330 Oslo Lufthaven
NORWAY

82. LT A.M. Weigel 3
4332 Great Oak Drive
Charleston, South Carolina 29418

83. Superintendent 2
Naval Postgraduate School
Attn: Library (Code 0142)
Monterey, California 93943-5002

18070 2

DUDLEY KNOX LIBRARY
NAVAL POSTGRADUATE SCHOOL
MONTEREY CALIFORNIA 93943-5002

Thesis
W3523 Weigel
c.1 Mesoscale variability in the West Spitsbergen Current and adjacent waters in Fram Strait.

DUDLEY KNOX LIBRARY
3 2768 00018109 3